



<https://theses.gla.ac.uk/>

Theses Digitisation:

<https://www.gla.ac.uk/myglasgow/research/enlighten/theses/digitisation/>

This is a digitised version of the original print thesis.

Copyright and moral rights for this work are retained by the author

A copy can be downloaded for personal non-commercial research or study, without prior permission or charge

This work cannot be reproduced or quoted extensively from without first obtaining permission in writing from the author

The content must not be changed in any way or sold commercially in any format or medium without the formal permission of the author

When referring to this work, full bibliographic details including the author, title, awarding institution and date of the thesis must be given

Enlighten: Theses

<https://theses.gla.ac.uk/>  
[research-enlighten@glasgow.ac.uk](mailto:research-enlighten@glasgow.ac.uk)

**PROTEIN-PROTEIN INTERACTIONS WITHIN THE  
2-OXOACID DEHYDROGENASE COMPLEXES.**

**Susan Diane Richards**

Thesis submitted to the University of Glasgow for the degree of Doctor  
of Philosophy

Division of Biochemistry and Molecular Biology, IBL  
October 1999

ProQuest Number: 10391208

All rights reserved

INFORMATION TO ALL USERS

The quality of this reproduction is dependent upon the quality of the copy submitted.

In the unlikely event that the author did not send a complete manuscript and there are missing pages, these will be noted. Also, if material had to be removed, a note will indicate the deletion.



ProQuest 10391208

Published by ProQuest LLC (2017). Copyright of the Dissertation is held by the Author.

All rights reserved.

This work is protected against unauthorized copying under Title 17, United States Code  
Microform Edition © ProQuest LLC.

ProQuest LLC.  
789 East Eisenhower Parkway  
P.O. Box 1346  
Ann Arbor, MI 48106 – 1346

GLASGOW  
UNIVERSITY  
LIBRARY

11712 (copy 2)

**'That is a good book which is opened with expectation, and closed with  
delight and profit'**

**Amos Bronson Alcott**

## Acknowledgements

This was probably the hardest page to write, as I didn't want it to turn into an epic Oscar acceptance speech. I'm afraid this was the shortest I could manage.

The first thank you must go to the BBSRC for their funding throughout this PhD and their kind donation which allowed me to participate in a conference in exotic Oxford. Next, a debt of gratitude to Professor Gordon Lindsay, whose enthusiasm, guidance and endless support helped turn many mountains into molehills.

Heather Lindsay; my 'mum-away-from-home'. Your practical and emotional support have been second to none.

Mum, Dad and Andrew; just how do you thank the best and most supportive family anyone could ever ask for?

Nick; for the love you have shown me and for turning my dreams into reality.

The 'Girlies' (you know who you are); for some wonderfully (dis)organised nights out!

Lab C35 past and present; thanks everyone. It's good to know that I'm not the only winner of the 'Dangerous Worker' award.

## **Abstract**

The 2-oxoacid dehydrogenase complexes; pyruvate dehydrogenase (PDC), 2-oxoglutarate dehydrogenase (OGDC) and branch-chain 2-oxoacid dehydrogenase (BCOADC), are mitochondrial multienzyme complexes which comprise of multiple copies of three different enzymes; E1, E2 and E3, that catalyse the oxidative decarboxylation of 2-oxoacids to their respective acyl CoA derivatives. The E2 enzyme forms the structural core, to which several copies of both E1 and E3 are non-covalently bound. Despite being three of the largest known proteins, relatively little is known regarding the interactions between the constituent components. This is due primarily to the flexibility within the complex which makes the generation of large quantities of material difficult.

In this thesis, we have demonstrated the ability to overexpress various subgenes of the complexes in *E. coli*. The first is a sub-gene of the E2-PDC enzyme from various sources and also the corresponding sub-gene of protein X, termed the di-domain. These di-domains, are comprised of the peripheral subunit binding domain and adjacent lipoyl domain. We have shown that the di-domains have retained their ability to fold correctly, by studying their lipoylation state. Their function to bind the E3 enzyme has been demonstrated by surface plasmon resonance. By binding purified E3 enzymes to the surface of a dextran-coated chip and passing crude extracts containing the overexpressed di-domains over the E3, we have determined that the strongest binding affinities were between human E3 and the protein X di-domain, further substantiating the hypothesis that protein X has evolved to bind E3. The binding affinities between E2-PDC and E3 are sufficiently high to suggest that in the absence of competition from E1, E3 may be able to form a stable complex with E2.

The sequences surrounding the lipoylation site, a conserved DKA motif within the lipoyl domain, have been investigated using a monoclonal Ab specific for the lipoylated form of the domain, to determine residues critical for recognition by the lipoylating

enzymes. To date, there has been some ambiguity with regard to the requirements of the lipoylating enzymes to enable lipoylation to occur. We have shown, with the use of lipoyl domain point mutants that the levels of lipoylation can be altered by mutating residues close to the critical lipoyl lysine.

The structure of OGDC has evolved with significant structural differences to PDC and BCOADC. In particular, the E1 component has the ability to interact directly with E3 as well as the E2 core. The N-terminal region of E1 is thought to be important in these interactions. Subsequently we have overexpressed, in *E. coli*, three N-terminal fragments for use as competitive inhibitors of OGDC reconstitution. Despite failing to bind E3, these fragments display inhibition following  $MgCl_2$  dissociation, suggesting interference with E1 binding to the E2 core.

Future work is planned to further investigate the divergent structure and protein-protein interactions of OGDC, along with interactions within the other two complexes. The overexpression and subsequent purification of each individual component should allow progress in this area.

## TABLE OF CONTENTS

	<b>PAGE</b>
<b>Declaration</b>	<b>ii</b>
<b>Quotation</b>	<b>iii</b>
<b>Acknowledgements</b>	<b>iv</b>
<b>Abstract</b>	<b>v</b>
<b>Table of contents</b>	<b>vii</b>
<b>List of figures</b>	<b>xiv</b>
<b>List of tables</b>	<b>xix</b>
<b>Abbreviations</b>	<b>xx</b>
<b>CHAPTER 1      INTRODUCTION</b>	<b>1</b>
<b>THE 2-OXOACID DEHYDROGENASE COMPLEXES.</b>	
1.1            Multienzyme Complexes.	2
1.2            The 2-Oxoacid Dehydrogenase Complexes.	3
1.2.1        General.	3
1.2.2        Quaternary Structure of the 2-Oxoacid Dehydrogenase Complexes.	5
1.3            The E2 Component.	9
1.3.1        Lipoyl Domains.	12
1.3.2        Flexible Linker Sequences.	17
1.3.3        Catalytic Domain.	17
1.3.4        Peripheral Subunit Binding Domain.	18
1.4            Dihydrolipoamide Dehydrogenase (E3) Component.	23
1.4.1        General.	23
1.4.2        Enzymatic reaction of E3.	24
1.5            The E1 Component.	26
1.5.1        General.	26
1.5.2        Enzymatic reaction of E1.	27

1.5.3	Control of E1 via Kinase and Phosphatase activity.	30
1.6	Protein X.	32
1.7	Regulation of 2-Oxoacid Dehydrogenase Complexes.	33
1.8	Physiological diseases associated with the 2-Oxoacid Dehydrogenase Complexes.	35
1.9	Mitochondrial Targeting.	37
1.10	Aims of this thesis.	40
<b>CHAPTER 2</b>	<b>MATERIALS AND METHODS</b>	<b>41</b>
2.1	MATERIALS.	44
2.1.1	Bacterial strains.	44
2.1.2	Bacterial Media.	44
2.1.3	Chemicals.	44
2.1.4	Enzymes.	44
2.1.5	Molecular Size & Weight Markers.	45
2.1.6	Oligonucleotides.	45
2.1.7	Photographic Materials.	45
2.1.8	Plasmid Vectors.	45
2.2	METHODS.	48
2.2.1	Determination of protein concentration.	48
2.2.2	Dialysis of protein samples.	48
2.2.3	Concentration of protein samples.	48
2.2.4	The Polymerase Chain Reaction (PCR) of the Di- domain.	48
2.2.5	The Polymerase Chain Reaction (PCR) of the E1-OGDC N-terminus.	50
2.2.6	Agarose gel electrophoresis.	50
2.2.7	DNA isolation from agarose gels.	51
2.2.8	Restriction Digests:	51

2.2.8.1	pET11a digestion with Nde I and Bam HI.	51
2.2.8.2	Di-domain PCR product with Nde I and BamHI.	51
2.2.8.3	E1-OGDC N-terminus PCR product with Bam HI.	52
2.2.8.4	pGEX-2T with Bam HI.	52
2.2.9	Ligations	52
2.2.9.1	Di-domain with pET11a vector.	52
2.2.9.2	E1-OGDC N-terminal fragments with pGEX-2T vector.	52
2.2.10	Preparation and transformation of <i>E. coli</i>	52
2.2.11	Isolation of plasmid DNA.	53
2.2.12	Preparation of supercompetent <i>E. coli</i> DE3plysS.	53
2.2.13	Overexpression of heterologous protein.	54
2.2.14	Large-scale overexpression of heterologous protein.	54
2.2.15	Large-scale preparation of bacterial PDC and E3.	54
2.2.16	SDS-Polyacrylamide Gel Electrophoresis.	55
2.2.16.1	Buffers used in the SDS-PAGE system.	56
2.2.17	Native Gel Electrophoresis.	56
2.2.17.1	Buffers used in Native Gel Electrophoresis.	57
2.2.18	Western Blotting and Immunological Detection of Proteins by Enhanced Chemiluminescence.	57
2.2.18.1	Buffers used in the ECL Western Blotting system.	58
2.2.19	GST-fusion Protein Purification.	59
2.2.19.1	Buffers used in the GST-fusion protein purification.	59
2.2.20	Surface Plasmon Resonance.	59
2.2.21	Isolation of PDC and OGDC from bovine heart mitochondria.	60

2.2.22	Preparation and purification of E3 from human OGDC.	61
2.2.23	Enzyme Assays.	62
2.2.23.1	2-Oxoacid Dehydrogenase Complexes.	62
2.2.23.2	Dihydrolipoamide Dehydrogenase (E3).	62

**CHAPTER 3 AMPLIFICATION AND EXPRESSION OF THE INNER  
LIPOYL AND ADJACENT PERIPHERAL ENZYME  
BINDING DOMAINS OF THE PROTEIN X AND E2  
COMPONENTS OF HUMAN PDC, BOVINE BCOADC  
AND *E. COLI* PDC.**

3.1	Introduction.	65
3.2	Materials.	67
3.3	Aims of this chapter.	72
3.4	Results.	72
3.4.1	Construction of di-domain DNA.	72
3.4.2	Construction of pET11a expression vector.	72
3.4.3	Overexpression of vector in <i>E. coli</i> DE3 (BL21)	75
3.4.4	Confirmation of correct folding of the di-domain	75
3.4.5	Enhancement of Lipoylation using exogenous Lipoic Acid.	84
3.5	Conclusions.	85
3.6	The effect of the presence of the mitochondrial presequence on the ability of the BCOADC di-domain to undergo lipoylation.	88
3.6.1	Construction of BCOADC sub-gene: presequence-di-domain.	88

3.6.2	Overexpression of BCOADC presequence-di-domain construct.	89
3.7	The effect of the presequence on the lipoylation of the di-domain, as shown by Western blotting.	89
3.8	Discussion.	92
<b>CHAPTER 4</b>	<b>INVESTIGATION INTO THE LIPOYLATION OF THE INNER APODOMAIN OF THE E2 COMPONENT AND THE PROTEIN X COMPONENT OF THE 2-OXOACID DEHYDROGENASE COMPLEXES.</b>	<b>93</b>
4.1	Introduction.	94
4.2	Initial lipoylation studies on the E2 component.	94
4.3	The <i>E. coli</i> system of lipoylation.	95
4.4	Lipoylation of mammalian E2.	96
4.5	Structure of lipoyl domains.	98
4.6	Aims of this chapter.	100
4.7	Materials and Methods.	100
4.8	Results.	100
4.8.1	Investigation into the lipoylation state of the PDC and OGDC complexes and also subgenes using the monoclonal antibody, PD1.	100
4.8.2	Sequence comparison around the attachment site of the lipoic acid moiety of the E2 and protein X.	101
4.8.3	Overexpression and subsequent purification of mutant human lipoyl domains.	105
4.8.4	Confirmation of lipoylation of mutant domains and recognition by monoclonal antibody PD1.	107

4.8.4.1	Western blot analysis of lipoyl domain mutants.	112
4.8.4.2	Native gel electrophoresis of lipoyl domain mutants.	112
4.9	Discussion and Conclusions.	116
4.9.1	Lipoylation states of intact complexes and subgenes.	116
4.9.2	Overexpression and purification of human lipoyl domain mutants.	117
4.9.3	Lipoylation of mutant lipoyl domains.	117
4.10	Concluding remarks.	120

**CHAPTER 5                    OVEREXPRESSION OF THE N-TERMINAL REGION OF THE E1 COMPONENT OF HUMAN OGDC AND COMPETITION STUDIES FOR BINDING OF THE E3 ENZYME AGAINST OGDC.**

5.1	Introduction.	122
5.2	Materials.	125
5.3	Methods.	125
5.4	Aims of this Chapter.	126
5.5	Polymerase Chain Reaction (PCR) of the E1-OGDC N-terminus.	126
5.6	Results.	127

**PART I**

5.6.1	PCR amplification of N-terminal fragments of E1-OGDC.	127
5.6.2	Construction of recombinant plasmid.	127
5.6.3	Overexpression of N-terminal fragments of E1-OGDC.	127
5.6.4	Purification of N-terminal fragments of E1-OGDC.	129

## PART 2

5.7	Competition studies using N-terminal fragments as inhibitors of OGDC reconstitution.	129
5.7.1	Dissociation of native OGDC using 1M NaCl.	129
5.7.2	Dissociation of native OGDC using 1M MgCl <sub>2</sub> .	132
5.8	Discussion.	138
5.8.1	Overexpression and purification of N-terminal fragments.	138
5.8.2	Dissociation of native OGDC.	138
5.8.3	Reconstitution of native OGDC.	140

## **CHAPTER 6 BIACORE STUDIES OF BINDING INTERACTIONS BETWEEN THE DI-DOMAINS OF PROTEIN X AND E2- PDC AND E3 ENZYME FROM VARIOUS SOURCES.**

6.1	Introduction.	144
6.2	Aims of the chapter.	147
6.3	Results	147
6.3.1	Immobilisation of E3 from various sources onto the CM5 sensor chip.	147
6.3.2	Interaction between the di-domains from protein X and E2-PDC with the immobilised E3 samples.	152
6.3.3	Interaction between full-length protein X and E2-PDC with the immobilised E3 samples.	157
6.4	Discussion.	159

## **GENERAL DISCUSSION** 164

## **BIBLIOGRAPHY** 168

## LIST OF FIGURES.

### CHAPTER 1

Figure 1.1	Metabolic Locations of the Mitochondrial 2-Oxoacid Dehydrogenase Complexes.	4
Figure 1.2	Reaction Scheme for the Oxidative Decarboxylation of the 2-Oxoacids by their Respective 2-Oxoacid Dehydrogenase Complex.	7
Figure 1.3	Schematic Representation of the Multidomain Structure of E2 and protein X.	10
Figure 1.4	Three-dimensional structure of the lipoyl domain from <i>B. stearothermophilus</i> PDC.	13
Figure 1.5	Structures of Lipoate and Octanoate.	15
Figure 1.6	Schematic representation of the organisation of the catalytic domain of CAT and E2p.	19
Figure 1.7	The E3-binding domain from the E2 core of the <i>E. coli</i> OGDC complex.	20
Figure 1.8	Electrostatic zipper formed between the E3 and E2 binding domain of <i>B. stearothermophilus</i> .	22
Figure 1.9	Schematic representation of the mechanism of dihydrolipoamide dehydrogenase (E3).	25
Figure 1.10	The catalytic mechanism of E1.	28
Figure 1.11	Two suggested mechanisms for the reductive transfer of the acetyl group onto the lipoyl moiety of the E2 lipoyl domain.	29
Figure 1.12	The regulation of mammalian PDC through the phosphorylation-dephosphorylation cycle.	34
<b>CHAPTER 2</b>		
Figure 2.1	Map of expression vector pET11a.	46

Figure 2.2	Map of the glutathione S-transferase fusion vector pGEX-2T.	47
------------	---	----

### CHAPTER 3

Figure 3.1	Schematic representation of the multidomain structure of E2 and protein X.	66
Figure 3.2a	The protein sequence of mammalian Pyruvate Dehydrogenase Complex E2.	68
Figure 3.2b	The protein sequence of E2-BCOADC gene.	69
Figure 3.2c	The protein sequence of the accF gene.	70
Figure 3.2d	The protein sequence of human protein X.	71
Figure 3.3	Primer sequences to allow the amplification of the di-domain from the E2 and protein X sources.	73
Figure 3.4	PCR amplification of the di-domain (DD) from various sources.	74
Figure 3.5a	Overexpression of the di-domain of human PDC, in <i>E. coli</i> DE3.	76
Figure 3.5b	Overexpression of bovine BCOADC di-domain.	77
Figure 3.5c	Overexpression of <i>E. coli</i> PDC di-domain.	78
Figure 3.5d	Overexpression of mammalian protein X di-domain.	79
Figure 3.6a	SDS-PAGE analysis of purified apo- and holo-lipoyl domain from human PDC.	80
Figure 3.6b	Immunoblot of apo- and holo-forms of the lipoyl domain.	81
Figure 3.7	Immunoblot of the di-domains of PDC and BCOADC E2 induced in the presence or absence of exogenous lipoic acid.	82
Figure 3.8	Immunoblot analysis of the di-domain of protein X, showing enhancement of lipoylation, in the presence	

	of exogenous lipoic acid.	<b>83</b>
Figure 3.9	Immunoblot on a native gel of the di-domain of PDC, showing the enhancement of lipoylation as a result of exogenous lipoic acid.	<b>86</b>
Figure 3.10	SDS-PAGE analysis of human protein X di-domain overexpression in <i>E. coli</i> DE3pLysS, in the absence and presence of exogenous lipoic acid.	<b>87</b>
Figure 3.11	Overexpression of BCOADC di-domain; comparison with clones overexpressing the di-domain plus the presequence.	<b>90</b>
Figure 3.12	Immunoblot of BCOADC di-domain, alongside the presequence-di-domain constructs using the lipoyl-specific monoclonal antibody, PD1.	<b>91</b>
 <b>CHAPTER 4</b>		
Figure 4.1	SDS-PAGE analysis of PDC and OGDC purified from bovine heart.	<b>102</b>
Figure 4.2	Western blot analysis of bovine PDC and OGDC, using a monoclonal antiserum specific for the lipoylated form of E2-PDC.	<b>103</b>
Figure 4.3	Western blot analysis of the PDC, BCOADC and protein X di-domains, blotting with antisera specific to the holodomains.	<b>104</b>
Figure 4.4	Features of pGEX vectors.	<b>106</b>
Figure 4.5	Overexpression of mutant forms of the lipoyl domain from human PDC, in <i>E. coli</i> DE3pLysS.	<b>108</b>
Figure 4.6	Overview of Glutathione Sepharose 4B column.	<b>109</b>
Figure 4.7	Purification of a mutant lipoyl domain-GST-fusion	

	protein by affinity chromatography on Glutathione Sepharose 4B.	<b>110</b>
Figure 4.8	Coomassie Blue-stained gel of the final purified mutant lipoyl domain proteins.	<b>111</b>
Figure 4.9	Western Blot of the lipoyl domain mutants induced in the presence or absence of exogenous lipoic acid.	<b>113</b>
Figure 4.10	Thrombin cleavage of GST-fusion proteins.	<b>114</b>
Figure 4.11	Native gel electrophoresis of the purified lipoyl domain mutants, following thrombin cleavage.	<b>115</b>
 <b>CHAPTER 5</b>		
Figure 5.1	Schematic representation of E1-OGDC.	<b>123</b>
Figure 5.2	Agarose gel showing the result of the PCR amplification of three N-terminal fragments of E1-OGDC.	<b>128</b>
Figure 5.3	SDS-PAGE analysis of the overexpression of the N-terminal fragments of E1-OGDC.	<b>130</b>
Figure 5.4	Purification profile of OGDC-60, purified as a GST-fusion protein on a Glutathione Sepharose 4B column.	<b>131</b>
Figure 5.5	Reconstitution of native OGDC in the absence and presence of the E1-OGDC N-terminal fragments.	<b>133</b>
Figure 5.6a	Reconstitution of native OGDC in the presence of OGDC-60, following dissociation in 1M MgCl <sub>2</sub> .	<b>135</b>
Figure 5.6b	Reconstitution of native OGDC in the presence of OGDC-110, following dissociation in 1M MgCl <sub>2</sub> .	<b>136</b>
Figure 5.6c	Reconstitution of native OGDC in the presence of OGDC-110, following dissociation in 1M MgCl <sub>2</sub> .	<b>137</b>

## CHAPTER 6

Figure 6.1	Elution profile obtained for the purification of the E3 enzyme from human OGDC complex, using the BioCAD sprint Perfusion Chromatography system.	148
Figure 6.2	Coomassie Blue-stained SDS-PAGE demonstrating the final step in the purification of the E3 from human OGDC.	149
Figure 6.3	Theoretical sensorgram.	151
Figure 6.4a	Immobilisation of human E3 to a CM5 sensor chip.	153
Figure 6.4b	Immobilisation of porcine E3 to a CM5 sensor chip.	154
Figure 6.4c	Immobilisation of yeast E3 to a CM5 sensor chip.	155

## LIST OF TABLES

### CHAPTER 1

Table 1.1	Enzyme Components of the 2-Oxoacid Multienzyme Complexes.	6
-----------	--	---

### CHAPTER 6

Table 6.1A	Rate and affinity constants for the protein X di-domain interacting with the immobilised E3 enzymes.	156
Table 6.1B	Rate and affinity constants for the E2-PDC di-domain interacting with the immobilised E3 enzymes.	156
Table 6.2A	Rate and affinity constants for full-length protein X interacting with the immobilised E3 enzymes.	158
Table 6.2B	Rate and affinity constants for full-length E2-PDC interacting with the immobilised E3 enzymes.	158

## ABBREVIATIONS

In addition to the abbreviations recommended (Instructions to authors, *Biochem. J.* (1992) **281**, 1-19), the following were used throughout this thesis.

Amp.	ampicillin
approx.	approximately
APS	ammonium persulphate
BCOADC	branched chain amino acid 2-oxoacid dehydrogenase complex
BSA	bovine serum albumin
CAT	chloramphenicol acetyltransferase
Da	daltons
DHL	dihydrolipoamide
DTT	dithiothreitol
DYT	dextrose, yeast, tryptone medium
E1	2-oxoacid dehydrogenase (decarboxylase)
E2	dihydrolipoamide acyltransferase
E3	dihydrolipoamide dehydrogenase
EDC	N-ethyl-N'- (3-dimethylaminopropyl) carbodiimide hydrochloride
EDTA	ethylenediaminetetra-acetic acid
ECL	enhanced chemiluminescence
GST	glutathione S-transferase
LB	Luria broth
Lipoamide	6,8-thioctic acid amide
LMP	low melting point
min	minutes
NHS	N-hydroxysuccinimide
OGDC	2-oxoglutarate dehydrogenase complex
PAGE	polyacrylamide gel electrophoresis
PBS	phosphate buffered saline

PCR	polymerase chain reaction
PDC	pyruvate dehydrogenase complex
PEG	polyethylene glycol
PMSF	phenylmethylsulphonyl fluoride
SDS	sodium dodecyl sulphate
TCA cycle	tricarboxylic acid cycle
TEMED	NNN'N'-tetramethylethylenediamine
ThDP	thiamine pyrophosphate
Tricine	N-tris[hydroxymethyl]methylglycine;N-[2-hydroxy-1,1-bis(hydroxymethyl)ethyl]glycine
Tris	2-amino-2-(hydroxymethyl)-1,3-propanediol
Tween 20	polyethylenesorbitan monolaurate
UV	ultraviolet
v/v	volume to volume
w/v	weight to volume

# INTRODUCTION

## The 2-Oxoacid Dehydrogenase Complexes

### 1.1 Multienzyme complexes

In order to maximise catalytic efficiency in metabolic pathways, enzymatic components are often coupled or complexed together. One means of clustering different enzyme functions is to assemble the polypeptide chains into complexes held together by non-covalent bonds. As well as enhancing complex activity, this also has the advantages of allowing substrate channelling and giving protection to reaction intermediates, which may be unstable.

The close proximity of each component enzyme and the substrate channelling act to increase local intermediate concentration, thus decreasing the effects of diffusion. Efficiency is further enhanced by the closeness of the active sites. Transfer of substrates between them is quicker and often carried out by flexible prosthetic groups, acting as "swinging arms" (Reed 1974).

Protein-protein interactions within a multienzyme complex can also enhance overall activity. Many enzymes are only active in an oligomeric form because residues from more than one monomer are required to form the active site. This is the case for the dihydrolipoamide dehydrogenase (E3) enzyme of the 2-oxoacid dehydrogenase complexes. A further advantage of a multienzyme complex is the speed at which regulatory control can be established. Many complexes have permanent or transient associations with regulatory enzymes such as kinases and phosphatases which enable rapid modulation of complex activity.

In the scope of this work, a family of multienzyme complexes called the 2-oxoacid dehydrogenases has been studied, which display many of the above mentioned

properties and serve as paradigms for the analysis of structure-function relationships in complex multimeric assemblies.

## 1.2. The 2-oxoacid dehydrogenase complexes

### 1.2.1. General

Loosely associated with the inner mitochondrial membrane is located a family of multienzyme complexes known as the 2-oxoacid dehydrogenase complexes. There are three principal members; pyruvate dehydrogenase (PDC), 2-oxoglutarate dehydrogenase (OGDC) and the branched chain amino acid 2-oxoacid dehydrogenase (BCOADC), each occupying a key position in intermediary metabolism.

The complexes consist of multiple copies of three distinct enzymes; E1, E2 and E3, (Table 1.1) which catalyse the lipoic acid-mediated oxidative decarboxylation of 2-oxoacids to their respective acyl CoA derivatives (reviewed in Perham, 1991). PDC converts pyruvate to acetyl CoA, CO<sub>2</sub> and NADH, an irreversible step in carbohydrate metabolism. The acetyl CoA is channelled either into the TCA cycle or used in the synthesis of compounds such as fatty acids, steroids and cholesterol. OGDC catalyses the oxidative decarboxylation of 2-oxoglutarate to succinyl CoA and is important in controlling flux through the TCA cycle. BCOADC is responsible for the committed steps in the degradation of the branched chain 2-oxoacids derived from valine, leucine and isoleucine, namely 2-oxo-valeric acid, 2-oxo-isocaproic acid and 2-oxo-3-methyl-valeric acid respectively, to produce the appropriate acyl CoA. Figure 1.1 illustrates the key metabolic steps controlled by these multienzyme complexes within the mitochondrial compartment.

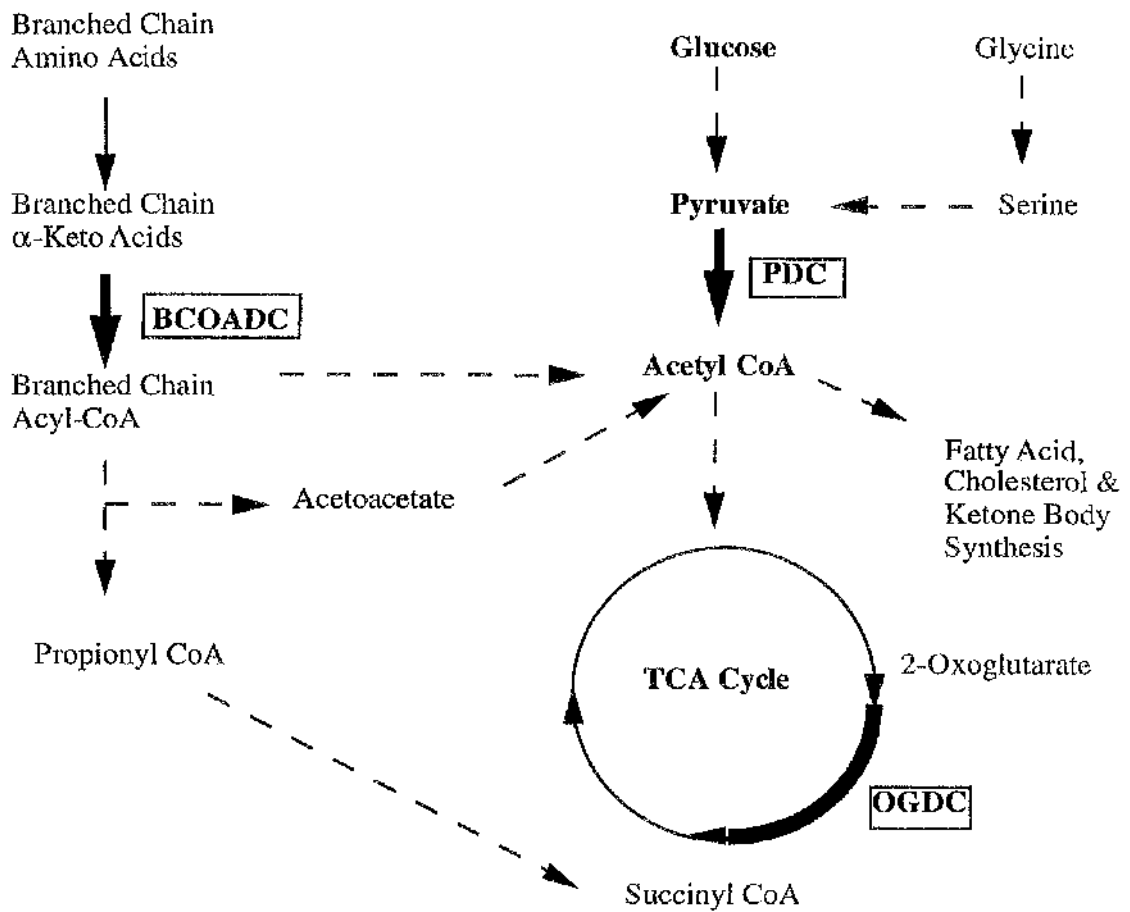


**Figure 1.1 Metabolic Locations of the Mitochondrial 2-Oxoacid Dehydrogenase Complexes.**

The E1 and E2 enzymes are complex-specific; however, in mammals the E3 component (dihydrolipoamide dehydrogenase) appears to be common to all three complexes (Table 1.1). The overall reaction catalysed by these three enzymes is outlined in Figure 1.2. The E1 enzyme catalyses i) the irreversible decarboxylation of the 2-oxoacid to a ThDP-linked intermediate (Frey *et al.*, 1989) and ii) the subsequent reductive acylation of the lipoyl moiety of E2 (Figure 1.2, reactions 1 & 2). The lipoyl group is reductively acylated, generating an 8 S-acyldihydrolipoamide intermediate. Acyl transfer can occur to produce S<sup>6</sup> isomers, but this does not normally occur during *in vivo* catalysis (Yang & Frey, 1986). E2 subsequently transfers the acyl CoA, leaving the lipoic acid in its reduced state (reaction 3). E3 then reoxidises the dihydrolipoyl group using its FAD co-factor (reaction 4) to generate NADH (reaction 5) as the final electron acceptor.

### 1.2.2. Quaternary structure of the 2-oxoacid dehydrogenase complexes

Each complex is organised around a core of E2 polypeptides, to which multiple copies of E1 and E3 are bound by non-covalent bonds. Two polyhedral forms of E2 cores have been observed using electron microscopy; the cube and the pentagonal dodecahedron (Oliver & Reed, 1982). The former design is common to Gram negative bacteria such as *E. coli*. (Reed, 1974) and *Azotobacter vinelandii* (Hanemaijer *et al.*, 1989) and the OGDC and BCOADC of eukaryotic organisms. They exhibit a core with 24 identical E2 subunits arranged with octahedral (432) symmetry (Oliver & Reed, 1982). These subunits are grouped in threes about the eight vertices of the cube. The latter design consists of 60 E2 subunits arranged with icosahedral (532) symmetry, again in groups of three about the 20 vertices of the pentagonal dodecahedron. This structure is found in PDC from the Gram positive bacteria *Bacillus stearothermophilus* (Henderson & Perham, 1980), *Bacillus subtilis* (Lowc *et al.*, 1983) the yeast *Saccharomyces cerevisiae* (Keha *et al.*, 1982; Stoops *et al.*, 1992) and mammals (Reed, 1974).

Complex Enzyme	PDC	OGDC	BCOADC
E1	E1p EC 1.2.4.1 Pyruvate Dehydrogenase	E1o EC 1.2.4.2 2-Oxoglutarate Dehydrogenase	E1b EC 1.2.4.4 Branched-chain 2-Oxoacid Dehydrogenase
E2	E2p EC 2.3.1.12 Dihydrolipoamide Acetyltransferase	E2o EC 2.3.1.16 Dihydrolipoamide Succinyltransferase	E2b Dihydrolipoamide Acyltransferase
E3	E3 EC 1.8.1.4 Dihydrolipoamide Dehydrogenase		

**Table 1.1.**

**Enzyme Components of the 2-Oxoacid Dehydrogenase Multienzyme Complexes.**

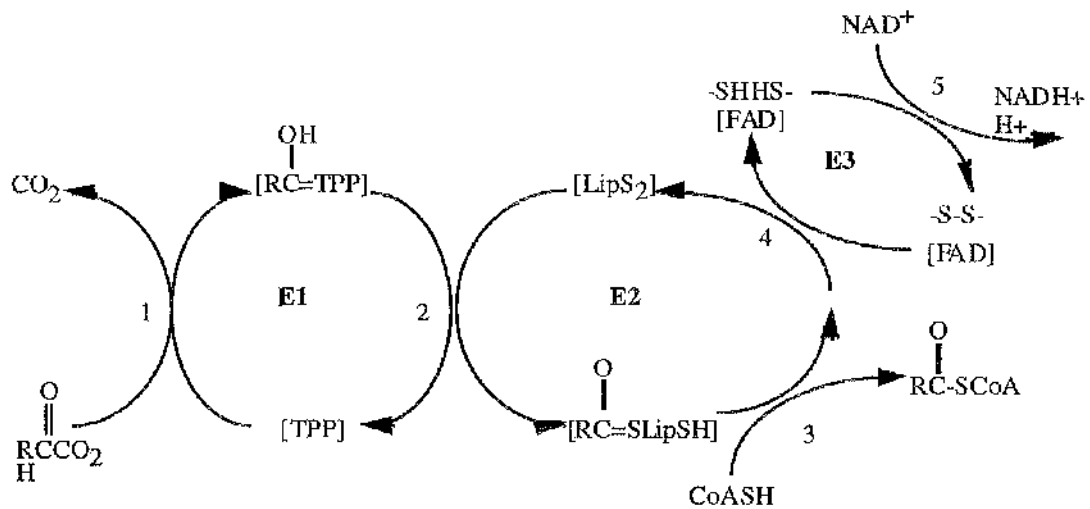


**Figure 1.2 Reaction Scheme for the Oxidative Decarboxylation of the 2-Oxoacids by their Respective 2-Oxoacid Dehydrogenase Complex.**

The numbers 1 to 5 represent the 5 reactions as detailed in the text. Abbreviations:

E1, E2 & E3 are the three enzymatic components of the multienzyme complexes, ThDP, thiamine diphosphate; LipS<sub>2</sub> & Lip(SH<sub>2</sub>); oxidised & reduced forms of the lipoyl moiety attached to E2; CoASH; Coenzyme A; FAD, flavin adenine dinucleotide; NAD<sup>+</sup> & NADH, oxidised & reduced forms of nicotinamide adenine dinucleotide.

(Adapted from Reed & Yeaman, 1987).

The 2-oxoacid dehydrogenase multienzyme complexes are among the largest enzymes known, with molecular masses of  $4 \times 10^6$ - $1 \times 10^7$  Da. Early electron microscopy studies (Oliver & Reed, 1982) suggested the complexes to be between 30 and 40nm in diameter, but recent work using cryoelectron microscopy suggests a value of at least 50nm (Wagenknecht *et al.*, 1991). The difference is thought to be caused by the dehydration associated with the negative staining process.

STEM imaging (scanning electron transmission electron microscopy) of bovine BCOADC has confirmed the cube (octahedral) model (Hackert *et al.*, 1989) and also shown the lipoyl domains of the *E. coli* core to be very mobile and cover an area with a radius of 17-18nm. This has also been shown by NMR (Green *et al.*, 1995). These lipoyl domains protrude to overlap with the E1 and E3 subunits (Hale *et al.*, 1992).

X-ray crystallography studies (Fuller *et al.*, 1979) suggest that homodimers (in *E. coli*) of E1, associate along the 12 edges of the octahedral core, whilst six homodimers of E3 associate along the faces. In icosahedral complexes, E1  $\alpha_2\beta_2$  tetramers and E3 dimers are thought to bind near the 30 edges and 12 faces respectively (Barrera *et al.*, 1972), but the exact ratios vary from one organism to another (Reed, 1974; Henderson & Perham, 1980).

The E1, E2 and E3 components are all required for catalysis, but not in a 1:1:1 stoichiometry. De Kok and Westphal (1985) reported the optimum binding stoichiometry of *E. coli* E1/E2 and E3/E2 to be 2:1 and 2.5:1 respectively, in PDC. Yang *et al.* (1985) showed purification of PDC to yield the ratio 1:1:0.5 (E1:E2:E3). The variation was initially thought to reflect binding competition between E1 and E3 for their respective binding sites. This has now been confirmed by Lessard *et al.* (1996).

In addition to the E1 and E3 enzymes, a further component known as protein X (E3-binding protein) has been identified in mammalian and yeast PDC (De Marcucci &

Lindsay, 1985; De Marcucci *et al.*, 1985; Jilka *et al.*, 1986; Behal *et al.*, 1989), which tightly associated with the E2 core as well as exhibiting structural and functional homology to this component.

A final pair of enzymes associated with the E2 core is a kinase and a phosphatase (Reed & Yeaman, 1987), the former being tightly bound whereas the latter interacts only loosely. These enzymes are involved in the overall regulation of the complexes. Phosphorylation causes complete inactivation, preventing breakdown of essential amino acids. Recent evidence now suggests that there are in fact four separate kinases, showing tissue specific expression (Popov *et al.*, 1993; Popov *et al.*, 1994; Popov *et al.*, 1995; Rowles *et al.*, 1996; Popov *et al.*, 1997).

### 1.3. The E2 Component

The E2 component of the 2-oxoacid dehydrogenase complexes plays a central role in the structure, assembly and catalytic activity of the complex. As mentioned above, it forms the symmetrical core about which the complex is assembled; it also provides the attachment site for the lipoic acid moiety, servicing the various active sites in addition to catalysing the formation of an acyl CoA product.

Initial structural characterisation was performed by Bleile *et al.* (1979) using limited tryptic digestion of the E2p protein from *E. coli*. They revealed a unique multidomain structure capable of independent folding and joined by flexible polypeptide linker segments (Figure 1.3). Under controlled conditions, the E2p protein yielded a structural domain consisting of the subunit binding and catalytic domains and a further extended region carrying the lipoic acid moieties. Limited chymotryptic cleavage of the E2p core of *B. stearothermophilus* (Packman *et al.*, 1988; Borges *et al.*, 1990) causes the release of its lipoyl domain leaving peptide chains of 45kDa. Further digestion with trypsin promotes the release of the E1 and E3 components previously bound to the peripheral subunit binding domain.

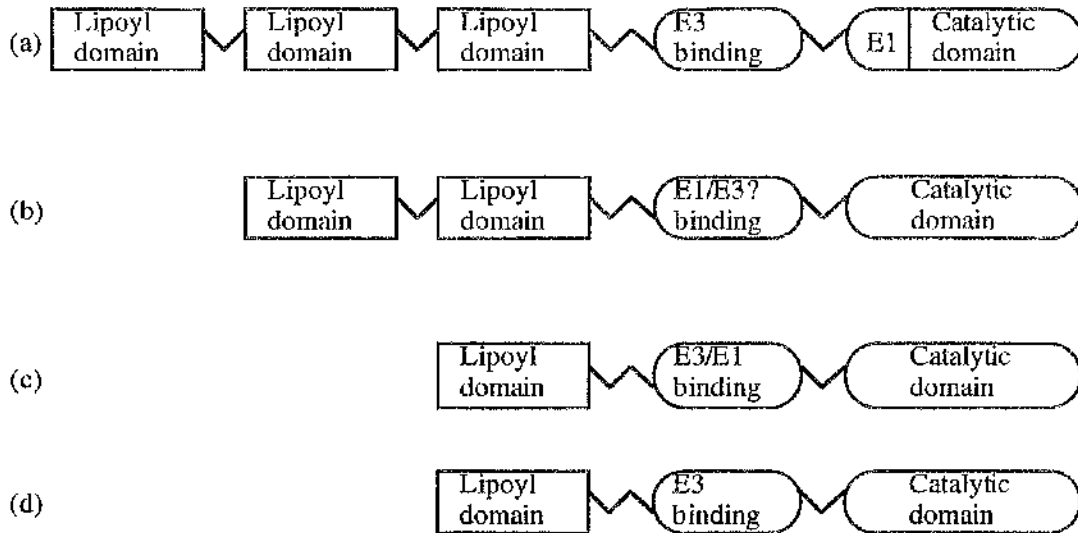


**Figure 1.3. Schematic Representation of the Multidomain Structure of E2 and Protein X**

- (a) *E. coli* PDC  
*A. vinelandii* PDC
- (b) Mammalian PDC  
*S. faecalis* PDC
- (c) Mammalian BCOADC  
Gram +ve bacteria
- (d) Protein X of mammals and yeast

Each domain is separated by linker regions (zig-zag lines). Subunit binding specificity is indicated as E1 and/or E3.

Additional limited proteolysis studies on the E2p and E2o from *E. coli* and other sources (Bicile *et al.*, 1981; Hale & Perham, 1979; Packman & Perham, 1986, 1987; Komuniccki *et al.*, 1992) have further substantiated similar multidomain structures and have also revealed that the number of lipoyl domains varies from one to three depending on both complex type and species. Each E2p of *E. coli* was shown to contain three lipoyl domains (Hale & Perham, 1979), following growth in the presence of [<sup>35</sup>S]-sulphate. Subsequent elucidation of the *E. coli* *aceF* gene sequence encoding the E2p polypeptide, showed 3 homologous domains arranged in tandem, each containing a conserved lysine residue which was capable of lipoylation (Stephens *et al.*, 1983).

These lipoyl domains, approx. 80 amino acids in length, are located in the N-terminal region of the E2 chain. They are joined by flexible linker regions of 25-30 amino acids, rich in proline and alanine residues. Miles *et al.* (1988) demonstrated that the mobility provided by the linkers is essential for complex activity by providing the lipoyl domain with freedom to interact with all the active sites.

Studies suggest that each lipoyl domain has the ability to fold independently and support overall catalysis (Graham *et al.*, 1986). Bates *et al.* (1977) proposed a mechanism of catalysis called "active site coupling", whereby acyl groups are transferred between the lipoic acid groups on different E2 polypeptide chains within an E2 core and that more than one lipoyl domain could interact with any E1 active site.

Arranged at the C-terminal end of the lipoyl domain(s) is the peripheral subunit binding domain of approximately 50 amino acids, which has the ability to bind E3 and/or E1 (source-dependent). In *E. coli* and *B. subtilis* PDC for example, both E1 and E3 components compete for the binding region, although, in the case of Gram negative organisms at least part of the site of E1 interaction is situated within the C-terminal core (see figure 1.3).

A 29kDa C-terminal domain (catalytic domain) is joined to the binding domain by a flexible linker peptide. It acts as the active site for the acetyltransferase reaction and is also involved in core assembly.

### 1.3.1. Lipoyl Domains

Lipoic acid is attached to a specific lysine residue via an amide linkage within each lipoyl domain. This residue provides the "swinging arm", allowing movement between the active sites of the complex. The attachment of the lipoic acid moiety to the mature domain seems to be essential for the reductive acetylation by the E1 enzyme as it has been demonstrated that free lipoic acid, lipoamide and also a lipoylated synthetic decapeptide are poor substrates (Graham *et al.*, 1989).

There is a poorly defined molecular recognition process occurring between the lipoyl domain and its cognate E1. The lipoyl domains from *E. coli* E2p and E2o can only act as substrates for E1p and E1o respectively (Graham *et al.*, 1989). This specificity provides a potent means of substrate channelling.

As previously mentioned, the number of lipoyl domains varies between species and even complex within the same species. The number does not correlate directly with the core symmetry (cubic versus dodecahedral). *E. coli* and *A. vinelandii* PDC have three domains per E2p chain, mammalian PDC and *S. faecalis* PDC have two and *B. stearothersophilus* (Figure 1.4) and yeast have only one. All OGDCs and BCOADCs carry one lipoyl domain per E2.

Guest *et al.* (1985) showed that *E. coli* PDC is fully catalytically active and capable of complex assembly when two of their three lipoyl domains are deleted. However, activity is lost when all three are removed or when the lipoylated lysine residue of a 'one lip E2p' is mutated to glutamine (Ali & Guest, 1990). Additional studies by Allen

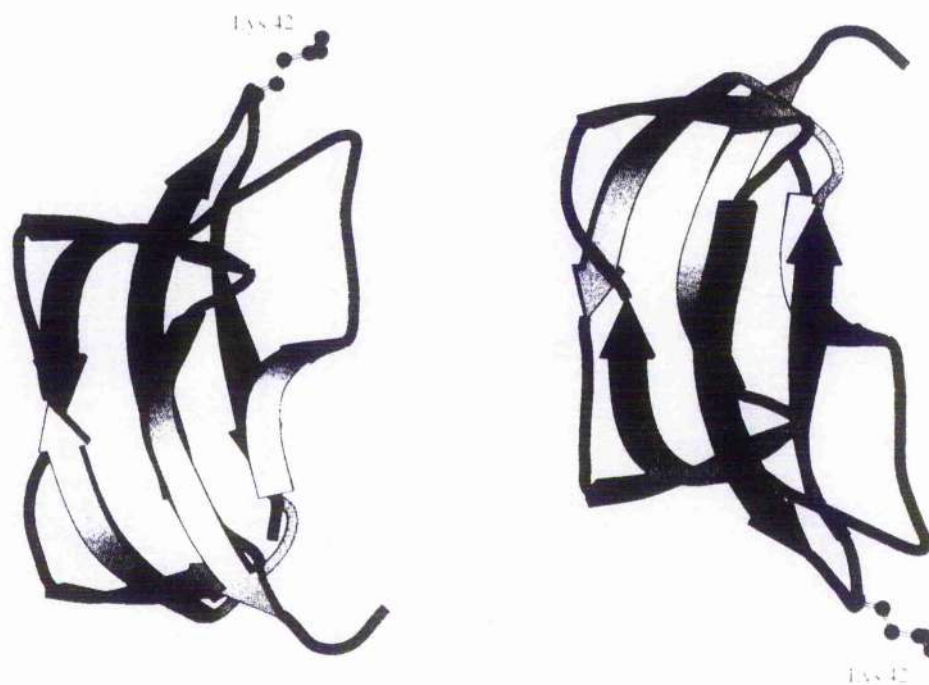


**Figure 1.4. Three-dimensional structure of the lipoyl domain from *B. stearothermophilus* PDC.**

The position of the lipoyl-lysine residue is shown, forming part of the exposed loop. The structure was taken from Wallis (1996) and was prepared using the programme MOLSCRIPT (Kraulis, 1991).

(1989) showed that each of the *E. coli* lipoyl domains is capable of independent functioning. Experiments by Machado (1993) demonstrated that the E3 binding domain of the three-lipoyl domain constructs show increased mobility compared to those with 1, 2 or 4 to 9 domains, suggesting the reason for the presence of three. This fails, however, to explain why other species function fully with one or no superfluous domains.

Until recently, little was known about the enzyme(s) responsible for the attachment of lipoic acid. The study of lipoate attachment has been enhanced by the creation of *E. coli* strains capable of overexpressing subgenes containing the lipoyl domain from *B. stearothersophilus* (Dardel *et al.*, 1990). Three forms were present upon purification; lipoylated (16%), unlipoylated (80%) and octanoylated (4%) (Fujiwara, 1992). As octanoic acid is a potential lipoic acid precursor (Figure 1.5), it remains unclear whether the octanoylated domain is a genuine reaction intermediate or whether it accumulates because of the limiting levels of lipoic acid in the culture medium.

Two lipoyl ligase enzymes lplA and lplB were described in *E. coli* by Brookfield *et al.* (1991) and initially by Reed (1958). They have the ability to activate lipoyl-deficient PDC complexes with the additional requirement of ATP and  $Mg^{2+}$ , using L-lipoate and lipoyl adenylate as substrates. LplB could also use octanoate as a further substrate, suggesting it could be responsible for the octanoylation of holo-lipoyl domain. More recently, two further enzymes have been characterised from *E. coli* (LipA and LipB), which are thought to play a role in lipoic acid synthesis and metabolism (Reed & Cronan, 1993). LipA is thought to add the first sulphur to octanoate. This is supported by its similar amino acid sequence to biotin synthase which catalyses the incorporation of sulphur into a biotin group (Hayden *et al.*, 1992). LipB seems to be involved in the process of actual lipoylation. It is possible to increase the degree of lipoylation by the *E. coli* enzymes by adding exogenous lipoate to culture media (see chapter 3). This further

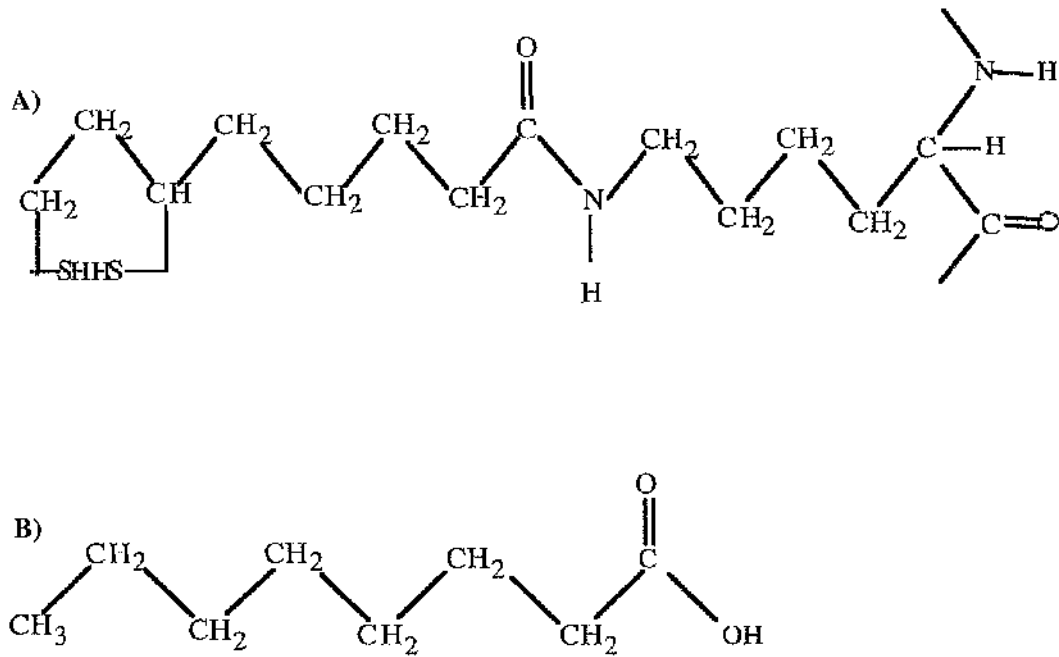


**Figure 1.5 Comparison of the Structures of A) Lipoate and B) Octanoic Acid.**

A) The lipoate moiety is shown attached to the specific lysine residue via an amide linkage

B) Octanoic acid is one of the precursor molecules of lipoic acid, before the addition of two sulphurs.

suggests that endogenous levels of lipoic acid act as the rate-limiting factor in lipoylation.

Little is known about the mechanism of lipoylation in mammals. It has been shown to occur within the mitochondrion (Griffin & Chuang, 1990; Fujiwara *et al.*, 1990). Mammalian lipoyl lipase has been partially purified from bovine liver mitochondria (Fujiwara *et al.*, 1992) and found to be unable to use free lipoic acid with ATP *i.e.* it is unable to activate lipoic acid to lipoyl adenylate. This infers that two separate enzyme-catalysed reactions may be required for lipoic acid attachment in mammals.

Both  $^1\text{H}$ - and  $^{15}\text{N}$ -NMR spectroscopy were used to determine the secondary structures of *B. stearrowthermophilus* and *A. vinelandii* lipoyl domains (Dardel *et al.*, 1991; Berg *et al.*, 1994). The former technique was able to show that the conformations of lipoylated and unlipoylated domains were identical.

The complete three dimensional structures of *B. stearrowthermophilus* (Dardel *et al.*, 1993) and *E. coli* (Green *et al.*, 1995) lipoyl domains have been elucidated, showing two 4-stranded  $\beta$ -sheets forming a flattened  $\beta$ -barrel around a hydrophobic core. These two sheets are related by a quasi 2-fold symmetry. The N and C termini are close together in space at the opposite end of the domain to the lipoyl-lysine. The polypeptide chain displays one tight type-I  $\beta$ -turn, which is where the lipoyl-lysine residue (Lys-42) is accessibly situated. The sequence surrounding Lys 42 is important in the recognition of E1, but other sequences must also be involved. It has been demonstrated that mutation of the adjacent residues does not prevent lipoylation, but does cause a reduction in the rate of reductive acetylation by E1 (Wallis & Perham, 1994).

### 1.3.2. Flexible Linker Sequences

For complex activity, the lipoyl domain must move between the active sites of each component enzyme (E1, E2 and E3) during catalysis. This active site coupling is facilitated in part by the lipoyl-lysine "swinging arm" (Reed, 1974) and also by flexible interdomain linker segments. The arm is 1.4nm, so has a maximum span of 2.8nm. Fluorescence studies of *E. coli* PDC showed the active sites of E1 and E3 to be at least 5nm apart (Shepherd & Hammes, 1976). Thus extra flexibility is required for active site coupling. Evidence for this comes from studies using genetically reconstituted PDC which had segments of linker deleted. Large deletions, shortening the 30 amino acid linkers by 50% or more, caused a drop of as much as 50% in complex activity (Miles *et al.*, 1987, 1988). Flexibility is reduced when the linker is removed.

Variation between linker sequences seems to fall into three categories. The most common is alanine-proline rich segments, found in *E. coli*. The second group is proline-rich and the final group is rich in charged and hydrophilic residues. The majority of the Ala-Pro peptide bonds are in the *trans* configuration, preventing the lipoyl domains collapsing into the core. The significances of these differences in linker design is not fully understood at present.

### 1.3.3. Catalytic Domain

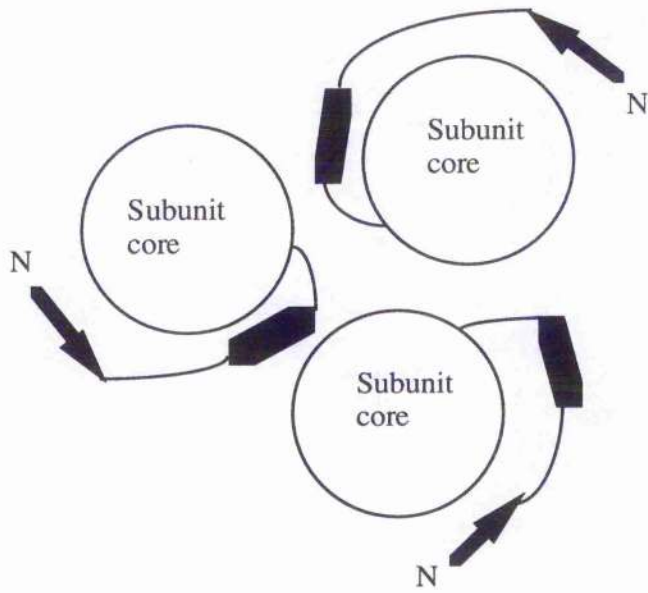
The C-terminal catalytic domain, consisting of between 200 and 250 amino acids, functions in the self-assembly of the E2 core and catalyses the formation of acyl CoA. The primary and secondary structures of the *E. coli* domain show some similarities to those of chloramphenicol acetyltransferase (CAT) (Guest *et al.*, 1987). CAT catalyses the acetylation (and thus inactivation) of chloramphenicol in antibiotic-resistant bacteria (Shaw, 1983). One interesting similarity is the positioning of the sequence -HXXXDG- in the active site of both enzymes (Guest, 1989). This suggests that the catalytic

domains are structurally related and that acetyl transfer is mediated by a related histidine-mediated mechanism (Kleanthous, 1985; Guest, 1987, 1989). The His acts as a general base and the Asn stabilises the transition state by hydrogen-bonding to it. Evidence in support of this comes from site-directed mutagenesis of the corresponding His in E2p of *E. coli* (Russell & Guest, 1990; Maedayorita *et al.*, 1994) and bovine E2b (Meng & Chuang, 1994). This resulted in loss of catalytic activity. However, the similar mutation in *S. cerevisiae* (Niu *et al.*, 1990) had no effect on enzyme activity. Several other residues of the CAT active site have been assigned catalytic roles (Lewendon, 1988) including Ser<sup>148</sup> and Asp<sup>199</sup>. Mutation of the corresponding residue (Ser<sup>550</sup>) of *E. coli* PDC reduces catalytic activity (Russell & Guest, 1991).

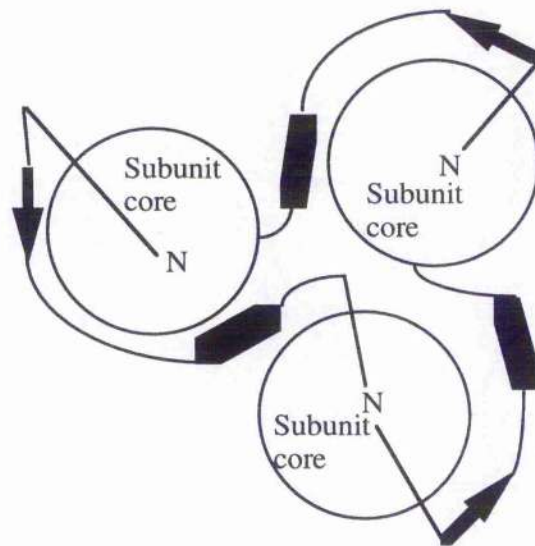
X-ray crystallography studies of the *A. vinelandii* core domain of E2p has given a high resolution structural insight into the similarities with the trimeric structure of CAT (Mattevi *et al.*, 1992, 1993) (Figure 1.6). Furthermore, each E2p core domain was seen to be folded into a six-strand  $\beta$ -sheet surrounded by five  $\alpha$ -helices and a small two-stranded  $\beta$ -sheet, demonstrating similarity to CAT (Mattevi *et al.*, 1993; Leslie *et al.*, 1990). Any differences in conformation were accounted for by the different substrates (chloramphenicol for CAT and lipoamide for E2p).

#### 1.3.4. Peripheral subunit binding domain

Located between the N-terminal lipoyl domains and the C-terminal catalytic domain lies the subunit binding domain. Depending on the source, this domain is the site for either E3 or E1 binding, or indeed both. The 3-D structures of the binding domain from *E. coli* OGDC (Robien *et al.*, 1992) (Figure 1.7) and *B. stearrowthermophilus* PDC (Kalia *et al.*, 1993) have been determined by means of 2D NMR spectroscopy. Both exhibit two parallel  $\alpha$ -helices, separated in the case of *E. coli* by a short extended strand and helical turn from a disordered loop structure and in *B. stearrowthermophilus* by a 3<sub>10</sub> helix from a highly structured loop. Kalia *et al.* (1993) also showed that the structure of



**Chloramphenicol Acetyltransferase (CAT)**



**E2p**

**Figure 1.6. Schematic Representation of the Organisation of the Catalytic Domain of CAT and E2p.**

The two cores display several similarities including their ability to form trimers. The shaded boxes represent common secondary structure regions. The arrows represent regions of  $\alpha$ -helix.

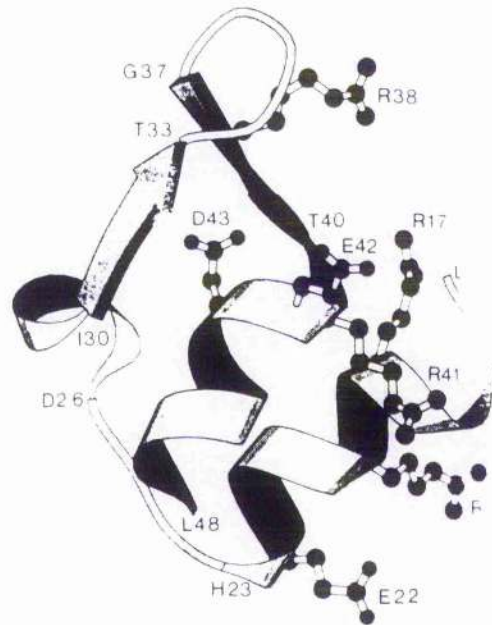


**Figure 1.7.** The E3-binding domain from the E2 core of the *E. coli* OGDC complex.

The schematic diagram shows the binding domain with the positions of conserved residues. The structure was taken from *Robien et al.* (1992).

the binding domain when complexed to E3 is similar to uncomplexed domain, implying a 'lock and key' mechanism of recognition, rather than 'induced fit'. In *B. stearothermophilus*, only the first helix interacts with E3. It has been suggested that helix 2 is involved in binding E1 (Mande *et al.*, 1996).

It has not been determined exactly which residues are involved in the binding of E1 and/or E3. The mode of binding may involve electrostatic interactions such as H-bonds and salt bridges between residues on the  $\alpha$ -helices of the binding domain and the E1 and E3 components. This was fuelled further by Russell and Guest (1991) who showed that under high ionic conditions, E1 and E3 are easily dissociated. The most recent work on the binding between the peripheral subunit binding domain and E3 was carried out by Mande *et al.* (1996). They showed that an electrostatic zipper was responsible for the main interactions (Figure 1.8) In *B. stearothermophilus*, this is formed between Arg135 and Arg139 of the binding domain and Asp344 and Glu431 of one of the E3 monomers. Sequence alignment studies highlighted the conserved tripeptide Gly155-Arg156-Val157. As well as its role in binding, it appears important for the stability of the binding domain. The Gly residue has a structural role, the Arg residue maintains the loop geometry in close proximity to the E3 while the Val residue contributes to the hydrophobic core of the domain.

It has been observed in *E. coli* that one E3 dimer can bind only to one binding domain (Higgs *et al.*, 1994; Maeng *et al.*, 1994). This could be either due to a change in conformation on binding to E2 or steric hindrance (Mande *et al.*, 1996) Studies of the binding of E1p to E2p in *B. stearothermophilus* have also shown that only one E1 heterotetramer ( $\alpha_2\beta_2$ ) can bind to each domain. Furthermore, E1 and E3 cannot bind to the same binding domain simultaneously (Mori *et al.*, 1994; Lessard & Perham, 1995) and E1 binds with a stronger affinity than E3 (Lessard & Perham, 1995). It could be proposed that, because E1 and E3 occupy different sites around the E2 core, they bind

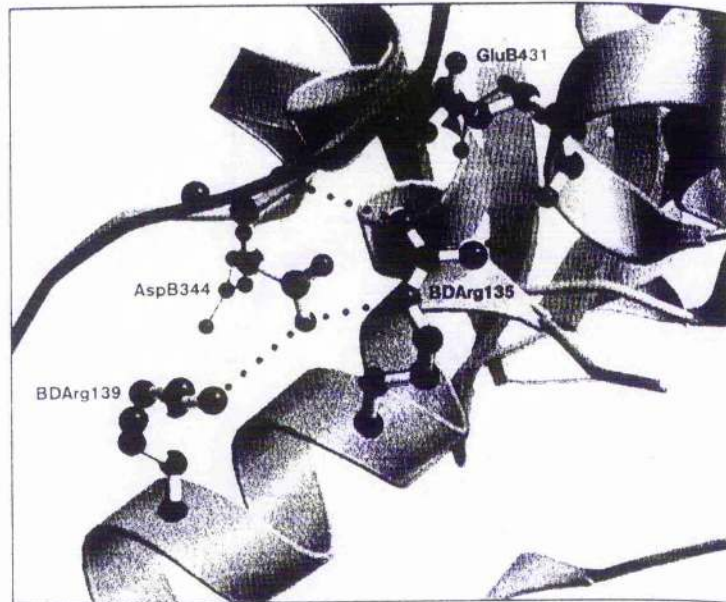


**Figure 1.8. Electrostatic zipper formed between the E3 and peripheral binding domain of E2 of *B. stearothermophilus*.**

The side chains of Asp344 and Glu431 of one monomer of E3 adopt a different conformation to that of uncomplexed E3 to allow binding to the peripheral subunit binding domain via salt bridges. (Adapted from Mande *et al.*, 1996).

to different binding sites within E2 and binding of one of these enzymes causes a steric hindrance effect, preventing binding by the other enzyme.

#### **1.4. The Dihydrolipoamide Dehydrogenase (E3) Component**

##### **1.4.1. General**

Dihydrolipoamide dehydrogenase is a flavoprotein belonging to the family of flavoprotein disulphide oxidoreductases that catalyses the reversible oxidation of the protein bound moiety of the E2 component of the 2-oxoacid dehydrogenase complexes.

Other such flavoproteins include glutathione reductase, NADH peroxidase and mercuric reductase. With the exception of the latter, they all catalyse electron transfer between disulphide compounds and nicotinamide dinucleotides (Roche & Patel, 1989).

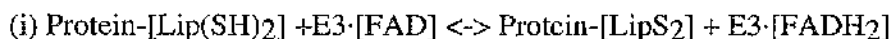
E3 has been isolated, sequenced and characterised from a variety of sources including *E. coli* (Stephens *et al.*, 1983b), *B. stearothermophilus* (Borges *et al.*, 1990), humans (Carothers *et al.*, 1989), *B. subtilis* (Hemila *et al.*, 1990) and *Halobacterium halobium* (Danson *et al.*, 1986). Their primary structures have been determined by nucleotide sequence analysis of the coding genes and found to be highly conserved (human liver E3 and porcine heart E3 have 96% sequence homology; Otulakowski & Robinson, 1987). Based on this information, the enzyme has a subunit size of approximately 50kDa.

Functional E3 is a homodimer with a non-covalently bound FAD co-enzyme associated with each subunit. X-ray crystallography studies have provided information regarding the overall structure of E3. Such studies on *A. vinelandii* (Mattevi *et al.*, 1991) show the presence of four domains per subunit; an FAD-binding domain, an NAD-binding domain, a central domain and an interface domain (in this order from the N-terminus to C-terminus). The two catalytic sites of the dimer contain sulphide bridges and are found

at the interface between the two subunits. Residues from both subunits form the active sites. There is a large area of contact upon dimerisation, with as much as 16% of previously accessible surfaces becoming buried.

#### 1.4.2. Enzymatic reaction of E3

The reaction catalysed by E3 (reviewed in Williams, 1992) is termed a ping-pong bi-bi mechanism, divided into two half reactions;



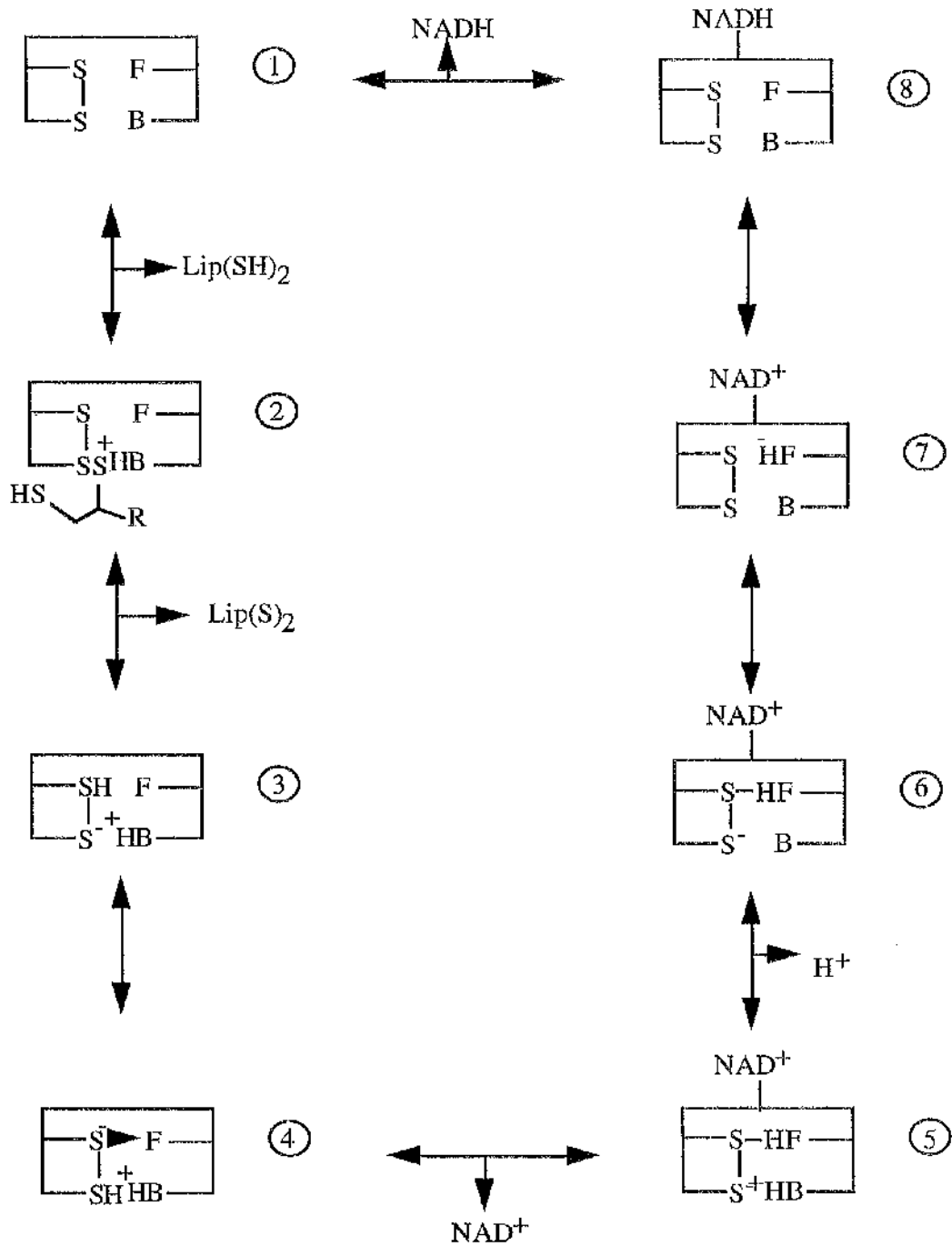
Reduction of the oxidised enzyme to the 2-electron reduced form (EH<sub>2</sub>), with the electrons being shared between the flavin and reactive disulphide.



Transfer of electrons from the 2-electron reduced form to the NAD<sup>+</sup> cofactor via the flavin to regenerate the oxidised enzyme (Figure 1.9).

Only the reduced (EH<sub>2</sub>) form can bind NAD<sup>+</sup>. The catalytic mechanism directly involves a histidine side chain donated by the opposite subunit to the reactive disulphide. This essential His has been identified by site-directed mutagenesis (Kim & Patel, 1992). Deletion and mutagenesis of residues in *A. vinelandii* E3 (Schulze *et al.*, 1991) has also demonstrated a conserved Tyr. Positional analysis suggests that a hydrogen bond is formed between this Tyr and the His of the second subunit.

One E3 dimer binds to only one peripheral subunit binding domain (Hipps *et al.*, 1994; Maeng *et al.*, 1994; Mandee *et al.*, 1996). This is thought to be due to a change in conformation or steric hindrance. Schulze *et al.* (1991) have shown that dimerisation is necessary for E2p binding, as both monomers provide residues forming the binding-site.



## 1.5. The E1 Component

### 1.5.1. General

The E1 component is a ThDP-dependent enzyme which catalyses the oxidative decarboxylation reaction with the concomitant transfer of the acyl group to the E2-bound lipoic acid. There are two forms of PDC E1; in octahedral PDC and OGDC complexes it is a homodimer ( $\alpha_2$ ) (Reed, 1974) and in octahedral BCOADC complexes and icosahedral complexes it is found as a heterotetramer ( $\alpha_2\beta_2$ ). In PDC, the  $\alpha$  subunit is 41kDa and the  $\beta$  subunit 36kDa. In the latter form, the  $\alpha$  subunit is thought to bind thiamine diphosphate (ThDP) (Stepp *et al.*, 1985) and the  $\beta$  subunit is involved in the reductive acetylation of the dithiolane ring of the lipoyl group (Yeaman, 1989; Patel & Roche, 1990). E1 $\alpha$  is thought to bind to E2 indirectly via binding to E1 $\beta$  (Rahmatullah *et al.*, 1989).

Lessard & Perham, (1994) have overexpressed the E1 $\alpha$  and E1 $\beta$  genes from *B. stearothermophilus* in *E. coli* and shown that E1 $\beta$  could bind to E2, without the presence of E1 $\alpha$ . The converse was not true, in that E1 $\alpha$  could not bind to E2, unless E1 $\beta$  was also present in the form of an E1 $\beta$ -E2<sub>p</sub> subcomplex.

The binding of E1 to E2 in mammalian sources relies on the peripheral binding domain (Wynn *et al.*, 1992). This was demonstrated by using truncated E2. Only the constructs devoid of the peripheral subunit binding domain were unable to bind E1.

This is in contrast to E1 binding in octahedral complexes, such as *E. coli* and *A. vinelandii*. It is still able to bind to the E2 core despite the removal of the peripheral subunit binding domain, showing the involvement of part of the inner catalytic domain (Packman *et al.*, 1988). Studies by Schulze *et al.* (1991) using site-directed mutagenesis of residues within the catalytic domain of *A. vinelandii* have confirmed the involvement of the inner domain in E1 binding. This group also showed that the

peripheral subunit binding domain and the core domain must be from the same species (Schulze *et al.*, 1992).

Sequence analysis of *E. coli* E1p and E1o has shown a lack of homology, in contrast to E2p with E2o (Stephens *et al.*, 1983b; Guest *et al.*, 1989). In fact, there seem to be sequences within the OGDC E1 enzyme which show similarities to those within E3 binding domains. There is also similarity to the putative E3 binding region of protein X. From this evidence, it has been suggested that the E1 component of OGDC has evolved to bind E3, in a similar way to protein X having apparently evolved as a separate gene product from E2-PDC, assuming a principal role in E3 binding in the process.

### 1.5.2. Enzymatic reaction of E1

The decarboxylation of pyruvate by E1 has been fairly well defined (Figure 1.10), but the final part of the catalytic reaction is still not fully determined. Two possible pathways for the reductive transfer of the acetyl group have been suggested (Gruys *et al.*, 1989; Frey *et al.*, 1989) (Figure 1.11).

In E1 from icosahedral complexes, it is the  $\alpha$  subunit which binds the ThDP. Primary sequence analysis has shown it contains a highly conserved sequence of approx. 30 amino acids, beginning -GDG- and ending with -NN-, which is common to other enzymes which also use ThDP as a cofactor, such as transketolases and pyruvate decarboxylases (Hawkins *et al.*, 1989). Several studies involving mutagenesis of various residues of both the  $\alpha$  and  $\beta$  subunits have suggested that up to six tryptophan residues are involved in cofactor binding (Ali *et al.*, 1995; Khailova *et al.*, 1989). Furthermore, it has been demonstrated that the presence of a  $\text{Ca}^{2+}$  ion is important for ThDP-binding (Lindquist *et al.*, 1992).

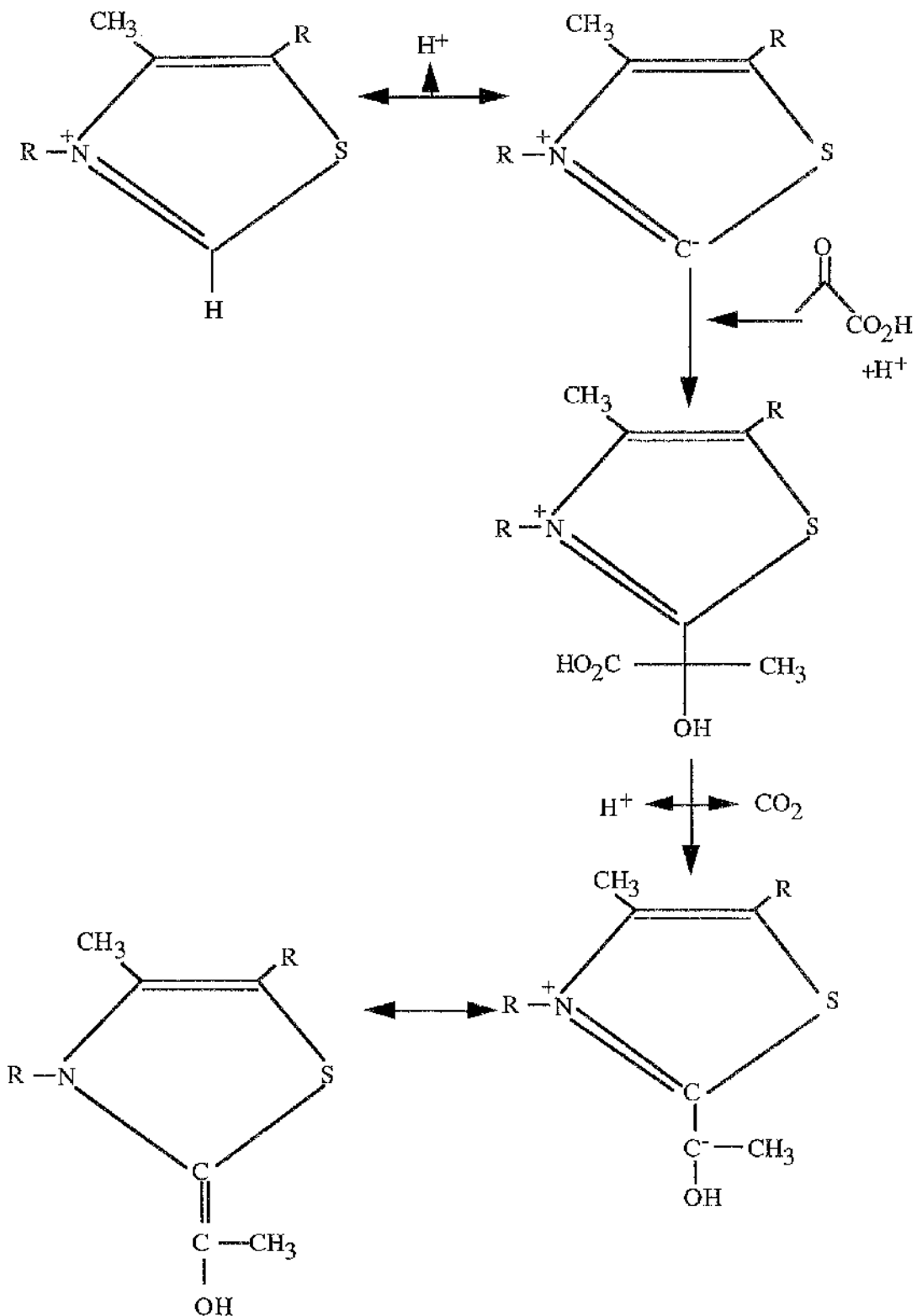


**Figure 1.10. The Catalytic mechanism of E1, involving the Decarboxylation of Pruvate to form 2-(1-hydroxyethylidene)-ThDP**

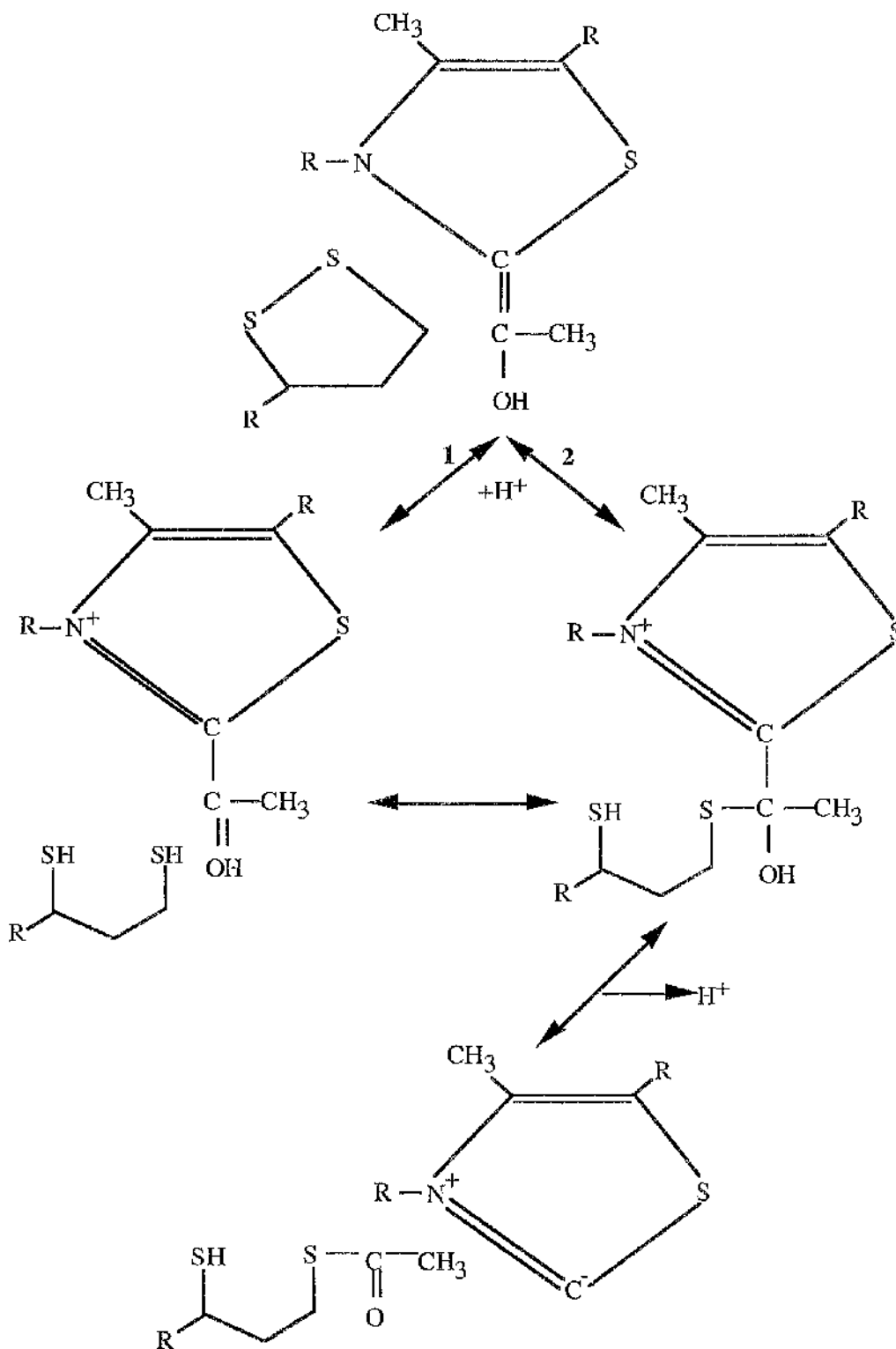


**Figure 1.11** Two suggested mechanisms for the reductive transfer of the acetyl group onto the lipoyl moiety of the E2 lipoyl domain

### 1.5.3. Control of E1 via Kinase and Phosphatase Activity

E1 catalyses the overall rate-limiting step in the sequence of reactions catalysed by the 2-oxoacid dehydrogenase complexes. Its activity is controlled by the phosphorylation and dephosphorylation of three specific serine residues in the  $\alpha$  subunit (reviewed in Reed & Yeaman, 1987; Patel & Roche, 1990). The  $Mg^{2+}$ -dependent kinase responsible for the phosphorylation and subsequent inactivation is tightly bound to the E2 core.

To date, four such kinases have been cloned. The first, BDK (branched chain  $\alpha$ -ketoacid dehydrogenase kinase) was cloned by Popov *et al.* (1992). It phosphorylates and inactivates the BCOADC complex. This conserves leucine, isoleucine and valine, when required for protein synthesis by all tissues. The phosphorylation of Ser<sup>293</sup> and Ser<sup>303</sup> of E1 $\alpha$  causes the inhibition of the ThDP-dependent step catalysed by E1 leading to inhibition of overall complex activity. BCOADC phosphatase is the enzyme responsible for the dephosphorylation and therefore activation of the complex.

The second kinase to be cloned (Popov *et al.*, 1993) is PDK (pyruvate dehydrogenase kinase). The phosphorylation of PDC causes a decrease in glucose utilisation and conserves the metabolic intermediates, alanine, lactate and pyruvate needed for the homeostasis of blood glucose levels. Phosphorylation can occur at 3 sites (Ser<sup>233</sup>, Ser<sup>240</sup> and Ser<sup>172</sup>) of the E1 $\alpha$  subunit (Yeaman *et al.*, 1978), the first of these being the main site of inactivation. Inhibition is enhanced by the concomitant phosphorylation of the other 2 sites. Inactivation is rapid, possibly due to the tight binding of the kinase to PDC. The inactivating effect of the kinase is reversed by PDC phosphatase.

The third kinase to be cloned (Popov *et al.*, 1994) also inactivates PDC upon phosphorylation, showing the existence of PDK isoforms in higher eukaryotes. The

amino acid sequences deduced from the full-length cDNAs encoding BDK, PDK1 and PDK2, show 30% homology between BDK and the PDKs, while the PDKs are 70% homologous.

The most recent PDK kinase to be cloned is the isoform PDK4, discovered by Rowles *et al.*, 1997. Harris *et al.* (1997) demonstrated starvation and also diabetes leads to an increase in the amount of the PDK4 isoform. In the rat model, it normally accounts for less than 30% of total PDK activity, but this was increased to above 50% in the starved state to 75% in the diabetic animals. As PDK4 activity is 7 times greater than the other isoforms, this isoenzyme shift resulted in greater phosphorylation and hence reduced PDC activities. Furthermore, due to PDK4 being less sensitive to pyruvate inhibition than PDK1 and PDK2 (Bowker-Kinley *et al.*, 1997), the PDC activity remains increased. Refeeding of the animals starved for 48h, reversed the increase in PDC activity. Insulin treatment of the animals leads to a decrease in PDK4 activity, although the mechanism has yet to be determined.

PDK3 and PDK4 have different allosteric and regulatory properties which are tailored to the distinctive energy demands of individual tissues. PDK3 and PDK4 are found at its highest levels in heart and skeletal muscle.

Mapping of the kinases reveals 5 highly conserved regions (Popov *et al.*, 1992), implicated as important for catalytic function. They may either directly form the active site or contribute structurally.

BDK expression in various tissues and its association with BCOADC under different physiological conditions is an important factor in regulating complex activity. The activity of BCOADC in the liver is greater than in any other tissue and it is here that BDK levels are lowest (Popov *et al.*, 1995). The tissue distribution of the PDKs has been determined by Northern blot analysis (Popov *et al.*, 1994). PDK1 mRNA is found

mainly in the heart. PDK2 mRNA is expressed in the heart and skeletal muscle but also to some degree in testes, liver, brain and kidney. PDK1/PDK2 ratios may alter according to physiological and pathological states.

### 1.6. Protein X

A fourth component has been identified associated with the PDCs of mammals and yeast (De Marcucci *et al.*, 1985). Initially it was assumed to be a proteolytic fragment of E2 or E3 as a band of approximately 50kDa was observed to migrate with the E2 component of bovine heart and kidney PDC. However, subsequent immunological, structural and genetic studies showed it to be an independent species (De Marcucci & Lindsay, 1985; De Marcucci *et al.*, 1986; Jilka *et al.*, 1986).

Sequence analysis of the protein X gene from yeast, *S. cerevisiae* (Behal *et al.*, 1989) and bovine heart (Neagle *et al.*, 1989) have shown it to possess a multidomain structure, similar to E2, comprising a single lipoyl domain and a peripheral subunit binding domain. The similarity does not extend to the C-terminal domain as it lacks the -HXXXDG- motif. The protein X lipoyl domain is capable of undergoing acetylation, deacetylation and reoxidation in the absence of E2 (Roche *et al.*, 1989b).

The most recent work involving protein X, suggests a role in the binding of E3 to the PDC complex (Neagle *et al.*, 1991). Indeed it now has the alternative name, E3 binding protein (E3BP). Native bovine kidney PDC was subjected to proteolysis with arg C. Selective degradation of protein X was shown to occur, by employing SDS-PAGE analysis. Two fragments were generated; a 35kDa fragment and an immunoreactive 15kDa species, the latter corresponding to the lipoyl peptide. Despite this degradation, there was a minimal effect of the overall PDC enzymatic activity. However, there was a decrease in the affinity of E3 for the E2 core and an enhanced sensitivity to high ionic strength. This suggested that either protein X is not essential for PDC activity or that the

35kDa truncated C-terminus peptide, still attached to the E2 core, is responsible for keeping the PDC function by positioning the E3 in the optimal location on the E2 core surface to facilitate its role in electron transfer. McCartney *et al.* (1997) showed that when protein X is removed, the PDC activity is reduced to between 10 and 15% of normal levels, but this can be enhanced by the presence of excess exogenous E3.

### 1.7. Regulation of the 2-Oxoacid Dehydrogenase Complexes

The location of the complexes within the energy-generating pathways of most aerobic tissues and cells means the requirement for close regulatory control. This is especially so for PDC, being located at a significant committed step in the metabolic pathway channelling intermediates into the TCA cycle. For example, during lipogenesis, increased PDC activity is required to supply acetyl CoA for fatty acid biosynthesis. On the other hand, in the presence of other substrates such as ketone bodies or fatty acids, suppression of complex activity is needed to allow carbohydrate 'sparing' for the brain, which is glucose-dependent. Thus the role of PDC could be looked upon as one of glucose homeostasis.

In other words, regulation must be both bioenergetically and biosynthetically sensitive. Three forms of control have been determined; end-product inhibition by NADH and acetyl CoA (Garland *et al.*, 1964; Kanzaki *et al.*, 1969), altered gene expression and through phosphorylation and dephosphorylation by the previously mentioned kinase and phosphatase. The latter mechanism is specific to PDC and is regulated by a number of effectors (Figure 1.12).

It has been demonstrated that hormones such as insulin are able to influence the activity of the complexes. In adipose tissues for example, PDC activity is increased several-fold. The mechanism of signalling between the insulin receptor and PDC is as yet unresolved, but several have been proposed, including the activation of secondary

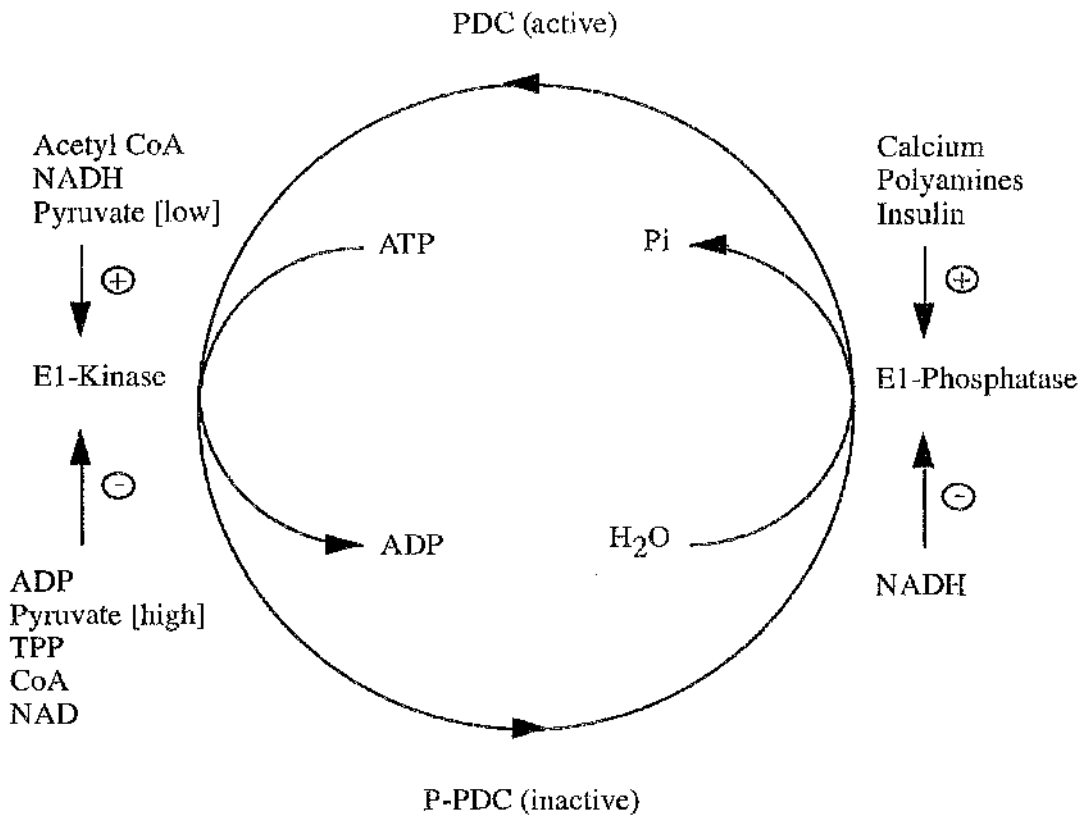


**Figure 1.12. The regulation of mammalian PDC through the phosphorylation-dephosphorylation cycle.**

messengers (Wieland *et al.*, 1989) and the production of small mediator molecules on the outside of the plasma membrane which interact with other cell surface receptors (Larner *et al.*, 1989) Gottschalk *et al.* (1992) have demonstrated that a 110 amino acid portion of the C-terminus of the insulin receptor may be involved in mediating PDC activity. It seems to possess determinants required for effective coupling to the PDC signalling system. Palmer *et al.* (1983) have shown that BCOADC activity in diaphragm muscle is inhibited following elevated levels of glucagon or adrenaline.

### **1.8. Physiological diseases associated with the 2-oxoacid dehydrogenase complexes**

A large number of related disorders have been attributed to deficiencies in the activities of the 2-oxoacid dehydrogenase complexes. Primary biliary cirrhosis (PBC) is a chronic autoimmune disease, characterised by progressive inflammatory destruction of intrahepatic bile ducts, leading to fibrosis and ultimately liver failure (Kaplan *et al.*, 1987; Sherlock & Dooley, 1993). A serological marker for diagnosis is the presence of antimitochondrial autoantibodies directed against the E2 components of PDC, OGDC and BCOADC (collectively termed the M2 antigens). Other antigenic components include protein X and the E1 $\alpha$  and E1 $\beta$  subunits of PDC (Yeaman *et al.*, 1988; Fussey *et al.*, 1988; Surh *et al.*, 1989). The vast majority (95%) of PBC sufferers have antibodies against the inner lipoyl domain of PDC-E2. Within the lipoyl domain, the site of attachment of the lipoic acid moiety is the most immunoreactive segment. Fussey *et al.* (1990) demonstrated that the lipoic acid itself has a role in the antibody recognition. Subsequent work (Joplin *et al.*, 1997) has suggested that the lipoic acid of protein X is involved in the aetiology of disease. The major autoantigen involved in PBC is located on the plasma membrane of bile duct epithelial cells. It can therefore be postulated that a defect in the targeting of PDC-E2 epitopes, or incorrect antigen processing, resulting in their wrongful location on the cell surface, could lead to the generation of an autoimmune response and disease promotion.

The largest group of PDC-related disorders are those resulting from a defect in the E1 genes. This is possibly due to the fact that one of the genes coding for E1, is located on the short arm of the X chromosome. The precise nature and degree of abnormality is dependent not only on the actual mutation, but also on the X-inactivation pattern in females. Most of the mutations occurring in exons I-IX are missense mutations, which allow some residual function. The insertion and deletion mutations in exons IX-XI result in an altered reading frame and the synthesis of truncated or elongated proteins, leading to inactive E1.

An example of an inborn error of metabolism caused by a defect in complex activity is the autosomal recessive 'Maple Syrup Urine Disease' (MSUD). This is characterised by a large number of phenotypes ranging from mental retardation and death to milder conditions with late onset. It results in the accumulation of branched-chain amino acids and derived products in the urine. The disease is caused specifically by a genetic defect in the E1 and/or E2 enzymes of BCOADC. The mutations are heterozygous and include deletion, insertion, missense and splicing abnormalities (Indo & Matsuda, 1996).

Studies have shown a possible link between OGDC deficiencies and Alzheimer's disease. Glutamate, which acts as a potent neurotoxin (Beal *et al.*, 1992) accumulates when 2-oxoglutarate oxidation is impaired. Sheu *et al.* (1994) demonstrated that patients with familial Alzheimer's had defective OGDC activity, possibly due to mutations in the E2 gene.

Deficiencies in the recently discovered protein X have been attributed to primary congenital lactic acidosis. In 1990, Robinson *et al.* described three patients with decreased PDC activity. The first patient had no E2 and decreased levels of protein X. The second had no protein X and the third showed a lower molecular mass form of protein X. In 1993, Marsac *et al.* also described three patients (two of whom were siblings) with defective protein X. This was followed by Geoffroy *et al.* (1996), then

De Meirleir *et al.* and Ling *et al.* (1998). The fact that some of the patients had no immunologically detectable protein X, yet retained partial PDC activity, further substantiates the E3-binding role of protein X, whilst confirming that E2-PDC displays low levels of E3 binding

To date very few E3-linked deficiencies have been documented. This is likely to be due to the severity of such diseases. A decreased E3 activity causes a reduction in each of the three complexes' activities, resulting in the accumulation of lactic, 2-oxo and branch chain amino acids (Liu *et al.*, 1993). Patel *et al.* (1997) were able, with the use of transgenic mice, to disrupt the E3 gene (*Dld*) by inserting a neomycin phosphatase gene into exon 10. The heterozygous animals showed a 50% reduction in the activity of the complex and a 50% reduction in the E3 mRNA, while displaying a normal phenotype. The homozygous animals, however, were embryonic lethal mutants. This highlights the importance of mitochondrial oxidative pathways during the implantation stage of development.

### **1.9. Mitochondrial Targeting**

It is known that the individual polypeptides making up the multienzyme complexes are nuclear encoded, as the translation products of the mitochondrial genome have been identified (Glover & Lindsay, 1992). The nascent precursor forms take only 2 to 5 minutes to cross the membrane, making detection and characterisation difficult. However, by uncoupling the electrochemical gradient necessary for translocation it has been possible to study the precursors via their accumulation in the cytoplasmic compartment.

There are three stages involved in the transfer of a newly synthesised mitochondrial polypeptide from the cytoplasm into the mitochondrion;

- (a) The maintenance of a translocational competent state *i.e.* unfolded polypeptide, involving chaperones and the presequence.
- (b) The targeting to the mitochondrion, involving binding proteins.
- (c) The translocation across the mitochondrial membrane.

The heat shock family of proteins, also termed chaperones, are important in keeping the precursor forms in an unfolded or translocation competent state and preventing self-aggregation. One such protein is the cytosolic Hsp70. It is also responsible for the uni-directional translocation of polypeptides through the mitochondrial membrane and for the correct folding once within the matrix (Stuart *et al.*, 1994). The presequences have been shown to be highly amphipathic and it is this characteristic which may promote binding by Hsp70 (Endo *et al.*, 1996). As well as Hsp70 is PBF (presequence binding factor) which may also bind the presequence after translation of the mRNA to polypeptide. PBF was shown by Murakami & Mori, (1990) to stimulate the import of precursor forms, but not the mature form of rat ornithine carbamoyltransferase.

Once the precursor arrives at the mitochondrial membrane, it is directed to a 'translocation contact site'. There are several receptors, called mitochondrial outer membrane proteins (MOMs) to which the precursor binds initially. They tend to be membrane bound with the receptor part on the cytosolic side, recognising either the signal peptide sequence or a bound cytosolic factor. On binding, the chaperone protein is removed, possibly involving another chaperone called Hsp40.

It has been suggested and demonstrated that not all the information required for targeting is confined to the presequence. There may be further information in the mature protein itself. This was shown to be the case in yeast, where mutants were able to transport mature mitochondrial proteins correctly as well as leaving synthetic fusion proteins in the cytosol (Schatz & Dobberstein, 1996). There is still a lot of ambiguity as to the full model of the translocation process itself. Many proteins are involved forming

a pore through which the polypeptide travels and others aiding the transfer across the membrane. Both a membrane potential and ATP supply are required.

Following the initial binding to the surface receptor, the polypeptide enters the outer membrane pore, then moves in to the innermembrane through a second pore. Mitochondrial proteins, including mt Hsp70, located in the matrix, bind the incoming polypeptide and aid its entry (Stuart *et al.*, 1994).

Processing of the polypeptide occurs immediately following translocation. the presequence is removed by MPP (mitochondrial processing peptidase) and the mature form adopted upon folding. MPP requires zinc and cleaves by recognising a particular 3D motif, rather than primary sequence.

Next, the mature polypeptide is either re-targeted or folded according to its final destination. Many polypeptides whose target is the intermembrane space or the inner membrane have a 'bipartite signal', which means that one sequence targets it to the mitochondrion then another is exposed to target it to its final destination.

The pre-sequence itself tends to be between 19 and 40 amino acids in length, although longer sequences have been identified. They contain high levels of serine, threonine and basic amino acids. In an  $\alpha$ -helical conformation, they are amphipathic *i.e.* hydrophilic on one side and hydrophobic on the other (Heijne *et al.*, 1989). There appears to be no sequence homology but there must be defined signals within these sequences.

### 1.10 Aims of this thesis.

Within this thesis there are several aims, which all tend towards obtaining a greater understanding into the interactions occurring within the 2-oxoacid dehydrogenase complexes.

The first was to devise a method to allow the amplification and subsequent overexpression of sub genes (the di-domain) of the E2 enzyme and the corresponding sequences of protein X. Following on from this is an investigation of the actual lipoylation of the E2 and protein X di-domains, including the use of site directed mutagenesis to determine specific residues essential for lipoylation. In addition, a preliminary study has been undertaken to investigate the effect that the large mitochondrial presequence has on the ability of the sub genes to fold and undergo lipoylation.

The N-terminal region of the E1 component of OGDC has been studied with the aim of studying its involvement in interacting with the E2 and E3 components.

Finally a study has been carried out, using the BIAcore instrumentation to obtain binding and affinity constants for interaction between the PDC di-domain and E3 and also between the protein X di-domain and E3. This was carried out to determine whether protein X has evolved with a greater ability to bind E3 than E2-PDC. Full-length protein X and full-length E2 has also been subjected to the same analysis.

## CHAPTER 2

### MATERIALS AND METHODS

## **2.1 MATERIALS**

- 2.1.1 Bacterial strains.
- 2.1.2 Bacterial Media.
- 2.1.3 Chemicals.
- 2.1.4 Enzymes.
- 2.1.5 Molecular Size & Mass Markers.
- 2.1.6 Oligonucleotides.
- 2.1.7 Photographic Materials.
- 2.1.8 Plasmid Vectors.

## **2.2 METHODS**

- 2.2.1 Determination of protein concentration.
- 2.2.2 Dialysis of protein samples.
- 2.2.3 Concentration of protein samples.
- 2.2.4 The Polymerase Chain Reaction (PCR) of the inner lipoyl domain plus peripheral subunit binding domain (di-domain) of the E2 enzyme or protein X.
- 2.2.5 The Polymerase Chain Reaction (PCR) of the N-terminal region of E1-OGDC.
- 2.2.6 Agarose gel electrophoresis.
- 2.2.7 DNA isolation from agarose gels.
- 2.2.8 Restriction Digests.
  - 2.2.8.1 pET11a digestion with Nde I and Bam HI.
  - 2.2.8.2 Di-domain PCR product digestion with Nde I and Bam HI.
  - 2.2.8.4 E1-OGDC N-terminus PCR product digestion with Bam HI.
  - 2.2.8.4 pGEX-2T digestion Bam HI.
- 2.2.9 Ligations.

- 2.2.9.1 Di-domain with pET11a vector.
- 2.2.9.2 E1-OGDC N-terminal fragments with pGEX-2T vector.
- 2.2.10 Preparation and transformation of *E. coli*
- 2.2.11 Isolation of plasmid DNA.
- 2.2.12 Preparation of supercompetent *E. coli* DE3plysS.
- 2.2.13 Overexpression of heterologous protein.
- 2.2.14 Large-scale overexpression of heterologous protein.
- 2.2.15 Large-scale preparation of bacterial PDC and E3.
- 2.2.16 SDS-Polyacrylamide Gel Electrophoresis.
  - 2.2.16.1 Buffers used in the SDS-PAGE system.
- 2.2.17 Native Gel Electrophoresis.
  - 2.2.17.1 Buffers used in Native Gel Electrophoresis.
- 2.2.18 Western Blotting and Immunological Detection of Proteins by Enhanced Chemiluminescence (ECL<sup>TM</sup>).
  - 2.2.18.1 Buffers used in the ECL Western Blotting system.
- 2.2.19 GST-fusion protein purification.
  - 2.2.19.1 Buffers used in the GST-fusion protein purification.
- 2.2.20 Surface Plasmon Resonance.
- 2.2.21 Isolation of PDC and OGDC from bovine heart mitochondria.
- 2.2.22 Preparation and purification of E3 from human OGDC, using the BioCAD Sprint Perfusion Chromatography system.
- 2.2.23 Enzyme Assays.
  - 2.2.23.1 2-oxoacid dehydrogenase complexes.
  - 2.2.23.2 dihydrolipoamide dehydrogenase (E3).

## 2.1 MATERIALS.

### 2.1.1 Bacteria.

Five strains of *E.coli* were employed:

*Escherichia coli* DH5 $\alpha$  : (Stratagene). For general propagation of plasmid vectors.

*Escherichia coli* XL1 Blue : (Stratagene). For propagation of plasmid vectors.

*Escherichia coli* XL-10 Gold: (Stratagene). For the propagation of pET vectors.

*Escherichia coli* DE3 (BL21): (Novagen). For the expression of the pET vectors carrying the T7 promoter.

*Escherichia coli* DE3 pLysS: (Novagen). For the expression of the pET vectors carrying the T7 promoter.

### 2.1.2 Bacterial Media.

Cultures were grown in either LB (10g bacto-tryptone, 10g NaCl and 5g yeast per litre) or DYT (16g bacto-tryptone, 5g NaCl and 10g yeast per litre). Media was autoclaved prior to use. Where necessary, media and plates were supplemented with ampicillin at 50 $\mu$ g/ml and/or chloramphenicol at 34 $\mu$ g/ml.

### 2.1.3 Chemicals.

Fisons, Loughborough supplied the Polyethylene glycol 6000 and Triton X-100. Pyronin dye was obtained from George T. Gurr, London. Mikrobiologie supplied the growth media for bacterial cultures. Reagents for SDS-PAGE and native gel electrophoresis were obtained from BDH Chemicals Ltd., Poole. All other chemicals were at least of analytical grade. Unless stated, water was glass-distilled.

### 2.1.4 Enzymes.

DNA restriction enzymes and DTT were supplied by Boehringer Mannheim Ltd. *Taq* DNA polymerase, calf intestinal alkaline phosphatase, proteinase K and DNA ligase

were supplied by Promega Ltd., Southampton. Cloned Pfu DNA Polymerase was supplied by Stratagene.

### **2.1.5 Molecular Size & Weight Markers.**

For agarose gel electrophoresis, 50bp, 100bp and 1kb ladders were used (GIBCO BRL) and also HindIII/EcoRI digested Lambda phage (Pharmacia). For SDS-PAGE analysis of proteins, broad-range molecular weight markers were used (NEB Biolabs).

### **2.1.6 Oligonucleotides.**

Primers for PCR were designed in the laboratory and synthesised by GIBCO BRL, Paisley or Genosys Biotechnologies (Europe) Ltd., Cambridgeshire.

### **2.1.7 Photographic Materials.**

Hyperfilm was obtained from Amersham, Bucks. The X-Omat-100 processor was supplied by Kodak.

### **2.1.8 Plasmid Vectors.**

**pHUMIT** (Kind donation by Dr. E. Gershwin). This vector contained the entire human PDC E2 gene.

**pTSE2a1** (Kind donation by Dr. D. Danner). This vector contained the bovine BCOADC E2 gene.

**pGS623** (Kind donation by Prof. J. Guest). This vector contained the *E. coli* PDC E2 gene.

**pET11a** and **pET11d** (Novagen). These vectors were used for the overexpression of heterologous proteins in *E. coli*. (Figure 2.1)

**pGEX-2T** (Pharmacia). This was used for the overexpression of GST-Fusion proteins in *E. coli*. (Figure 2.2)

**pGLIP-2T** (Kind donation by J. Quinn). This vector contained the lipoyl domain of human E2-PDC.

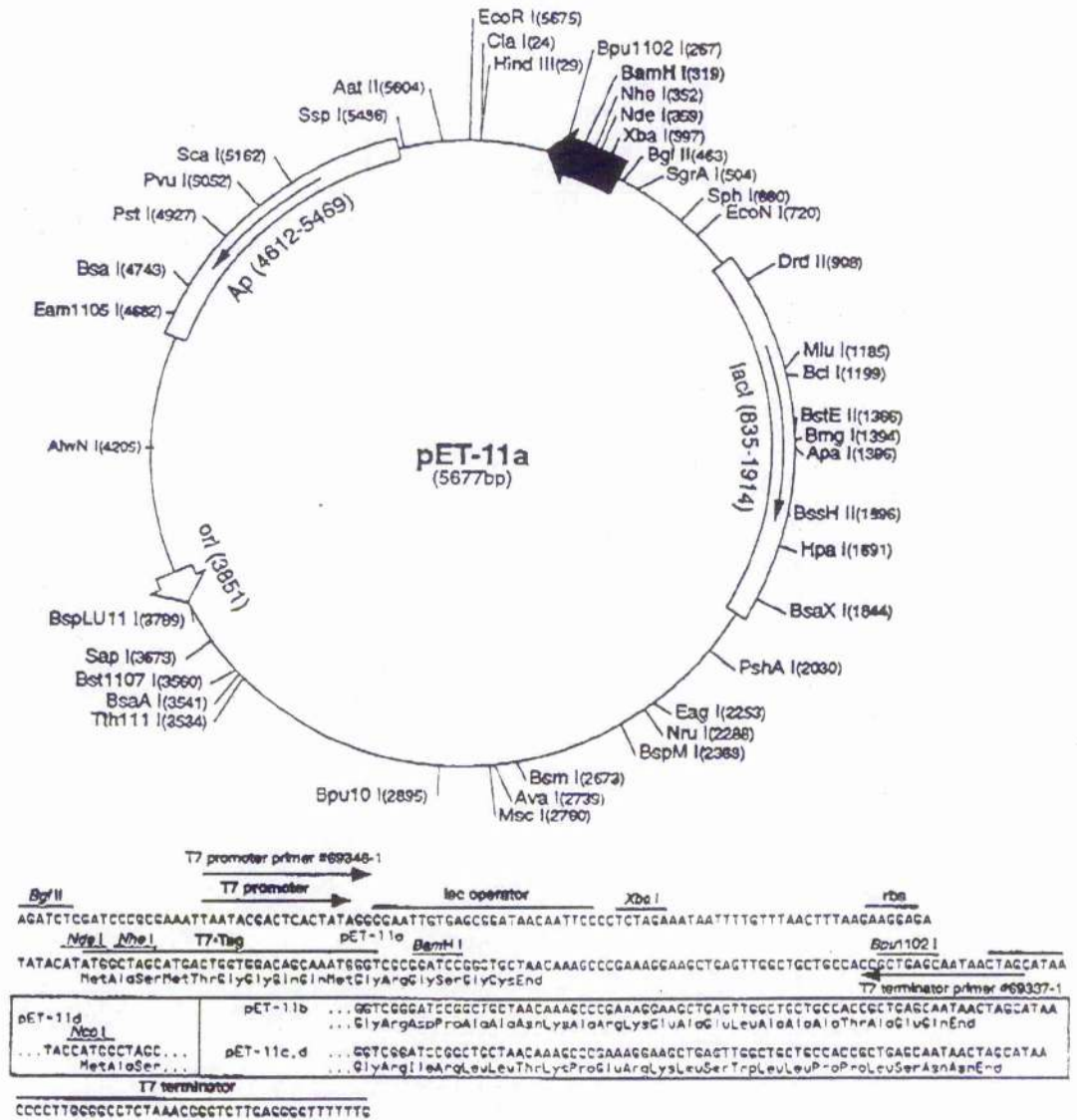


**Figure 2.1** Map of expression vector pET11a. The pET11a-d vectors carry an N-terminal T7-Tag sequence and Bam HI cloning site. The circular map shows the unique sites. The cloning region of the coding strand transcribed by T7 RNA polymerase is shown below. The expression region is reversed on the circular map as the sequence is transcribed by the pBR322 convention. The pET11d vector has the following exceptions to the above map; it is a 5674bp plasmid and an Nco I site is substituted for the Nde I site with a net 1bp deletion at position 359 of pET11c. As a result, Nco I cuts pET11d at position 355.

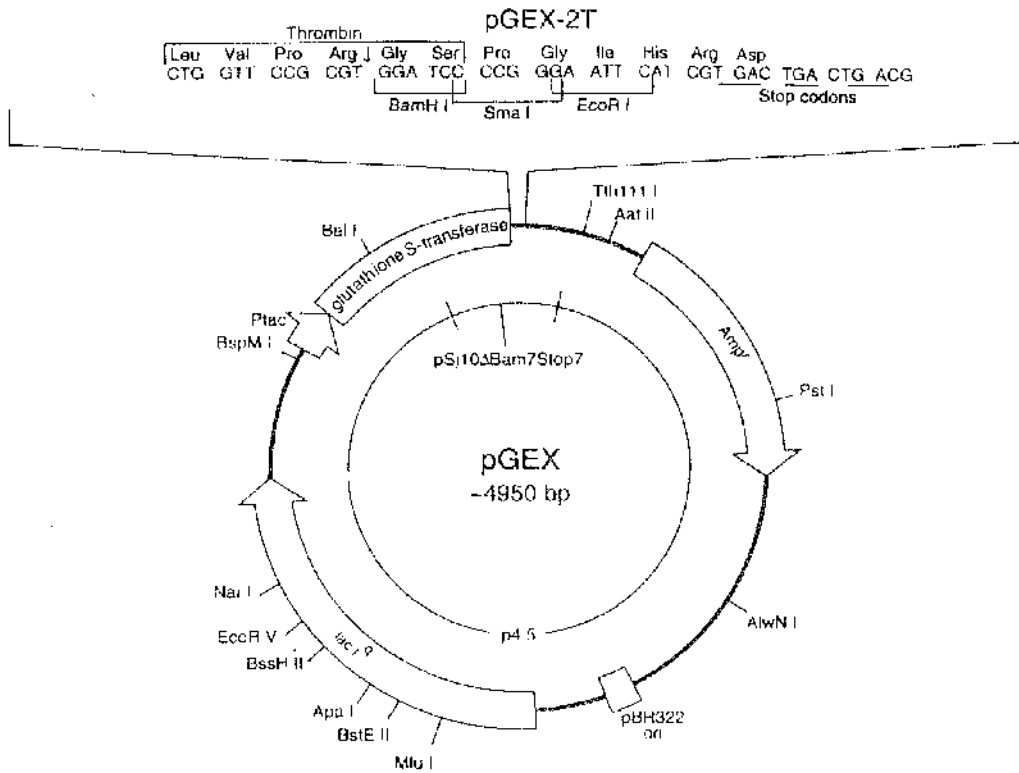


**Figure 2.2** Map of the glutathione S-transferase fusion vector, pGEX-2T, showing the reading frames and main features of the multiple cloning site. The vector has a tac promoter, for chemically inducible expression. A thrombin recognition site is located immediately upstream of the cloning site, allowing cleavage of the desired protein from GST.

## 2.2. METHODS

### 2.2.1 Determination of protein concentration.

Proteins concentrations were determined by the method of Lowry *et al.* (1951), modified by Markwell *et al.* (1976). For low concentrations, the Micro BCA assay was employed (Biorad). Protein standards were constructed using bovine serum albumin or IgG and absorbancies read at 595nm.

### 2.2.2 Dialysis of protein samples.

Dialysis was carried out at 4°C in Visking Tubing which had previously been boiled for 10 min in 1mM EDTA (pH 8.0) and 10mM sodium bicarbonate, then rinsed with distilled water and stored in 100% (v/v) ethanol.

### 2.2.3 Concentration of protein samples.

Protein samples were concentrated in Visking Tubing by covering with polyethylene glycol-6000 (PEG-6000) at room temperature until the volume inside the tubing had been sufficiently reduced.

### 2.2.4 Polymerase Chain Reaction (PCR) of the E2 or protein X di-domain.

The oligonucleotides (see below) were obtained from Life Technologies, Paisley. The underlined sequences in the 5' primers indicate the Nde I restriction site. The underlined sequences in the 3' primers indicate the Bam HI restriction site.

a) **Human PDC 5' Primer:**AGG CTC CTC ATA TGT CAT ATC CCC CTC ACA TG**Human PDC 3' Primer:**CTT GGC ACG GAT CCA GTG ATA TCC TTC CTG GTGb) **Bovine BCOADC 5' Primer:**GCT GCT CAT ATG GGA CAG GTT GTT CAG TTC AAG**Bovine BCOADC 3' Primer:**CAA TAT AGC GGA TCC AGT CCT TTC CAA ATA GTTc) ***E. coli* PDC 5' Primer:**GTG ACT GAA CAT ATG GTG AAA GGC GAC AA***E. coli* PDC 3' Primer:**GAT AGC TTC GGA TCC AGT AGC CTG AAC GTC TTCd) **Human protein X 5' Primer:**ACG CAG TGG CAT ATG GGT GAT CCC ATT AAG ATA CTA**Human protein X 3' Primer:**TCC AGA TGT GGA TCC AGT GGG CGA AGG TGC TGT

PCR reactions were carried out in a 50µl volume containing 50ng template DNA, 0.25mM dATP, dGTP, dCTP & dTTP (Promega), 5µg each primer, 1.5mM MgCl<sub>2</sub>, 1x Taq Polymerase buffer, 1 unit Taq Polymerase (Promega). Each reaction was overlaid with 50µl paraffin to prevent evaporation. Amplification was carried out on a PTC-100 thermocycler (GRI) for 30 cycles (30 sec at 92°C, 30 sec at 53°C, 1.5 min at 72°C) preceded with an initial denaturation step of 3 min at 94°C and concluding with a 5 min extension time at 72°C. Prior to further analysis, the PCR products were stored at 4°C.

### 2.2.5 Polymerase Chain Reaction (PCR) of the OGDC E1 N-terminus

The four oligonucleotides designed following careful study of previously published sequences, were obtained from Life Technologies, Paisley. The underlined sequences in all the primers indicate the Bam HI restriction site.

Upstream primer:	CAGATTCGGGGATCCTCTGCACCTGTTGCTGCTG
OGDC-60	CACAGCAGCGGATCCAGTTCGGCTCAGGGAAGG
OGDC-110	CAGATCAGCGGATCCAGTCCCCAGGGGTCCAG
OGDC-160	GATCTCCCGGATCCAGTTGCTGATTCCTGTCC

OGDC-60 was used to amplify the first 60 amino acids, OGDC-110 the first 110 and OGDC-160 the first 160.

PCR reactions were carried out in 50 $\mu$ l volumes containing 50ng human foetal heart cDNA, 0.25mM dATP, dGTP, dCTP & dTTP (Promega), 5 $\mu$ g each primer, 1x Pfu DNA polymerase buffer, 2 units Pfu DNA Polymerase (Stratagene). Each reaction was overlaid with 50 $\mu$ l paraffin to prevent evaporation. Amplification was carried out on a PTC-100 thermocycler (GRI) for 35 cycles (45sec at 95 $^{\circ}$ C, 30sec at 65 $^{\circ}$ C, 10 min at 72 $^{\circ}$ C) preceded with an initial denaturation step of 45 sec at 95 $^{\circ}$ C and concluding with a 15 min extension time at 72 $^{\circ}$ C. Prior to further analysis, the PCR products were stored at 4 $^{\circ}$ C.

### 2.2.6 Agarose gel electrophoresis of the amplified DNA encoding the di-domain.

10 $\mu$ l of PCR product was electrophoresed on a 2% (w/v) agarose gel, with 2 $\mu$ l of bromophenol blue/xylene cyanol loading buffer (Promega). The gel was run in 1x TAE buffer at 75V until the dye front was within 1 cm of the end of the gel. A 100bp ladder was used as a molecular mass marker (Life Technologies, Paisley). The gel was stained with ethidium bromide (10mg/ml) (Sigma) for 1h, destained for 1h in distilled water

and the banding pattern visualised under transillumination with an ultraviolet (UV) light source.

#### **2.2.7 DNA isolation from agarose gels.**

The PCR product was run on a 2% low melting point TAE-agarose gel and the DNA recovered using the Promega Wizard<sup>TM</sup> PCR Preps kit or Qiagen prep kit and provided protocol. The DNA was eluted into 50µl distilled water.

#### **2.2.8 Restriction digests.**

Both Nde I and Bam HI were supplied by Boehringer. Nco I was supplied by Stratagene, and NEBuffer 2 was supplied by New England Biolabs.

##### **2.2.8.1 pET11a digestion with Nde I and Bam HI.**

Digests were carried out in a 40µl volume, containing the following components; 15µl pET11a vector, 15 units Nde I, 15 units Bam HI, 4µl Buffer B and 18µl distilled water. The mixture was incubated in a water bath at 37°C for 2h. After the first hour, 1µl alkaline phosphatase was added to prevent self-ligation. The 40µl digestion mix was run on a 1.5% TAE-agarose gel. DNA was recovered using the Promega Wizard<sup>TM</sup> PCR Preps kit and the provided protocol. The DNA was eluted into 50µl distilled water.

##### **2.2.8.2 Di-domain PCR product digestion with Nde I and Bam HI.**

Digests were carried out in a volume of 40µl, containing the following components; 20µl di-domain product, 15 units Nde I, 15 units Bam HI, 4µl Buffer B and 13µl distilled water. The mixture was incubated in a water bath at 37°C for 2h and the resultant products run on a 2% low melting point (LMP) agarose gel. DNA was recovered using the Promega Wizard<sup>TM</sup> PCR Preps kit, and the provided protocol.

### **2.2.8.3 OGDC N-terminal fragment PCR product digestion with Bam HI.**

Digests were carried out in 40 $\mu$ l volumes, containing the following components; 20 $\mu$ l PCR product, 15 units Bam HI, 4 $\mu$ l Buffer B and 12 $\mu$ l distilled water. The mixture was incubated in a water bath at 37 $^{\circ}$ C for 2h and purified DNA recovered using the Qiagen Preps kit and the provided protocol.

### **2.2.8.4 pGEX-2T digestion with Bam HI.**

Digests were carried out in 40 $\mu$ l volumes, containing the following components; 15 $\mu$ l pGEX-2T, 15 units Bam HI, 4 $\mu$ l Buffer B and 7 $\mu$ l distilled water. The digestion was incubated at 37 $^{\circ}$ C for 3h, then for a further 30 min with the addition of 1 $\mu$ l alkaline phosphatase. The DNA was purified using a Qiagen Preps kit and the provided protocol.

## **2.2.9 Ligations.**

### **2.2.9.1 Ligation of E2 di-domain with pET11a vector.**

The ligation of the vector with the E2 di-domain was carried out for 10h; 5h at 16 $^{\circ}$ C followed by 5h at 10 $^{\circ}$ C. Various ratios of insert to linearised vector were tried, with the optimal ratio being approx. 1:1. Each reaction was carried out in a 10 $\mu$ l volume, containing DNA, T4 ligase buffer, 2 units T4 ligase and distilled water.

### **2.2.9.2 Ligation of OGDC E1 N-terminal fragments with pGEX-2T vector.**

The same protocol was employed as detailed above.

### **2.2.10 Preparation and Transformation of *E. coli*.**

DH5 $\alpha$  or XL1-Blue cells were grown overnight in 5ml LB, then 1ml per transformation were made supercompetent, using the following method (2.2.12), prior to being transformed with the 10 $\mu$ l ligation mixes. For each transformation, 1ml of

overnight culture was pelleted in a microcentrifuge for 1 min. The cells were resuspended in 500µl ice-cold, sterile 0.1M CaCl<sub>2</sub> and left on ice for 10 min. They were then pelleted for 1 min, resuspended in 300µl 0.1M CaCl<sub>2</sub> and incubated on ice for 30 min. At this point the 10µl ligation mixes were added and each sample left on ice for at least 30 min. Heat shock was carried out in a water bath at 42°C for exactly 90 sec, then 1ml LB was added to each sample. After 1h of shaking incubation at 37°C, the cells were pelleted in a microcentrifuge, resuspended in 100µl LB and spread on agar plates containing ampicillin. The plates were incubated overnight at 37°C.

The plates were made by dissolving 15g of agar in a litre of LB broth. Following autoclaving, the broth was allowed to cool to below 50°C before adding antibiotic (final concentration 50µg/ml) and pouring under sterile conditions.

#### **2.2.11 Isolation of plasmid DNA.**

A single colony was used to inoculate 5ml LB and grown overnight at 37°C in the presence of ampicillin. The plasmid DNA was then isolated using the Promega Wizard™ Minipreps kit and the provided protocol.

#### **2.2.12 Preparation of supercompetent DE3 or DE3pLysS *E. coli* cells.**

A single colony was used to inoculate a 5ml culture of LB, which was supplemented with ampicillin (plus chloramphenicol if using DE3pLysS). After overnight growth at 37°C, a 1ml sample was then used to inoculate 50ml of LB, again containing ampicillin and the culture grown until an A<sub>600</sub> of 0.3 was reached. The sample was stored on ice for 15 min, then centrifuged at 5000 x g for 10 min at 4°C. The resultant pellet was resuspended in 10ml of 0.1M ice-cold MgCl<sub>2</sub> and centrifuged again at 5000rpm for 10 min at 4°C. The resultant pellet was resuspended in 10mls ice-cold 0.1M CaCl<sub>2</sub> and left on ice for 30 min before a final centrifugation at 5000 x g for 10 min at 4°C. The

resultant pellet was resuspended in 2ml 0.1M ice-cold CaCl<sub>2</sub> and aliquoted into 200µl samples, with 200µl 50% (v/v) glycerol. Storage was at -80°C.

#### **2.2.13 Overexpression of heterologous protein.**

A single colony was used to inoculate a 5ml culture of LB, which was supplemented with the appropriate antibiotic. After overnight growth at 37°C, a 1ml sample was then used to inoculate 50ml of LB, again containing ampicillin, and the culture incubated in a 37°C orbital shaker at 225rpm until an A<sub>600</sub> of 0.5 was reached. At this point, the cells were induced with 0.4mM IPTG. Samples (1ml) were removed at 0, 1, 2 and 3h following induction, and their A<sub>600</sub> determined. The cells were then pelleted in a microcentrifuge and resuspended in Laemmli sample buffer (10µl per absorbance unit), containing 10mM DTT. Samples (20µl) were loaded onto a 15% SDS-polyacrylamide gel, following 5 min boiling in a water bath.

#### **2.2.14 Large-scale overexpression of heterologous protein.**

A single colony was used to inoculate a 5ml culture of LB, which was supplemented with the appropriate antibiotic. After overnight growth at 37°C, the 5ml sample was then used to inoculate 330ml of LB, again containing ampicillin with or without chloramphenicol, and the culture grown at 225rpm until an A<sub>600</sub> of 0.8 was reached. A total of 1l of LB was used for each sample. At this point, the cells were induced with 0.4mM IPTG. The flasks were shake-incubated for a further 3h at 37°C, then the contents spun for 15 min at 5000 x g. The pellet was resuspended in a minimal volume of Resuspension buffer (20mM potassium phosphate (pH 7), 0.02% (w/v) sodium azide) then subjected to disruption in a French Pressure cell (2x 950MPa). The sample was then centrifuged for 45 min at 5,000 x g.

#### **2.2.15 Large-scale preparation of Bacterial PDC and E3.**

2l of ampicillin (50µg/ml) and 0.2% (w/v) glucose-supplemented LB were inoculated with overnight cultures of plasmid JRG 2872. The flasks were shake-incubated at 37°C

until the  $A_{600}$  reached 0.5, when the cultures were induced with  $60\mu\text{M}$  IPTG. The cells were harvested by spinning at  $5000 \times g$  for 40 min, following an 8h incubation. The pellet was resuspended in Buffer A ( $\text{KH}_2\text{PO}_4$ , 2mM EDTA (disodium salt), 1mM benzamidine). This was repeated a twice more, with the final resuspension volume being 15ml. The cells were broken by two passages through the French press at 95MPa. The extract was then clarified by a 30 min spin at  $40,000 \times g$ . PDC was sedimented by spinning for a further 4h. The resultant supernatant contains the E3. The PDC pellet was resuspended in Buffer A. To purify the E3, the supernatant was heated to  $65^\circ\text{C}$  for 10 min then spun in a microcentrifuge at  $14,000 \times g$ .

#### **2.2.16 SDS-polyacrylamide gel electrophoresis.**

Samples ( $20\mu\text{l}$ ) were electrophoresed on  $20\text{cm} \times 20\text{cm}$  slab gels, using a model V-16 polyacrylamide gel apparatus (Life Technologies). The glass plates were cleaned with 100% (v/v) ethanol, prior to pouring. 30ml resolving gel solution was made up (15ml resolving gel buffer, 15ml 29:1 acrylamide:bisacrylamide solution,  $360\mu\text{l}$  10% (w/v) ammonium persulphate,  $36\mu\text{l}$  TEMED). The gel was overlaid with 100% isopropanol until set. Excess fluid was poured off and a stacking gel solution layered on top (8.2ml stacking gel buffer, 1.8ml 29:1 acrylamide:bisacrylamide,  $120\mu\text{l}$  10% (w/v) ammonium persulphate,  $12\mu\text{l}$  TEMED) Once set, the comb was removed and the wells washed out with distilled water. Prior to loading, the samples were boiled for 5min at  $95^\circ\text{C}$  in Laemmli sample buffer. The gel was run in 1x electrode buffer containing 0.02M Tris, 0.05M glycine and 3mM SDS. Electrophoresis was carried out until the dye front was within 2cm of the end of the gel. Staining was performed using a Coomassie Brilliant Blue R stain (0.1% (w/v) Coomassie blue, 10% (v/v) acetic acid, 50% (v/v) methanol) for 1h. The banding pattern was visualised on a transilluminator, following overnight destaining in 10% (v/v) acetic acid, 25% (v/v) isopropanol.

### 2.2.16.1 Buffers used in the SDS-PAGE electrophoresis system.

Resolving Gel (pH 8.8)	15% (w/v) Acrylamide
	0.3% (w/v) Bis-acrylamide
	0.75M Tris
	0.2% (w/v) SDS
	0.1% (v/v) TEMED
	1% (w/v) Ammonium persulphate
Stacking Gel (pH 6.8)	6.5% (w/v) Acrylamide
	0.2% (w/v) Bis-acrylamide
	0.17M Tris
	0.2% (w/v) SDS
	0.1% (v/v) TEMED
	1% (w/v) Ammonium persulphate
Electrode Buffer (pH 8.3)	0.02M Tris
	0.05M Glycine
	3mM SDS
Laemmli Sample Buffer	62.5mM Tris
	2% (w/v) SDS
	10% (w/v) Sucrose

### 2.2.17 Native Gel Electrophoresis.

Samples (20 $\mu$ l) were electrophoresed on a 20cm x 20cm slab gel as before. The casting technique was identical to that for SDS-PAGE. The 10% gel was run for 2-3h at a constant current of 65mA in electrode buffer. Electrophoresis was performed until the dye front was within 2cm of the end of the gel. Staining was carried out using a Coomassie Brilliant Blue R stain (0.1% (w/v) Coomassie blue, 10% (v/v) acetic acid, 50% (v/v) methanol) for 1h. The banding pattern was visualised on a transilluminator, following overnight destaining in 10% (v/v) acetic acid, 25% (v/v) isopropanol.

### 2.2.17.1 Buffers used in the Native Gel electrophoresis system.

Resolving Gel (pH 8.8)	10% (w/v) Acrylamide
	0.3% (w/v) Bis-acrylamide
	0.75M Tris
	0.1% (v/v) TEMED
	1% (w/v) Ammonium persulphate
Stacking Gel (pH 6.8)	6.5% (w/v) Acrylamide
	0.2% (w/v) Bis-acrylamide
	0.17M Tris
	0.1% (v/v)TEMED
	1% (w/v) Ammonium persulphate
Electrode Buffer (pH 8.3)	0.02M Tris
	0.05M Glycine
Loading Buffer	62.5mM Tris
	10% (w/v) Sucrose
	0.5% (w/v) Xylene cyanol

### 2.2.18 ECL<sup>TM</sup> Western Blotting

In order to confirm the presence of the di-domain in the crude *E. coli* extract, Western blotting, in the form of enhanced chemiluminescence (ECL) was employed.

Crude extract samples were subjected to SDS-PAGE, then transferred overnight onto a nitrocellulose membrane (Amersham), at a constant current of 40mA. Non-specific sites were then blocked for 6h at room temperature, using blocking buffer (see below). The blot was then incubated in primary antibody solution (see below) overnight, at 4°C. The following day the blot was washed 4 times for 30 min in wash buffer (see below), then incubated for 2h with the secondary antibody which was conjugated to horseradish peroxidase. Following a further 3 x 30 min. washes, the blot was incubated in high salt buffer for 30 min, then exposed to X-ray film (Hyperfilm<sup>TM</sup> ECL<sup>TM</sup>, Kodak).

**2.2.18.1 Buffers used in the ECL Western Blotting system.**

Transfer Buffer (10x) (1l)	30.3g Tris base 144g Glycine 2g SDS
Blocking Solution	20mM Tris (pH 7.2) 15mM NaCl 5% (w/v) Non-fat milk 5% (v/v) Donkey serum 0.2% (v/v) Tween 20
Primary Antibody Solution	20mM Tris (pH 7.2) 1% (w/v) Non-fat milk 1% (v/v) Donkey serum 0.1% (v/v) Tween 20 1:1000 dilution of primary antibody
Wash Solution	20mM Tris (pH 7.2) 15mM NaCl 1% (w/v) Non-fat milk 1% (v/v) Donkey serum
Secondary Antibody Solution	20mM Tris (pH 7.2) 150mM NaCl 1% (w/v) Non-fat milk 1% (v/v) Donkey serum 1:5000 dilution of secondary antibody

*Primary PD (antibody) 1:1000*



flow cell was achieved with HBS buffer (10mM HEPES, (pH 7.4), 15mM 3.4mM EDTA, NaCl, 0.005% surfactant P20). Regeneration was achieved with 1M NaCl. The amount of E3 immobilised was between 1000 and 2000 resonance units (RUs).

For the collection of kinetic data, 60µl of the *E. coli* cell extracts containing the overexpressed di-domains were passed over the chip (association phase) at concentrations between 250nM and 50µM. The flow was continued for a further 1min with the equilibrium buffer (dissociation phase). 10µl of 1M NaCl was passed over the chip for regeneration.

### **2.2.21 Isolation of PDC and OGDC from bovine heart mitochondria.**

The isolation of the complexes from bovine heart tissue was carried out at 4°C using the method of Stanley & Perham (1980), with several modifications as detailed here. To 600g of fresh heart tissue, the following was added; 500ml of 3% (v/v) Triton X-100 buffer (50mM MOPS, 2.7mM EDTA, 3% (v/v) Triton-X 100, 0.1mM DTT, 1mM PMSF, 1mM benzamidine, 0.2% (v/v) anti-foam, adjusted to pH 7 with 6M NaOH), before blending for 5 min, after which time the volume was made up to 2l with more buffer. The homogenate was then clarified at 10,000 x g for 20min, the pellets discarded and the supernatant adjusted to pH 6.45 with 10% (v/v) acetic acid. The complexes were precipitated by adding 0.12 vol. of 35% (w/v) PEG, stirred for 30min and pelleted at 18,000 x g for 15min. The pellets were resuspended by homogenisation in 400ml 1% (v/v) Triton X 100 buffer, this time with the addition of 1.5µM leupeptin, and the pH adjusted to 6.8, before clarification at 25,000 x g for 40 min.

The supernatant was filtered through muslin and 0.013vol. of 1M MgCl<sub>2</sub> and 0.05vol. 1M sodium phosphate buffer (pH 6.3) were added with 0.5M NaOH to maintain the pH at 6.8. Acetic acid was added to lower the pH to 6.45 then a second 0.12 vol. of 35% (w/v) PEG was added and the supernatant stirred for 30min at 4°C. The complexes were pelleted at 25,000 x g for 10min, resuspended by homogenisation in

160ml of 1% Triton-X 100 buffer (pH 6.8) and fresh solutions of 1mM PMSF, benzamidine, leupeptin plus 0.5% (v/v) rat serum added and left overnight at 4°C.

Re-homogenisation was followed by a clarifying spin at 25,000 x g for 1h and the supernatant adjusted to pH 6.45 before the addition of 0.04-0.06 vol. of 35% (w/v) PEG for 30min with stirring. This differential cut enables the separation of OGDC (pelleted at 25,000 x g for 10min) from PDC which remains in the supernatant and is pelleted by an ultracentrifugation step of 200,000 x g for 2.5h.

The pelleted complexes were subsequently resuspended in 1% (v/v) Triton-X 100 buffer (pH 6.8) and further purified using a 100cm x 3cm Sepharose CL-2B gel filtration column, equilibrated overnight at 4°C with 50mM sodium phosphate buffer (pH7.0) containing 2.7mM EDTA and 1% (v/v) Triton X 100. Approx. 100mg of protein were routinely resolved. The individually purified complexes were then pelleted at 200,000 x g for 2.5 h and resuspended in 1% (v/v) Triton X 100 buffer.

#### **2.2.22 Preparation of E3 from human OGDC.**

The human OGDC was kindly provided by Professor Steve Yeaman, University of Newcastle, in 50% glycerol at 9.25 mg/ml. The sample was cooled to 4°C for 20 min, then heated to 65°C for 10min in the presence of 1M NaCl and 20mM potassium phosphate buffer (pH 7.6). Cell debris was removed by centrifuging the sample at 14,000 x g for 15 min. The supernatant was transferred to dialysis tubing and dialysed for 2h against a 25mM Tris/Bis-Tris Propane buffer (pH 7.6). Following a 10min centrifugation step at 14,000 x g, 1ml was loaded on to a Poros 20Pi column and the following programme run;

To equilibrate the column, 25mM Tris buffer (pH 9) was blended with 25mM Tris buffer (pH 6) to give a working buffer at pH 7.5 and 10 column vols passed through the column. After injecting the sample onto the column an NaCl gradient was started, ranging from 400mM to 800mM. Fractions (1ml) were collected for analysis by SDS-

PAGE. A final wash step was added, whereby 10 column volumes of 2M NaCl was passed through the column.

### **2.2.23 Enzyme Assays.**

#### **2.2.23.1 2-Oxoacid Dehydrogenase Complexes**

The activities of PDC and OGDC were determined spectrophotometrically at 340nm as the rate of formation of NADH, at 30°C. Approx. 2-5µg of complex was added to 670µl of solution A (50mM potassium phosphate buffer (pH 7.6) containing 3mM NAD<sup>+</sup>, 2mM MgCl<sub>2</sub> and 0.2mM TPP), 14µl solution B (0.13M cysteine HCl, 0.13mM Li<sub>2</sub>CoASII) and 14µl solution C (100mM pyruvic acid (for PDC assay) or 2-oxoglutarate (for OGDC assay)). The reaction was initiated by the addition of enzyme to the above solutions and carried out at 30°C. Activity was expressed as nkatals (the amount of enzyme required to produce 1nmole of NADH per sec).

#### **2.2.23.2 Dihydrolipoamide Dehydrogenase (E3)**

The activity of the E3 enzyme was determined spectrophotometrically at 340nm as the rate of formation of NADH, at 30°C, from the conversion of dihydrolipoamide to lipoamide. Dihydrolipoamide was prepared from the oxidised form of DL-6,8-thioctic acid amide using the method of Kochi & Kikuchi (1976), whereby 60mg of DL-lipoamide was dissolved in 1.2ml of 50% (v/v) ethanol in 1M potassium phosphate buffer (pH 8) to which 2.4ml 5% (w/v) NaBH<sub>4</sub> (in 10mM NaOH) was added, for 10min followed by neutralisation with 1.2ml of 3M HCl. The dihydrolipoamide was then extracted into the upper solvent layer by the addition of 3 x 3ml vols of toluene. Evaporation of the toluene under nitrogen gas left the dihydrolipoamide which was stored at -20°C until use at which time 20.7mg was dissolved in 1ml of 70% (v/v) ethanol.

For the assay itself, approximately 2-5 $\mu$ g of E3 were added to 670 $\mu$ l of solution A (50mM potassium phosphate buffer, pH 7.6, containing 3mM NAD<sup>+</sup>, 2mM MgCl<sub>2</sub> and 0.2mM TPP) and 10-20 $\mu$ l fresh dihydrolipoamide (preincubated at 30°C in a quartz cuvette) and the activity expressed as nkatal (the amount of enzyme required to produce 1nmole of NADH per sec at 30°C).

### CHAPTER 3.

AMPLIFICATION AND EXPRESSION OF THE LIPOYL  
AND ADJACENT PERIPHERAL ENZYME BINDING  
DOMAINS OF THE E2 COMPONENTS OF HUMAN PDC,  
HUMAN PROTEIN X, BOVINE BCOADC AND *E. COLI*  
PDC.

### 3.1 Introduction

A solid knowledge and precise understanding of protein function can be enhanced greatly by obtaining detailed structural information. X-ray crystallography and NMR spectroscopy are two of the major techniques currently employed to gain such insights. The requirement to produce well-ordered crystals for high-resolution structural analysis is an important limiting factor in X-ray crystallographic studies, though easier when the protein of interest displays a relatively rigid structure. In the case of the 2-oxoacid dehydrogenase complexes, the flexibility of N-terminal domains is considered to prevent the formation of highly ordered crystals.

The E2 component of each complex consists of three types of independently folded protein domains (lipoyl domain, peripheral subunit binding domain and catalytic domain) joined by flexible polypeptide linker regions (Figure 3.1). The flexibility of the structure is necessary for multienzyme function, but appears to greatly reduce the ability to form intact crystals. For this reason, previous studies have attempted to overexpress and characterise the individual domains of the E2 component and also a truncated E2 core, lacking the N-terminal region, from several sources.

The lipoyl domain(s) and subgenes of the domains have been successfully overexpressed and shown to function independently (Miles & Guest, 1987; Ali & Guest, 1990; Dardel *et al.*, 1990). 3-D structures have been obtained using NMR spectroscopy, of the lipoyl domains from PDC of *B. stearrowthermophilus* (Dardel *et al.*, 1993) and *E. coli* (Green *et al.*, 1995). The catalytic domain from PDC of *A. vinelandii* has been overexpressed, leading to the three dimensional structure elucidation of the octahedral inner core complex (Mattevi *et al.*, 1992). However, attempts at the overexpression of the peripheral subunit binding domain alone, from any source, have proved unsuccessful. This has been overcome for the bacterial subunit binding domain by co-expression with the adjacent lipoyl domain (Hipps *et al.*, 1992; M.D. Allen, PhD thesis, 1995). This di-domain of *B. stearrowthermophilus*, comprising the lipoyl domain

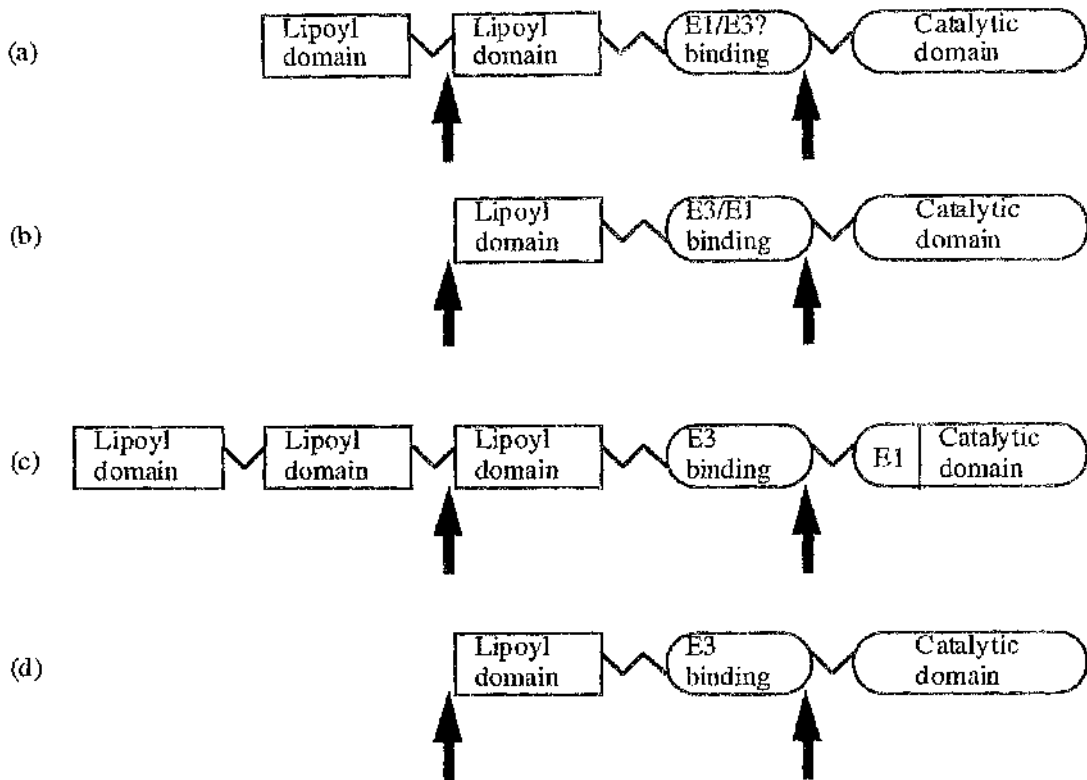
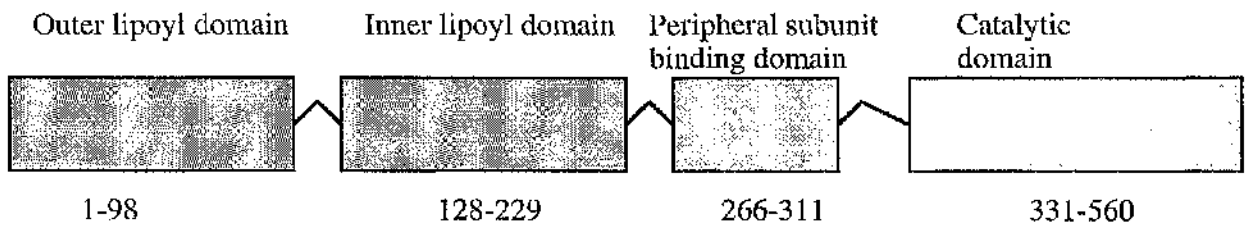


**Figure 3.1. Schematic representation of the multidomain structure of E2 and protein X.**

- (a) Mammalian PDC
- (b) Mammalian BCOADC
- (c) *E. coli* PDC
- (d) Protein X

The arrows define the boundaries of the di-domain.



Schematic representation of human E2-PDC demonstrating the approximate amino acid positions of each domain. The inner lipoyl domain DKA lipoic acid binding motif encompasses residues 172 to 174.

The numbering system is similar to that used by Gershwin *et al.*, 1990 and Quinn *et al.*, 1993.

and binding domain, joined by the flexible linker region was overexpressed in *E. coli*. The independently folded binding domain was then obtained following limited proteolytic digestion and purification (Hipps *et al.*, 1994).

To facilitate studies involving the subunit binding domain and inner lipoyl domain (the di-domain), large quantities of the domains are needed. None of the previous studies have involved the use of domains from mammalian sources. This chapter describes the molecular biological techniques employed to make the expression vectors allowing the overexpression of the di-domains from several sources; human PDC-E2, protein X, bovine BCOADC and *E. coli* PDC-E2. Successful overexpression will greatly facilitate crystallography studies and also permit investigation of domain interactions with the E1 and E3 enzymes, by surface plasmon resonance, leading to a greater understanding of the molecular recognition phenomena and active-site coupling within these complex multimeric assemblies.

### 3.2 Materials

The di-domain was PCR amplified from one of three plasmid sources:

Plasmid pHUMIT was the source of the human E2-PDC (kind donation by Dr. E. Gershwin). Plasmid pTSE2a1 was the source of the bovine BCOADC (kind donation by Dr. D.J. Danner). Plasmid pGS623 was the source of the *E. coli* PDC (kind donation by Prof. J. Guest). Human fetal liver cDNA was the template for the protein X di-domain.

The sequences of these sources are shown in Figures 3.2a to d.

The resultant product was amplified following ligation into the expression vector pET11a (Novagen) and insertion into *E. coli* DH5 $\alpha$ . Recombinant plasmid was subsequently used to transform the *E. coli* strains DE3 (BL21), or DE3plyS. This resulted in the production of large quantities of polypeptide in all cases.

1-MSPHCSTTYLRTLGRITTFWKTTEGRDGMKMAVQEFSEFGLLLQLLGSPGR  
 RYYSLPPHQKVPLPSLSPTMQAGTIARWEKKEGDKINEGDLIAEVETDKATVGF  
 ESLEECYMAKILVAEGTRDVPIGAIICTVVGKPEDIEAFKNYTLDSAAPTPQAAP  
 APTPAATASPPTPSAQAPGSSYPPHMQVLLPALSPTMTMGTVQRWEKKVGEKL  
 SEGDLLAEIETDKATIGFEVQEEGYLAKILVPEGTRDVPLGTPLCIIVEKEADISA  
 FADYRPTEVTDLKPQVPPPTPPPVAAVPPTPQPLAPTSTPCPATPAGPKGRVVFV  
 DPLAKKLAVEKGIDLTQVKGTGPDGRITK**KDIDSFVPSKV**APAPAAVVPPTGPG  
 MAPVPTGVFTDIPISNIRRVIAQRLMQSKQTIPHYLLSCKYGEVLLVRKELNKI  
 LEGRSKISVNDFIKASALACLKVPEANSSWMDTVIRQNHVVDVSVAVSTPAGL  
 ITP IVFNAHIKGVETIANDVVSLATKAREGKLPHEFQGGTFTISNLGMFGIK  
 NFSAIINPPQACILAIGASEDKLVPADNEKGFVDVASMMSVTLSCDHRVVDGAVG  
 AQWLAEFRKYLEKPTIMLL-613

**Figure 3.2a. The protein sequence of the E2 component of human PDC.**

The underlined sequences indicate the sequences to which the di-domain primers were made. The conserved DKA motif, to which the lipoic acid co-factor is attached, is highlighted in bold. The E2 gene is encoded by 613 amino acids, including a mitochondrial targeting sequence located at the N-terminus. The di-domain itself encompasses Ser-128 to Val-311.

-61MAAVRMLRTWSRNAGK**LICVRYFQTCGNVHVLKPNYVCF**FGYPSFKYSH**P**  
 HHFLKTT**AALRGOVVQFKLSDIGEGIREVT**VKEWYVKEGDTVSQFDSICE  
 VQSDKASVTTTSRYDGV**IKKLYYNLDDIAYVGKPLVDIETEAL**KDSEEDVVETP  
 AVSHDEH**THQEI**KGRKTLATPAV**RR**LAMEN**NIK**LSEV**VGS**GKDGRILKEDIL**N**  
**YLEKQTGAILPPSPKVEIMPPPPKPKDM**TV**PILVSKPPVFTGKDKTEPIKGFQKA**  
 MVKTMSAALKIPHF**GYCDEIDL**TEL**VKLREELKPIAFARGIKLSFMPFFLKAASL**  
 GLLQFPILNASVDENCQNITYKASHNIGIAMDTEQGLIVPNVKNVQICSIFDIATE  
 LNRLQKLGSV**GQLSTTDLTGGTFTLSNIGSIGGTF**AKPVIMPPEVAIGALGSIKA  
 IPRFNQKGEVYKAQIMNVSW**SADHRVIDGATMSRFSNLWKSYLE**NP**AFMLLD**  
 LK-482.

**Figure 3.2b. The protein sequence of bovine BCOADC E2 component.**

The underlined sequences indicate the sequences to which the di-domain primers were made. The conserved DKA motif, to which the lipoic acid co-factor is attached, is highlighted in bold. The E2 gene is encoded by 482 amino acids, including a mitochondrial targeting sequence located at the N-terminus. The di-domain itself encompasses Ala-58 to Leu-217.

1.MAIEIKVPDIGADEVEITEILVKVGDKVEAEQSLITVEGDDKASMEVPSPQAGI  
 VKEIKVSVGDKTQTGALIMIFDSADGAADAAPAQAFFKKEAAPAAAPAAAAAK  
 DVNVPDIGSDEVEVTEILVKVGDKVEAEQSLITVEGDKASMEVPAPFAGTVKEIL  
 VNVGDKVSTGSLIMVFEVAGEAGAAPAAKQEAAAPAAAPAPAAGVKEVNVDPDIG  
 GDEVEVTEVMVLVGDKVAAEQSLITVEG**DK**ASMEVPAPFAGVVKELKVNVD  
 KVKTGSLIMIFEVEGAAPAAAPAKQEAAAPAPAAKAEAPAAAPAAKAEGKSEP  
 AENDAYVHATPLIRRLAREFGVNLAKVKGTGRLGRILREDVQAYVKEAIKRAF  
 AAPAATGGGIPGMLPWPKVDFSKFGEIEEVELGRIQKISGANLSRNWVMIPIV  
 THFDKTDITELEAFRKQQNEEAARKKLDVKITPVVVFIMKAVAAALEQMPRFNSS  
 LSEDGQRLTLKKYINIGVAVDTPNGLVVPVFKVNKKGIHLSRELMTISKKARD  
 GKLTAGEMQGGCFTISSIGGLGTTHFAPIVNAPEVAILGVSKSAMEPVWNGKE  
 FVPRLMLPISLSFDHRVIDGADGARFITIINNTSDIRRLVM-627

**Figure 3.2c. The protein sequence of the *aceF* gene, encoding the E2 component of the *E. coli* PDC.**

The underlined sequences indicate the sequences to which the di-domain primers were made. The conserved DKA motif, to which the lipoic acid co-factor is attached, is highlighted in bold. The E2 gene is encoded by 627 amino acids. The di-domain itself encompasses Val-221 to Ile-369.

-53MAASWRLGCDPRLRLYLVGFPGCRSVGLVKGALGWSVSRG  
 ANWRWFHSTQWLRGDPIKILMPSLSPTMEEGNIVKWLKKEGEAVSAGDAL  
 CEIET**DKA**VVTLDASDDGILAKIVVEEGSKNIRLGSLIGLIVEEGEDWKHVEIPK  
 DVGPPPPVSKPSEPRPSPEPQISIPVKKEHIPGTLRFRLSPAARNILEKHSILDASQ  
 GTATGPRGIFTKEDALKLVQLKQTGKITESRPTPAPTATPTAPSPLQATSGPSYP  
 RPVIPPVSTPGQPNAVGTFTFTEIPASNIRRVIAKRLTESKSTVPHAYATADCDLGA  
 VLKVRQDLVKDDIKVSVNDFIIKAAAVTLKQMPDVNVSWDGEKPKQLPFIDISV  
 AVATDKGLLTPIIKDAAAKGIQEIADSVKALSKKARDGKLLPBEYQGGSFISISNL  
 GMFGIDEFTAVINPPQACILAVGRFRPVLKLTDEEENAKLQQRQLITVTMSSDS  
 RVVDDELATRFLKSFKANLENPIRLA-448

**Figure 3.2d. The protein sequence of protein X from a human fetal liver source.**

The underlined sections indicate the sequences to which the di-domain primers were made (to). The conserved DKA motif, to which the lipoic acid co-factor is attached, is highlighted in bold. The protein X gene is encoded by 448 amino acids. The di-domain itself encompasses Gly-1 to Gly-199.

### 3.3 Aims of this chapter

- (i) Generation of PCR-amplified di-domains.
- (ii) Engineering of *E. coli* strains capable of overexpressing the di-domains.
- (iii) Confirmation of the correct folding of the di-domains.
- (iv) Investigation into the effect of exogenous lipoic acid on the lipoylation of the di-domains.
- (v) Investigation into the effect of the presence of the mitochondrial presequence on the folding and lipoylation of the BCOADC di-domain.

### 3.4 Results

#### 3.4.1 Construction of di-domain DNA

The PCR reactions were carried out using the oligonucleotides described in Figure 3.3 and the products analysed on 2% agarose gels (Figure 3.4). PCR mutagenesis was employed such that each upstream primer was designed so as to create an Nde I restriction site on the resultant PCR product. The site also incorporates an ATG start codon. Each downstream primer was designed to create a Bam HI restriction site in the PCR product. These allowed incorporation into the multiple cloning site of the pET11a expression vector (Novagen).

#### 3.4.2 Construction of pET11a expression vector

The expression vector pET11a (Novagen) was digested with the Nde-I and Bam III, as detailed in section 2.2.9.1 and treated with calf intestine alkaline phosphatase. The PCR fragments containing the di-domains were then ligated into the pET vector. Ligation was carried out as detailed in Materials and Methods section 2.10. *E. coli* DH5 $\alpha$  cells were transformed with the resultant plasmid and grown on plates containing LB medium supplemented with ampicillin (Materials and Methods section 2.12). Colonies

**Human PDC**

5'Primer: AGG CTC CTC ATA TGT CAT ATC CCC CTC ACA TG  
 3' Primer: CTT GGC ACG GAT CCA GTG ATA TCC TTC CTG GTG

**Bovine BCOADC**

5' Primer: GCT GCT CAT ATG GGA CAG GTT GTT CAG TTC AAG  
 3' Primer: CAA TAT AGC GGA TCC AGT CCT TTC CAA ATA GTT

***E. coli* PDC**

5' Primer: GTG ACT GAA CAT ATG GTG AAA GGC GAC AA  
 3' Primer: GAT AGC TTC GGA TCC AGT AGC CTG AAC GTC TTC

**Human protein X**

5' Primer: ACG CAG TGG CAT ATG GGT GAT CCC ATT AAG ATA CTA  
 3' Primer: TCC AGA TGT GGA TCC AGT GGG CGA AGG TGC TGT

**Figure 3.3. Primer sequences to allow the amplification of the di-domain from the E2 and protein X sources.**

The underlined portion of the 5' primer indicated the site of the Nde I restriction digest site and the underlined portion of the 3' primer indicates the site of the Bam HI restriction digest site.

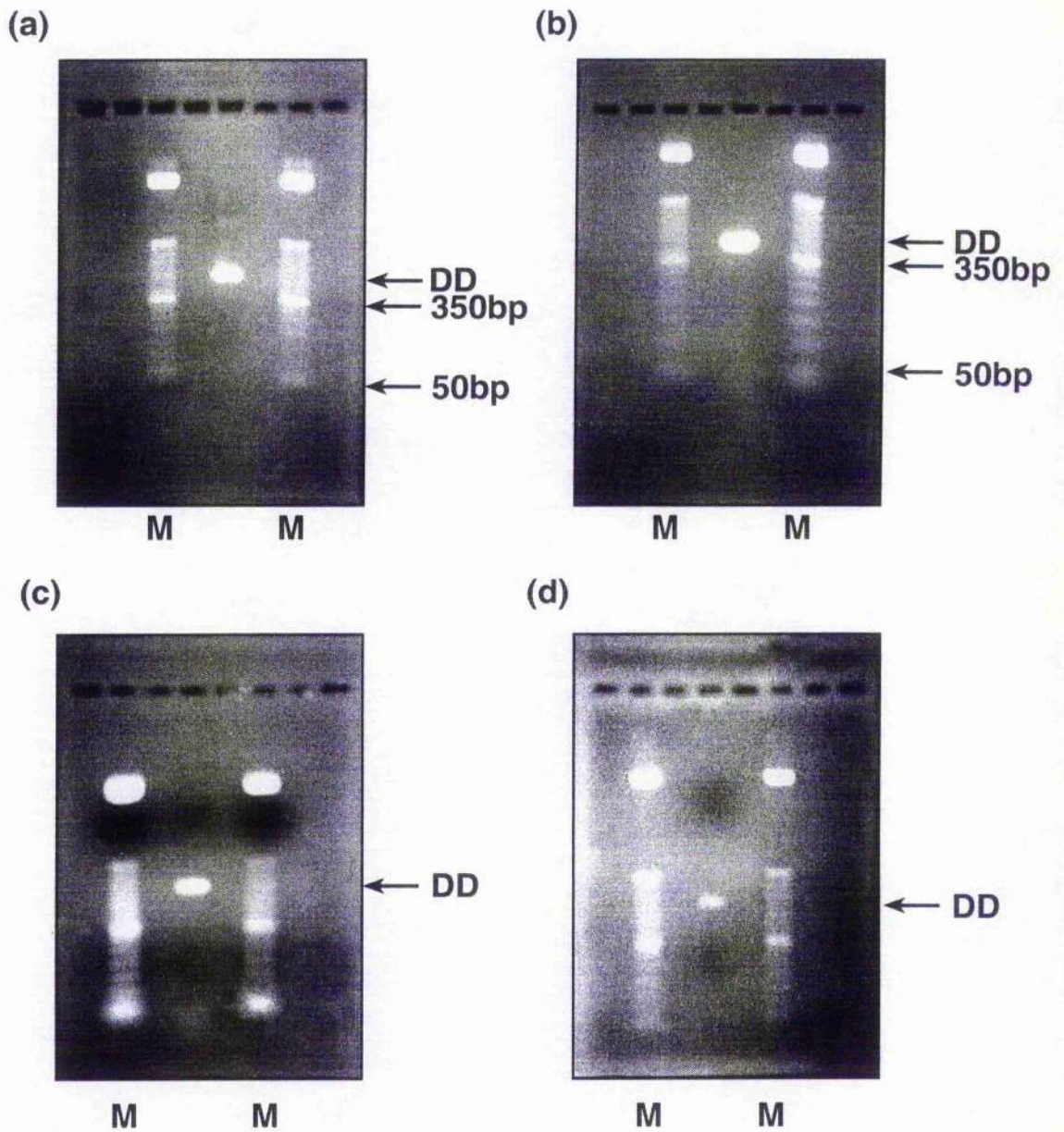


**Figure 3.4. PCR amplification of the di-domain (DD) from various sources.**

(a) Bovine BCOADC-E2 (b) *E. coli* PDC-E2 (c) Human protein X (d) Human PDC-E2  
 Samples were run on 2% agarose gels, then visualised using UV illumination following ethidium bromide staining. M, molecular mass marker (50bp ladder).

were picked and grown overnight in 5ml aliquots of ampicillin-supplemented LB. Minipreps were carried out (Promega) to obtain plasmid DNA for the subsequent transformation of the expression strains *E. coli* DE3 or DE3 pLysS.

### **3.4.3 Overexpression of vector in *E. coli* DE3 (BL21)**

Overexpression of each of the four sources of di-domain was observed following the transformation of *E. coli* DE3 (BL21) cells (Materials and Methods section 2.15) using IPTG induction (Materials and Methods section 2.16). Visualisation of the protein was carried out by resolution on a 15% SDS-polyacrylamide gel (Materials and Methods section 2.2.16) and staining with Coomassie Brilliant Blue. A substantial overexpression was observed within an hour of induction in all cases (Figure 3.5a-d).

### **3.4.4 Confirmation of correct folding of the di-domain**

The lipoylation of the heterologously-expressed domains can only occur after correct folding of their respective lipoyl domains. Access to a monoclonal antibody (PD1) which exclusively recognises the holodomain form of the human inner E2 lipoyl domain was generously provided by Prof. F. Stevenson, University of Southampton. (Figure 3.6b). Initially the specificity of the antibody for the holodomain was tested using purified human unlipoylated and lipoylated domain (kind donation from Dr. J. Palmer, University of Newcastle). Samples of each domain were initially resolved on a 15% SDS-polyacrylamide gel and stained with Coomassie Brilliant Blue (Figure 3.6a) to confirm their purity, prior to being used for immunoblotting. It is clear from figure 3.6b that monoclonal PD1 displays strong reactivity solely with the lipoylated form of the domain. Figures 3.7 and 3.8 demonstrate that, in addition to E2-PDC, a high level of reactivity is observed with the di-domains of BCOADC and protein X. This indicates that both of these di-domains are also recognised by the *E. coli* lipoyl ligase. No cross reactivity was observed with *E. coli* E2-PDC.

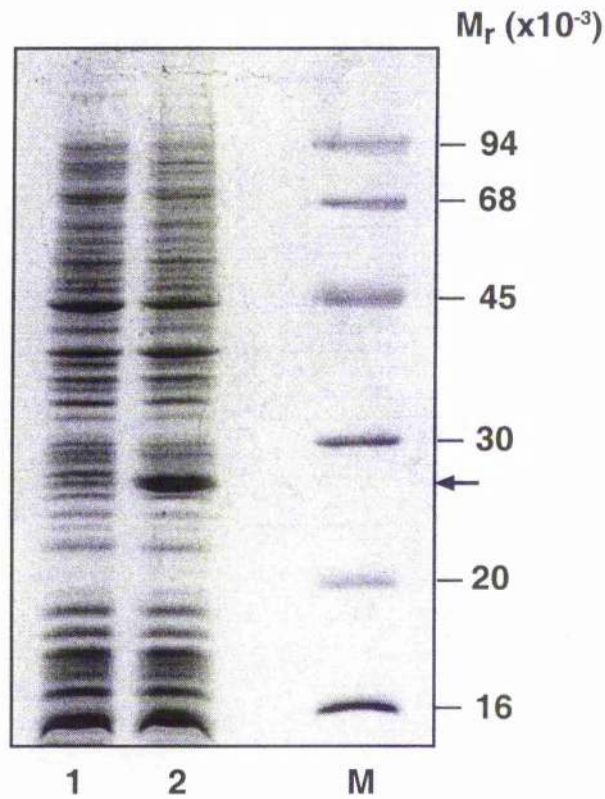


**Figure 3.5 (a) Overexpression of the di-domain of human PDC in *E. coli* DE3.**

Following IPTG-induction, total *E. coli* extracts were run on a 15% SDS-PAGE gel (see Materials and Methods). Lane 1, sample taken prior to induction and lane 2, sample taken 3h after induction. Lane M, molecular mass marker. The arrow indicates the overexpressed protein.

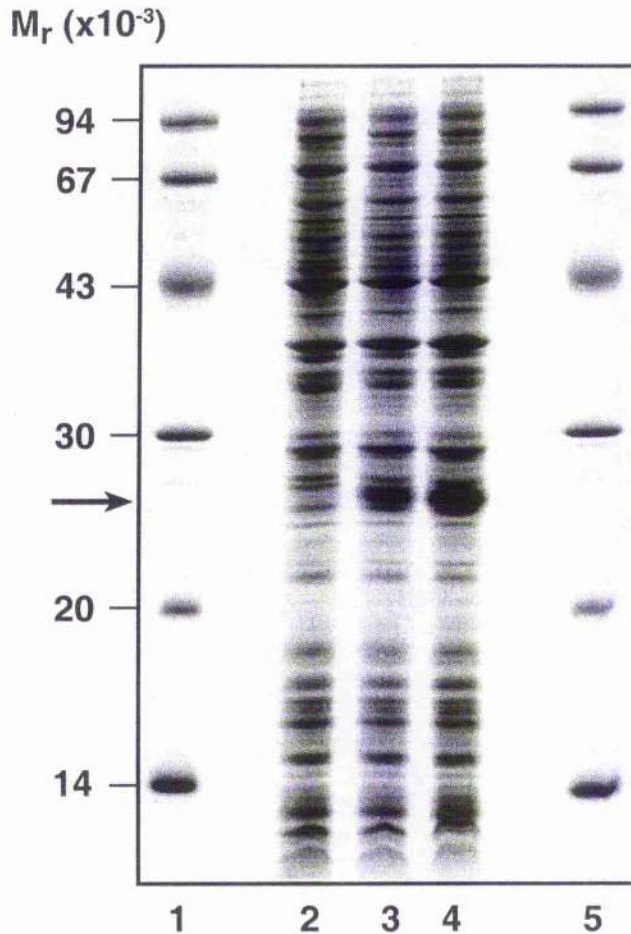


**Figure 3.5 (b) Overexpression of the bovine BCOADC di-domain in *E. coli* DE3.**

*E. coli* extracts were prepared from cultures and samples were collected prior to and 1 and 3h following IPTG-induction, then run on a 15% SDS-PAGE gel. Lanes 1 and 5, molecular mass marker. The pre-induced sample is in lane 2, the 1h post-induction sample in lane 3 and the 3h post-induction sample in lane 4. The arrow indicates the di-domain.

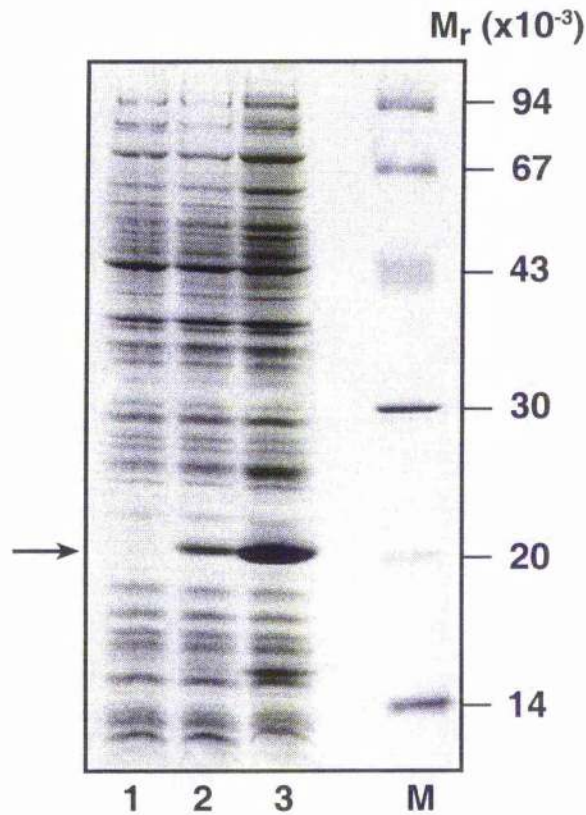


**Figure 3.5 (c) Overexpression of *E. coli* PDC di-domain in *E. coli* DE3.** *E. coli* extracts were prepared from cultures and samples collected prior to and then 1 and 3h following IPTG-induction (Lanes 1, 2 and 3 respectively). Lane M, molecular mass marker. Samples were resolved on a 15% SDS-PAGE gel. The arrow indicates the di-domain.

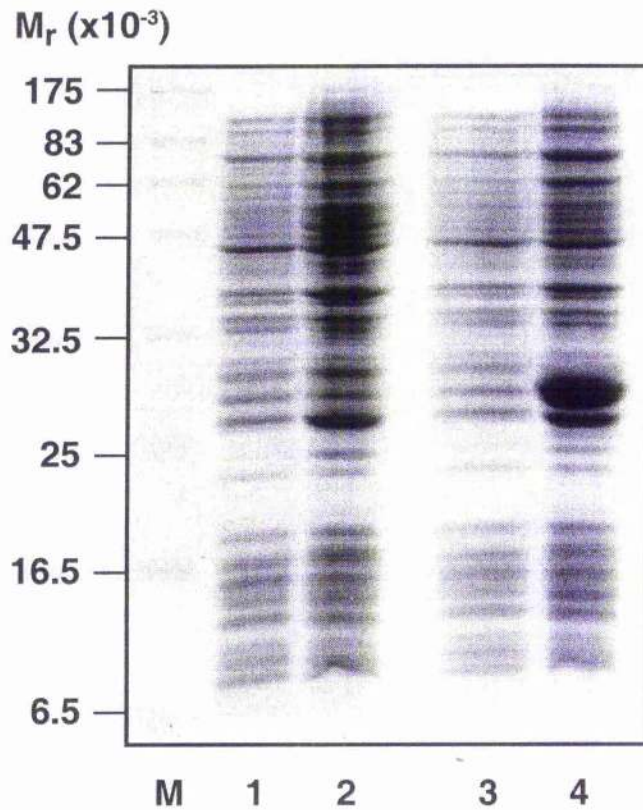


**Figure 3.5 (d) Overexpression of human protein X di-domain in *E. coli* DE3pLysS.**

*E. coli* extracts were prepared from cultures and samples collected prior to and 3h following IPTG-induction, then run on a 15% SDS-PAGE gel. Lanes 1 and 2 show a non-expressing clone, prior to and 3h after induction. Lanes 3 and 4 show the overexpression of the di-domain after 3h. Lane M, molecular mass marker.

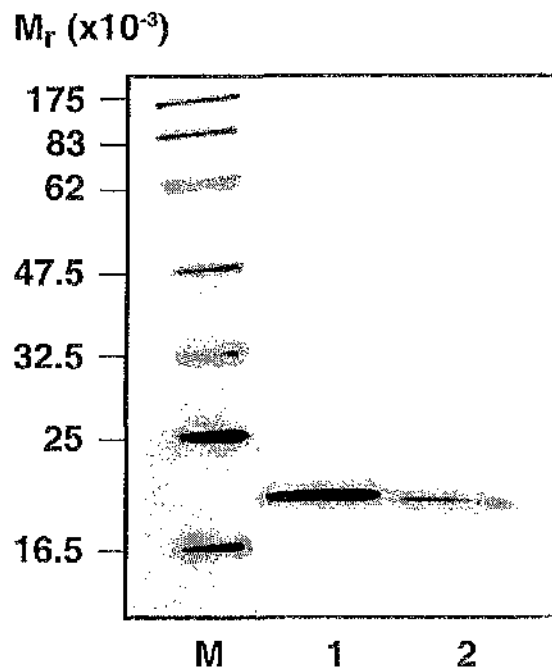


**Figure 3.6 (a).** SDS-PAGE analysis of purified apo- and holo-lipoyl domain from human PDC.

Samples were run on a 15% SDS gel and stained with Coomassie Blue. Lane 1, the unlipoylated protein (3  $\mu\text{g}$ ) and Lane 2, the lipoylated protein (1.5  $\mu\text{g}$ ). M, molecular mass marker.

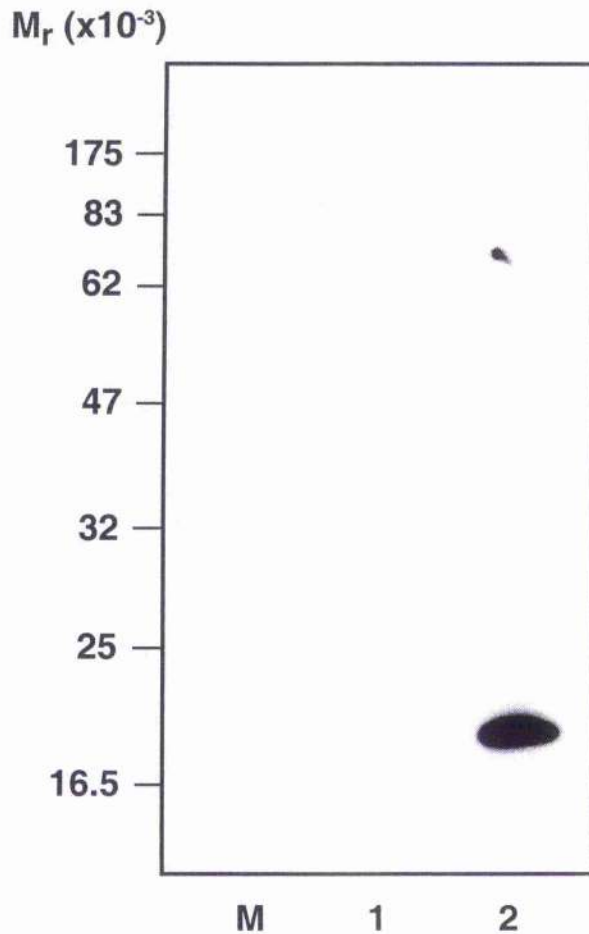


**Figure 3.6(b). Immunoblot of apo- and holo-forms of the lipoyl domain.**

Samples of purified unlipoylated ( $1\mu\text{g}$ ) and lipoylated ( $1\mu\text{g}$ ) human lipoyl domain were resolved on a 15% SDS-polyacrylamide gel prior to Western blotting with a monoclonal antibody, specific for the holodomain.

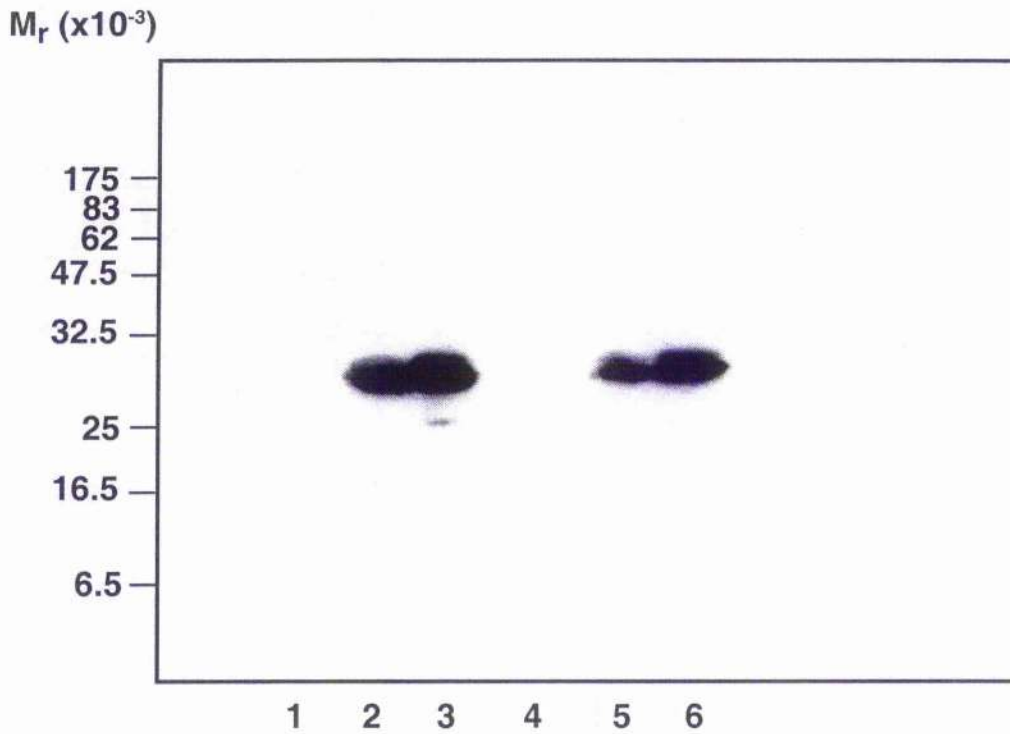


**Figure 3.7. Immunoblot of the di-domains of E2-PDC and E2-BCOADC induced in the presence or absence of exogenous lipoic acid.**

Lanes 1 and 4 contain pre-induced di-domain. Lanes 2 and 5 contain samples of E2-PDC and E2-BCOADC respectively, collected 3h following IPTG induction. Lanes 3 and 6 contain samples collected 3h after induction, in the presence of lipoic acid (10 $\mu$ g/ml).

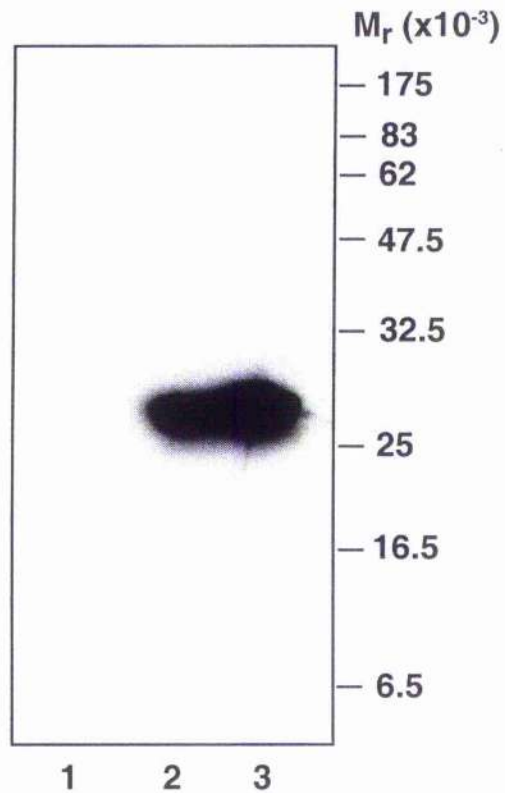


**Figure 3.8.** Immunoblot analysis of the di-domain of protein X, showing enhancement of lipoylation in the presence of exogenous lipoic acid.

Lane 1 contains the pre-induced sample. Lane 2 contains the 3h post-induction sample, grown without lipoic acid, and Lane 3, the 3h post-induction sample grown with lipoic acid.

### 3.4.5 Enhancement of Lipoylation using exogenous Lipoic Acid

The immunoblots also demonstrate the ability to enhance the amount of domain that has been lipoylated by the addition of lipoic acid (10µg/ml) to the cultures at the time of IPTG-induction. The immunoblots were also analysed on native gels (Figure 3.9) but the signal was not as strong or specific, so SDS gels were employed in subsequent studies.

In the case of the protein X di-domain, a mobility shift can clearly be observed on enhanced lipoylation, as monitored by SDS-PAGE and staining with Coomassie Blue (Figure 3.10). In the absence of lipoic acid, two bands of approx. equal intensity were seen to be overexpressed (apo- and holo-domain). When lipoic acid is added to the culture, there is a marked shift to the lower band (the holo-domain). The lipoylated domain runs faster presumably as a result of a change in conformation caused by the presence of the lipoic acid co-factor.

## 3.5 Conclusions

A prerequisite for in-depth analysis of interactions between the constitutive components of the 2-oxoacid dehydrogenase complexes is the ability to produce large quantities of native protein. In this chapter, a method has been devised to allow the production of large amounts of the requisite lipoyl domain linked to the adjacent peripheral subunit binding domain (termed the di-domain). It has been possible to overexpress successfully the di-domain from 4 sources; human E2-PDC, bovine E2-PDC, *E. coli* E2-PDC and human protein X using the expression vector pET11a. Indeed, high levels of protein were detected within 1h of induction with IPTG. The overexpression was attempted over a series of temperatures, (data not shown) and 37°C deemed optimal, in all cases.

It has also been demonstrated that the heterologously-expressed mammalian di-domains retain their ability to fold correctly and act as substrates for the *E. coli* lipoylation system as evidenced by their cross reactivity with monoclonal antibody PD1. Previously studies with this antibody have been performed with native polyacrylamide gels (Quinn, 1997), so it was necessary to determine its ability to cross-react specifically with the holodomain under denaturing conditions. It has been shown here that the denaturing conditions did not affect the specificity or inhibit the cross-reactivity of the antibody, despite the fact that many monoclonals are only active against native protein, since they are raised against non-contiguous epitopes. In the absence of exogenous lipoate, it is apparent that incorporation of the lipoic acid prosthetic group into the apodomains of E2-PDC and BCOADC and protein X is incomplete. Best estimates are that approx. 50% lipoylation occurs in the absence of added cofactor as there is a 1.5-2.5-fold enhancement in cross reactivity with PD1 when induction is performed in the presence of lipoate (10µg/ml). Due to the high levels of expression of the di-domains (approx. 20% of the whole cell extract appears to be the di-domain protein) the lipoylating apparatus of the *E. coli* is not capable of attaining 100% lipoylation without exogenous assistance. The rate of production of endogenous lipoic acid is not capable of meeting the rate of production of the di-domain.

In retrospect, a different expression vector may have been chosen to carry out these studies. Following the overexpression of the di-domain, a method to purify it is required for many types of biochemical and biophysical analyses. It would seem more advantageous to produce the di-domains as GST-fusion proteins or His tagged proteins, which would greatly simplify their purification. Indeed, various members of the laboratory are presently undertaking this work.

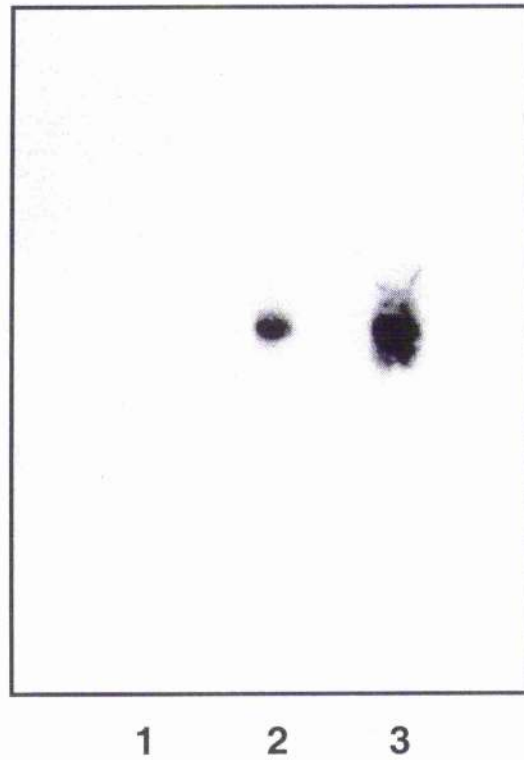


**Figure 3.9. Immunoblot on a native gel of the di-domain of E2-PDC, showing the enhancement of lipoylation as a result of exogenous lipoic acid.**

Lane 1 contains the pre-induced sample. Lane 2 contains the 3h post-induction sample, grown without lipoic acid, and lane 3, the 3h post-induction sample grown with lipoic acid.

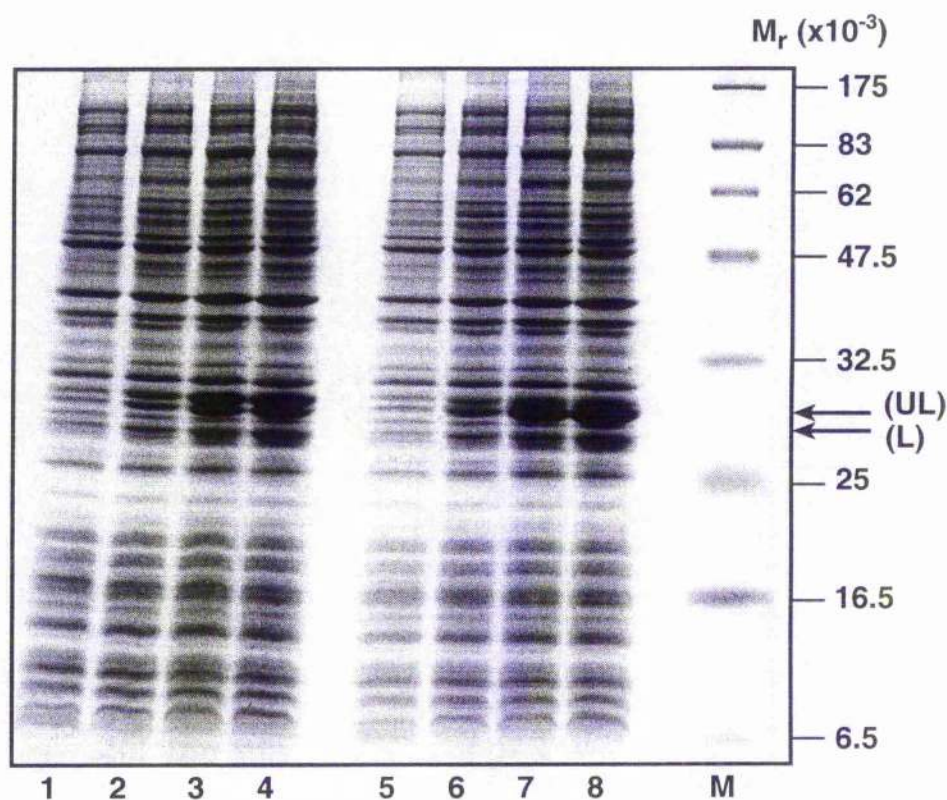


**Figure 3.10. SDS-PAGE analysis of human protein X di-domain overexpression in *E. coli* DE3pLysS, in the absence and presence of exogenous lipoic acid.**

Lanes 1 to 4 represent pre-induced, then 1, 2, and 3h post-induction samples grown without exogenous lipoic acid. Lanes 5 to 8 represent the same culture grown in the presence of exogenous lipoic acid (10 $\mu$ g/ml). Two proteins seem to be overexpressed, representing the unlipoylated (UL) and lipoylated (L) forms. An obvious shift to the lipoylated form is seen when lipoic acid is added. Lane M, molecular mass marker.

The generation of *E. coli* with the ability to express the di-domains to such high levels provides a method of producing sufficient protein to further investigate protein-protein interactions within these important multienzyme complexes. It will allow the study of the kinetics of the various domain interactions with the aim of generating affinity and binding constants, which until now has been hampered by the low levels of material available. An investigation into this area is detailed in chapter 6 of this thesis.

### **3.6 The effect of the presence of the presequence on the ability of the BCOADC di-domain to undergo lipoylation.**

As an adjunct to this chapter, it was decided to investigate the effect that the presence of the mitochondrial presequence has on the ability of the BCOADC di-domain to fold and undergo lipoylation. As previously mentioned, the components of the 2-oxoacid dehydrogenase complex are nuclear encoded and therefore require to be transported to and then across the mitochondrial membrane. The precursor polypeptide has a long presequence attached at the N-terminus, which is involved in the targeting to the organelle.

#### **3.6.1 Construction of BCOADC sub gene:**

##### **Presequence-di-domain.**

In order to do this, a primer was designed to the N-terminus of the precursor polypeptide and used along with the existing primer designed to sequence downstream of the di-domain to amplify the intermediate sequence from the vector pTSE2a1. This contains the entire bovine BCOADC E2 gene. The primers were both designed with restriction sites (Nde I on the upstream primer and Bam HI on the downstream primer) to facilitate ligation to the pET11a expression vector. Following propagation in *E. coli*

DH5 $\alpha$ , *E. coli* DE3 were transformed with the plasmid and colonies chosen, on the basis of restriction digests (data not shown), for further study. Professor Gordon Lindsay kindly carried out these initial stages.

### **3.6.2 Overexpression of BCOADC presequence-di-domain construct.**

Two colonies referred to here as B4 and C5 were chosen for the overexpression studies. Following IPTG induction, the cultures were left to grow at 37°C for 4h before the cells were harvested and samples resolved by 15% SDS-PAGE. Visualisation of the proteins was carried out on a light box, following staining with Coomassie Blue dye. Significant overexpression of a protein, larger than the native protein, was seen after this time (Figure 3.11).

### **3.7 The effect of the presence of presequence on the lipoylation of the di-domain, as shown by Western Blotting (ECL).**

Having established the correct construction of the presequence-di-domain subgene, the next study involved investigating whether the di-domain segment was capable of undergoing lipoylation. To do this, B4 and C5 were induced in the presence and absence of exogenous lipoic acid, as was a BCOADC di-domain clone as a control and then the samples blotted with the monoclonal Ab (PD1) specific for the lipoylated domain (Figure 3.12). The immunoblot shows reactivity with the di-domain alone, which is enhanced by inducing in the presence of lipoic acid. It also shows that there is no reactivity with the presequence-di-domain clones, even when the cultures are supplemented.

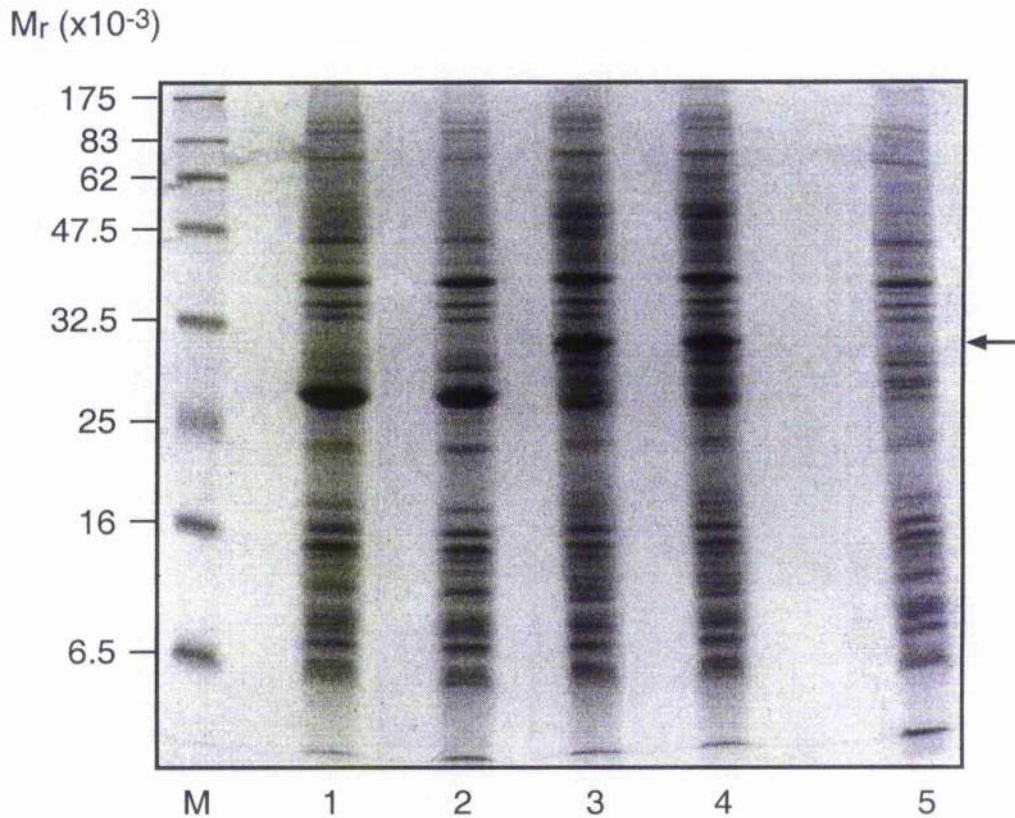


**Figure 3.11. Overexpression of BCOADC di-domain, alongside clones B4 and C5 which overexpress the di-domain plus pre-sequence construct.** Lanes 1 and 2 show the BCOADC di-domain overexpressed without and in the presence of exogenous lipoic acid respectively. Lanes 3 and 4 show clones B4 and C5 respectively overexpressing the pre-sequence di-domain constructs, in the presence of exogenous lipoic acid. Lane 5, un-induced extract. Lane M, molecular mass marker.

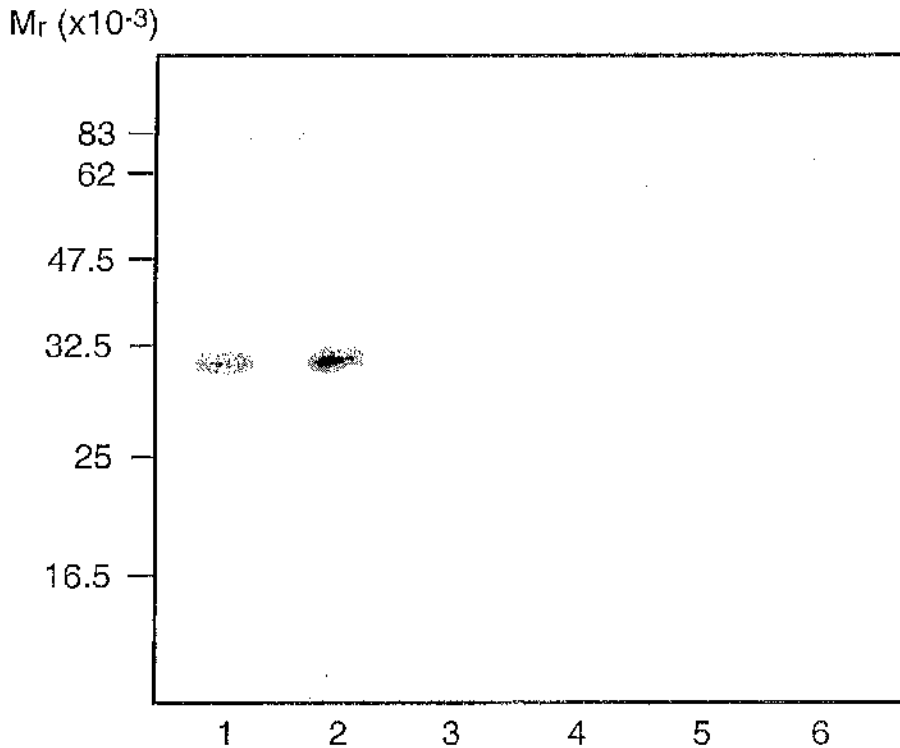


**Figure 3.12.** Immunoblot showing the detection of the BCOADC di-domain and the BCOADC pre-sequence-di-domain constructs, using the monoclonal antibody, PD1, specific for the lipoylated form of the lipoyl domain. Lanes 1 and 2 respectively, BCOADC di-domain overexpressed in the absence and presence of exogenous lipoic acid. Lanes 3 and 4 respectively, clone B4, overexpressing the BCOADC pre-sequence-di-domain construct in the absence and presence of exogenous lipoic acid. Lanes 5 and 6 respectively, clone C5, overexpressing the BCOADC pre-sequence-di-domain construct in the absence and presence of exogenous lipoic acid.

### 3.8 Discussion

These preliminary studies show that it is possible to attain the overexpression of the BCOADC di-domain with the mitochondrial pre-sequence also attached. The fact that the pre-sequence-di-domain constructs are apparently unable to undergo lipoylation could be explained by the presence of the pre-sequence leading to or preventing the correct folding of the di-domain. This would result in the inability to undergo lipoylation, as only the correctly folded domain can be recognised by the lipoylating apparatus. Furthermore, the incorrect folding may increase the susceptibility of the construct to degradation. It has not yet been determined which part, indeed if all the pre-sequence is required for targeting and maintaining the immature folded structure necessary for entry into the mitochondrion. To this end, work is currently being undertaken in our laboratory using deletion mutants of the pre-sequence-di-domain construct. It is hoped to discover which residues or regions of the pre-sequence are essential for keeping the di-domain unfolded. The work should also show which regions are essential for targeting to the mitochondrion. These experiments are yet another example of work which has now been made possible by developing a method for overexpressing sub genes of the vast 2-oxoacid dehydrogenase complexes.

**CHAPTER 4.**

**INVESTIGATION INTO THE LIPOYLATION OF THE APODOMAINS  
OF THE E2 AND PROTEIN X COMPONENTS OF HUMAN  
PYRUVATE DEHYDROGENASE COMPLEX.**

#### 4.1 Introduction.

The oxidative decarboxylation of 2-oxoacids carried out by the complexes is mediated partially by the sulphur-containing prosthetic group, lipoic acid that is located on the E2 or protein X components on these complexes. This prosthetic group is covalently bound via an amide linkage between the carboxyl group of lipoic acid and the  $\epsilon$ -amino group of a specific lysine residue. The lipoyl-lysine residue has a side chain 1.4nm long, which acts as a "swinging arm", carrying the substrate between three active sites; additional flexibility of the domain itself is provided by ala-pro rich sequences linking the lipoyl domains to each other and to the C-terminal half of these polypeptides, allowing interaction with all 3 active sites. Although the role of lipoic acid in the catalytic cycle has been well studied, it is only recently that research on the enzymes responsible for the insertion of the lipoyl group and their recognition properties has started to be examined in detail.

There are 2 types of systems responsible for lipoylation, both using lipoyl-AMP as an intermediate:

- (i) In *E. coli*, there is a single enzyme (lipoate-protein ligase), which activates and ligates the lipoyl groups to the apoenzyme.
- (ii) In mammalian systems there are 2 separate enzymes; lipoyltransferase, responsible for the transfer of lipoyl groups from the lipoyl-AMP intermediate to the apoenzyme and lipoic acid activating enzyme, which initially activates the lipoic acid moiety.

#### 4.2 Initial lipoylation studies on the E2 component

In 1958, Reed *et al.* first described the lipoylation of PDC, using lipoic acid deficient *S. faecalis* cells. Following incubation with [ $^{35}\text{S}$ ] lipoic acid, increases in both the amount of bound lipoic acid and in PDC activity were noted. Subsequent precipitation steps isolated the system responsible for protein lipoylation. This comprised 2 fractions, a heat-labile and a heat-stable fraction, both required for the activation of the apo-PDC.

The heat-labile fraction catalysed the activation of the lipoic acid. Further work by the group showed that in order to activate apo-PDC, the intermediate lipoyl-AMP is required. This then suggested that the attachment of the lipoic acid to the E2 polypeptide occurred in two consecutive reactions;

(i) Lipoic Acid + ATP  $\rightarrow$  Lipoyl-AMP + PPi

(ii) Lipoyl-AMP + Apoprotein  $\rightarrow$  Lipoylated Holoenzyme + AMP

Until recently, little progress had been made in the study of lipoylation, owing to lack of a suitable substrate for the lipoylation reaction. Overexpression of subgenes using recombinant DNA techniques has allowed studies to progress in eukaryotes as well as bacteria. Overexpression of subgenes encoding single lipoyl domains from *E. coli*, *B. stearothermophilus* and human sources provides both lipoylated and unlipoylated domains as the host cells are often unable to synthesise lipoate in sufficient amounts to meet the levels of overexpression.

### 4.3 The *E. coli* system of lipoylation

In *E. coli*, holo- and apolipoyl domains of PDC were overexpressed and purified (Ali and Guest, 1990). Two independent lipoate-protein ligase activities were then determined (LPL-A and LPL-B) (Brookfield *et al.*, 1991). Both have subunit  $M_r$  values of approx. 45,000 and catalyse lipoylation of apo-domain in the presence of lipoic acid, ATP and  $Mg^{2+}$ . The main difference is in the inability of LPL-A to use octanoic acid as a substrate.

Wallis and Perham (1994) demonstrated that *E. coli* lipoate-protein ligase can lipoylate the correct lysine residue of foreign lipoyl domains. To confirm the necessity for the specific lysine residue, site-directed mutagenesis was carried out on a sub-gene encoding the lipoyl domain of *B. stearothermophilus* PDC, expressed in *E. coli*. Either the target lysine was moved or an extra one was introduced. In both cases, the ligase

was unable to recognise any lysine other than that located in the original position (Lys 42).

In 1994, Morris *et al.* using transposon mutagenesis to isolate mutants, which can only grow under conditions that bypass any requirement for the lipoate-dependent enzymes, isolated the gene encoding the *E. coli* lipoate-protein ligase. This *lpl-A* gene was cloned and sequenced and found to encode a 338 amino acid protein with an upstream ribosome-binding site and a downstream Rho-independent transcriptional terminator. Overexpression and purification of the *lpl-A* gene product allowed studies which confirmed that the enzyme is ATP-dependent, catalysing both the activation of lipoic acid to lipoyl-AMP as well as the transfer of the activated species to apoprotein, with the concomitant release of AMP. Morris *et al.* (1994) also suggested that the two lipoylation activities described by Brookfield *et al.* (1991) were isoforms of the *lpl-A* gene product, as neither was detectable in *lpl-A* null mutants.

In 1995, Morris *et al.* proposed a second pathway of lipoylation, not involving the *lpl-A* gene product. They demonstrated, using null mutants, that *lip-B* (a gene previously thought to be involved in lipoic acid biosynthesis or metabolism) is responsible for *lpl-A*-independent lipoylation, using lipoic acid generated endogenously. If free lipoic acid is available, the *E. coli* use *lpl-A* to catalyse lipoyl-AMP formation. When there is no exogenous lipoic acid present, the *lip-B*-dependent ligase second pathway forms lipoyl groups by *de novo* synthesis. Both reactions appear to be catalysed by single enzymes in *E. coli*.

#### 4.4 Lipoylation of mammalian E2

With the advent of recombinant DNA technology, it has now been possible to generate lipoylated and unlipoylated forms of mammalian lipoyl domain. Quinn *et al.* (1993) overexpressed a subgene encoding the fusion protein of the inner lipoyl domain of human E2-PDC with glutathione S-transferase in *E. coli*. Both forms of the domain

have been purified. Brookfield *et al.* (1991) incubated the unlipoylated form with partially purified lipoate-ligase B from *E. coli* (Brookfield *et al.*, 1991) and the majority was converted to the lipoylated form, although at a considerably reduced rate. The presence of lipoylation activity in the mitochondrial matrix was demonstrated by Griffin *et al.* (1990). Recombinant mature bovine E2 (E2b) was overexpressed in *E. coli* and used as a substrate. Following incubation with [2-<sup>3</sup>H] lipoic acid, ATP and a soluble extract from the matrix of bovine liver mitochondria, incorporation of the radiolabelled lipoic acid into E2b was detected. It was also shown to be ATP-dependent. Having established the presence in mitochondria of the lipoyltransferase enzyme, attempts were made to purify it from bovine liver mitochondria (Fujiwara *et al.*, 1994). Partial purification on hydroxylapatite columns resolved 2 peaks of activity.  $M_r$  determinations of both forms showed proteins of subunit  $M_r$  40,000.

Both lipoyltransferases I and II catalysed lipoylation of apo-protein, being absolutely dependent upon lipoyl-AMP and apo-protein (Fujiwara *et al.*, 1996). In contrast to *E. coli* lipoate-protein ligase, these enzymes could not use lipoic acid plus Mg-ATP as the lipoyl donor. The bovine lipoyltransferases, when incubated with lipoyl-AMP and various apolipoyl domains were able to recognise and lipoylate rat E2p and E2o. This initially suggested that the enzyme recognises some features of the primary structure. Fujiwara *et al.* (1991) carried out site-directed mutagenesis studies on H-protein. This is one of 4 proteins making up the glycine cleavage system, which catalyses the reversible oxidation of glycine to yield carbon dioxide, ammonia, 5,10-methylenetetrahydrofolate and NADH. H-protein shows significant sequence homology with the corresponding region of E2 and also uses lipoic acid as a cofactor in its catalytic mechanism. They showed that conversion of a Glu residue, (3 residues upstream from the lipoyl lysine) to glutamine, alanine, or aspartic acid inhibited lipoylation by up to 60%. They also showed the positioning of a glycine residue 11 residues downstream was involved in lipoylation. These results indicate that both charge and structure are both important for maximal lipoylation.

#### 4.5 Structure of lipoyl domains.

A subgene encoding the N-terminal 85 amino acids (Ala-1 to Phe-85) of native E2 from *B. stearrowthermophilus* PDC has been overexpressed in *E. coli* and the structure determined by NMR spectroscopy (Dardel *et al.*, 1993). Similarly, the structure of *E. coli* lipoyl domain from the E2p chain has been determined by Green *et al.* (1995).

The domain is composed of two four-stranded  $\beta$ -sheets, forming a flattened  $\beta$ -barrel, with a core of well-defined hydrophobic residues. The polypeptide chain weaves back and forth between the sheets, with one exception; a type-I  $\beta$ -turn in one sheet that incorporates the lipoyl-lysine at its tip (Lys-42 in *B. stearrowthermophilus* and Lys-40 in *E. coli*). The N- and C-termini are close together in space, at the opposite ends of the molecule, in the other  $\beta$ -sheet. There are a further 6 to 8 amino acids at the C-terminus which form part of the linker region joining the lipoyl domain to the peripheral subunit binding domain. The  $\beta$ -barrel displays a 2-fold axis of quasisymmetry, reflecting a weak similarity between the N- and C-terminal halves of sequence noticed by Spencer *et al.* (1984).

Lipoylation of the specific lysine residue causes no detectable change in conformation, as shown by NMR spectroscopy of the lipoylated and unlipoylated forms of the domain of the E2-PDC component from *B. stearrowthermophilus* (Dardel *et al.*, 1990) and *A. vinelandii* (Berg *et al.*, 1994).

The E1 enzyme of the PDC complex requires the presence of the entire lipoyl domain in order to carry out efficient reductive acetylation of the lipoyl group. Various other substrates were substituted for the lipoyl domain (free lipoic acid, lipoamide, or a lipoylated decapeptide with the identical sequence to that around the lipoyl-lysine) and all were shown to be extremely poor substrates for E1. In particular, the lipoylated

decapeptide was not recognised to any greater extent than free lipoamide. Evidence for specific E1-lipoyl domain interaction was shown by Graham *et al.* (1989) whereby the E1 of *E. coli* OGDC was unable to recognise the lipoyl domain from *E. coli* PDC and vice versa.

The residues around the lipoyl-lysine are highly conserved in lipoyl domains from different sources. Many display the DKA motif that forms part of the exposed turn. The aspartic acid and alanine residues can be changed by site-directed mutagenesis with no effect on the lipoylation of the domain from *B. stearrowthermophilus* *in vivo* in *E. coli*. (Wallis and Perham, 1994).

In contrast, the recognition of the domain by E1 may be dependent on the side chains around the lipoyl lysine. Replacing the aspartic acid and alanine residues decreases the rate of reductive acetylation of *B. stearrowthermophilus* PDC domain by the cognate E1 (Wallis and Perham, 1994). The substitution of aspartic acid with large residues may obstruct access to other residues within the cleft-like structure of which aspartic acid is located at the mouth. If the alanine is replaced by charged residues (lysine and glutamate), a reduction in the rate of reductive acetylation is observed, suggesting a hydrophobic interaction between the alanine residue and the E1 enzyme (Wallis and Perham, 1994).

More recently, work has been carried out suggesting the importance of various residues surrounding the lipoylation site for the functioning of lipoyltransferases (Fujiwara *et al.*, 1996).

However, this is still a largely under-investigated area, particularly in the mammalian system; thus a series of experiments were undertaken here to further determine the requirements within the lipoyl domain for lipoylation, specifically in conserved residues adjacent to the lipoylation site.

#### **4.6 Aims of this chapter**

- (i) Investigation into the reactivity of the lipoyl-containing polypeptides of bovine PDC and OGDC using the PD1 monoclonal antibody.
- (ii) Overexpression and subsequent purification of human lipoyl domain mutants.
- (iii) Confirmation of lipoylation of mutant domains and recognition by PD1 monoclonal antibody.

#### **4.7 Materials and Methods**

The monoclonal antibody PD1 was obtained from Professor Freda Stevenson, University of Southampton, shown previously on native gel electrophoresis to cross-react with the lipoylated form of the human lipoyl domain. ECL was employed to detect reactivity.

Purified human lipoylated and unlipoylated lipoyl domain samples were obtained from Dr. J. Palmer, University of Newcastle.

A series of mutant human lipoyl domains, expressed as GST-fusion proteins were obtained from Dr. Janet Quinn in Newcastle. They encompassed the residues Serine 181 to Lysine 282 of the E2-PDC gene.

#### **4.8 Results**

##### **4.8.1 Investigation into the reactivity of the lipoyl-bearing subunits of bovine the PDC and OGDC and the lipoylation state of E2 subgenes using the PD1 monoclonal antibody.**

The PD1 monoclonal was used on purified PDC and OGDC isolated from bovine heart (see Materials and Methods). Prior to Western blotting, enzyme assays were carried out to determine the purity of the PDC and OGDC. It was established that the OGDC contained 2% PDC activity and that the PDC was cross-contaminated with OGDC activity to a significant extent (15-17%). Each sample (10 $\mu$ g) was resolved by 10%

## **Production of human anti-PDC-E2 monoclonal antibodies**

The monoclonal antibody, PD1, was a kind donation from Professor Freda Stevenson, University of Southampton. It was generated by immortalising B lymphocytes from a patient with the autoimmune disease, Primary Biliary Cirrhosis (PBC). Venous blood was drawn and the B lymphocytes exposed to Epstein Barr Virus. Following incubation in supplemented-RPMI, the cells were hybridised with mouse myeloma cells. Once of the hybridomas were visible, each clone was screened for reactivity with E2-PDC, which is the major autoantigen in PBC. Positive clones were selected and cloned until stable monoclonal populations were established.

SDS-PAGE (Figure 4.1) and a corresponding gel run for Western blotting (Figure 4.2).

Western Blot analysis revealed that only the PDC-E2 and not the OGDC-E2 reacted with monoclonal PD1. This result was somewhat surprising in view of the strong dependence of this monoclonal Ab on the presence of lipoic acid; however having already made subgenes, in the form of the di-domains, of human PDC, *E. coli* PDC, BCOADC and protein X, these were also blotted against the PD1 antiserum (Figure 4.3). Immunoblot analysis demonstrated that the E2-PDC, protein X and branched chain di-domains reacted strongly, but not the E2 of the *E. coli* di-domain (data not shown for latter).

Following on from this observation, sequence similarities around the attachment site of the lipoic acid were investigated to determine whether variations in this sequence could be influencing reactivity with the antisera (see below).

#### **4.8.2 Sequence comparison around the attachment site of the lipoic acid moiety of the E2 and protein X subunits:**

PDC:	A E V E T D K A T V
BCOADC:	C E V Q S D K A S V
Protein X:	C E I E T D K A S V
OGDC:	D Q N V D K R T C
<i>E. coli</i> PDC:	L I T V G D K A S M

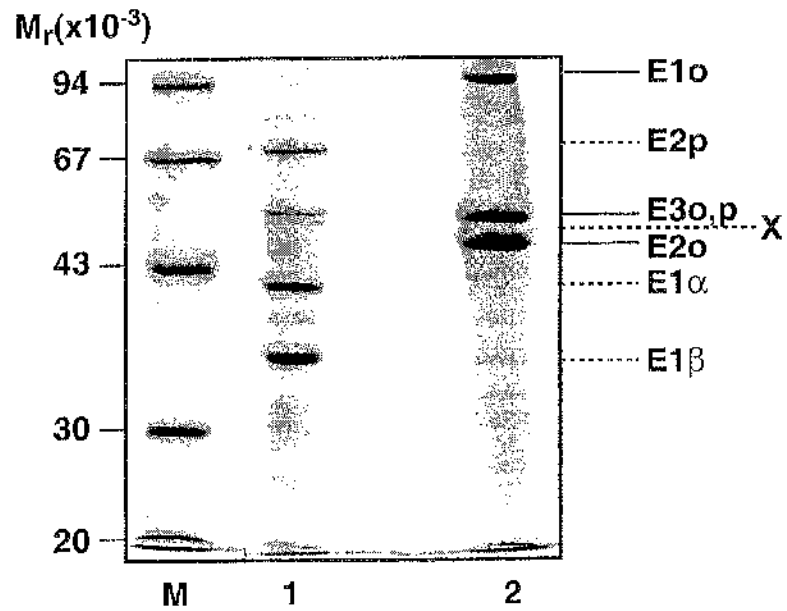


**Figure 4.1 SDS-PAGE analysis of PDC and OGDC purified from bovine heart.**

Purified PDC and OGDC (10 $\mu$ g of each) are resolved on a 10% SDS-polyacrylamide gel and stained with Coomassie Blue as described in Methods section. Lane 1, PDC; lane 2, OGDC sample. Lane M, M<sub>r</sub> marker.

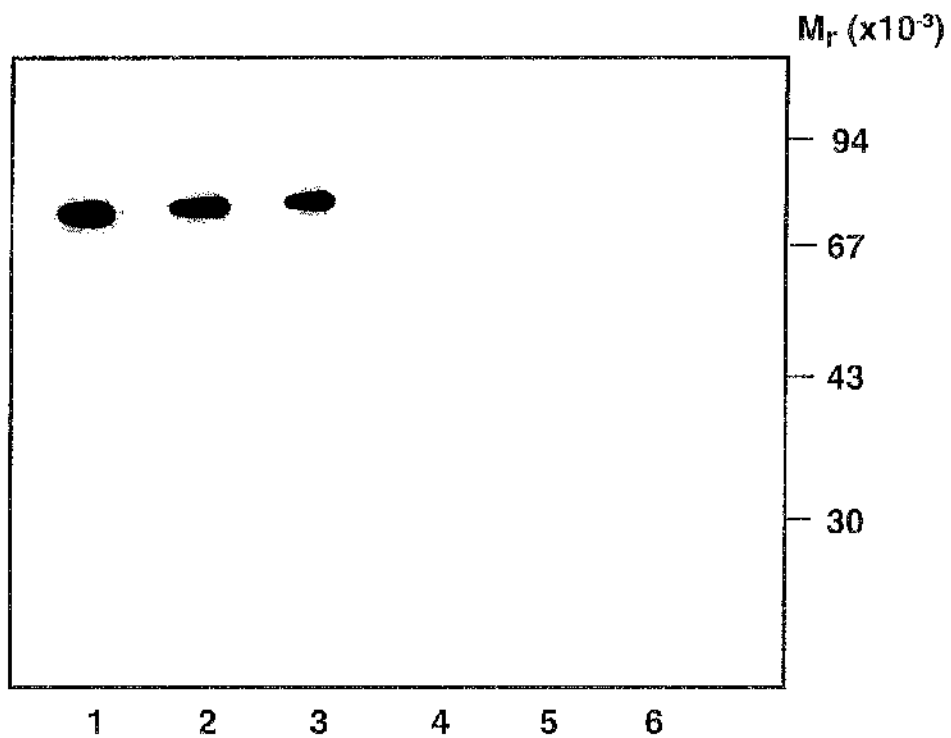


**Figure 4.2** Western blot analysis of bovine PDC and OGDC, using a monoclonal antiserum specific for lipoylated form of E2-PDC.

Lanes 1 to 3 contain 10, 5 and 2.5 $\mu$ g PDC respectively. Lanes 4 to 6 contain OGDC, loaded identically to the PDC samples.  $M_r$  standards were also run on the gel, as indicated.

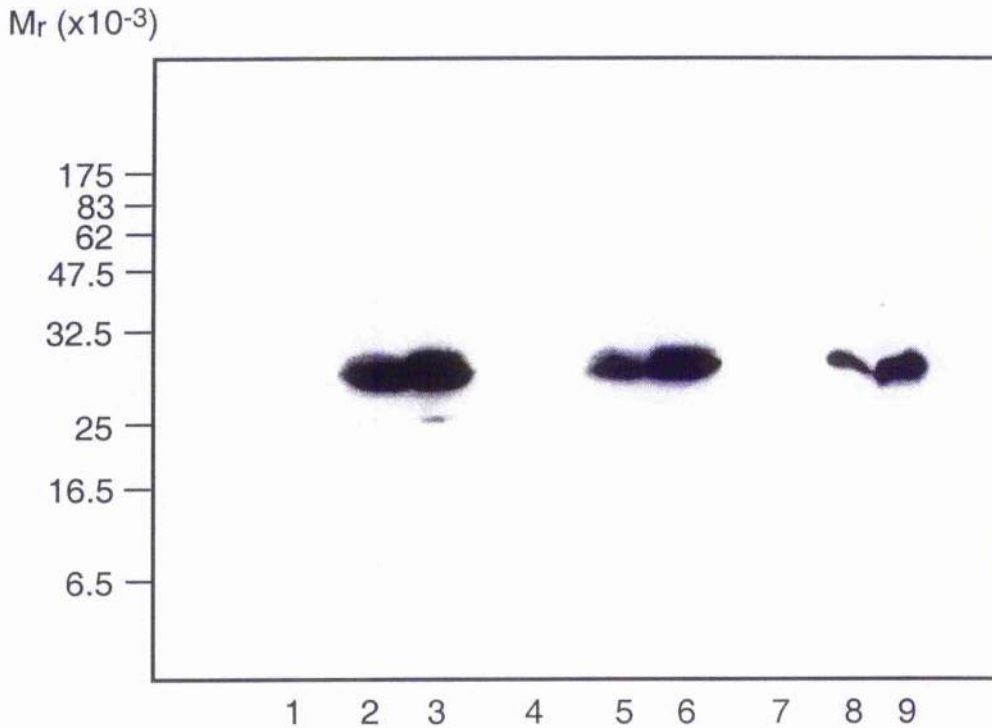


**Figure 4.3.** Western blot analysis of the PDC, BCOADC and protein X di-domains, blotting with antisera specific to the holo-domains.

Extracts were prepared from *E. coli* DE3 cultures expressing the di-domains at 0h and 3h after IPTG addition. Additional extracts were grown in the presence of lipoic acid at 10 $\mu$ g/ml. Lane 1, pre-induced human E2-PDC di-domain. Lane 2, 3 hour post-induction sample and lane 3, the equivalent sample with the exception of it being induced in the presence of lipoic acid. Lanes 4 to 6 contain the equivalent samples, but for E2-BCOADC di-domain. Lanes 7 to 9, as for lanes 1 to 3, but of protein X di-domain.

From the result of this comparison, there was no obvious distinction between the sequences of those which provoked a positive response with the monoclonal antibody and those which did not, with the exceptions of the lack of a conserved valine downstream of the lipoyl-lysine (situated within the DKA motif) and a conserved glutamate upstream. It was decided to further investigate the influence of the surrounding sequence using point mutations of the PDC-E2, originally generated by Dr. Janet Quinn, University of Newcastle. It was hoped that residues could be identified which were required for both the lipoylation reaction and antisera recognition

#### **4.8.3 Overexpression and subsequent purification of mutant human domains**

For this series of experiments, a series of point mutations in the conserved sequence adjacent to the E2 lipoyl attachment site were obtained from Dr. Janet Quinn in Newcastle. The inner lipoyl domain from human E2-PDC (107 amino acids) had been cloned into the pGEX-2T plasmid (Pharmacia Biotech) (Figure 4.4), using EcoRI and Bam HI and propagated in *E. coli*. XL1-Blue. The original lipoyl domain, referred to as pGLIP-2T, was subjected to one of five point mutations:

<b>Mutant Name</b>	<b>Mutation</b>
1A:	Ala174 to Ser
2A:	Glu170 to Gln
3A:	Lys173 to Gln
3B:	Gly180 to Asn
4A:	Asp172 to Asn

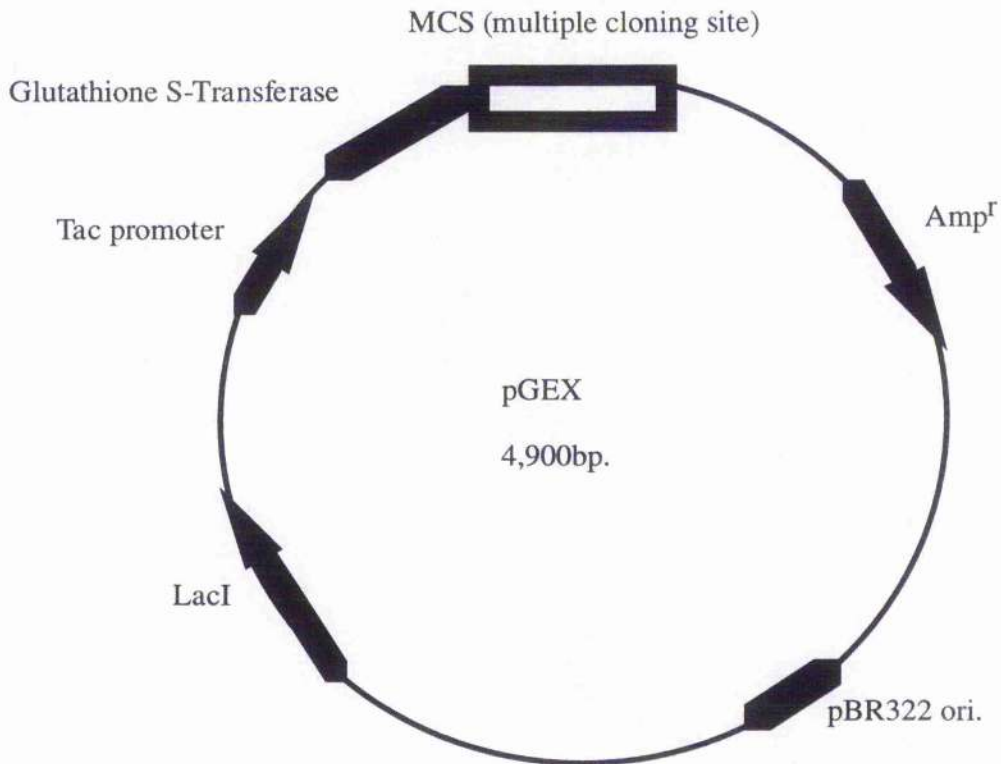


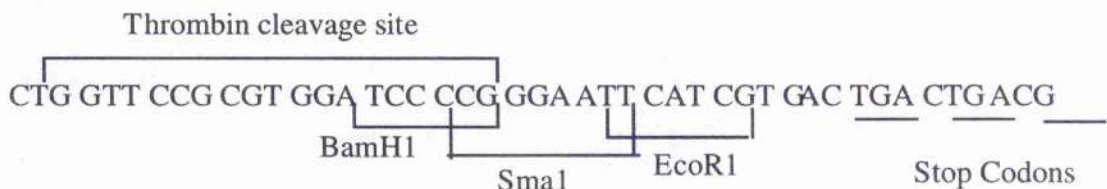
**Figure 4.4 Features of pGEX Vectors.**

Tac promoter for high-level expression, using IPTG.

Ampicillin resistance gene for selection.

Thrombin or Factor Xa protease recognition sites for cleavage of protein of interest from the fusion protein.

For these experiments, pGEX-2T was used, which contains a thrombin cleavage site within the multiple cloning site, shown below.



The aims were to investigate earlier claims of the importance of these residues in the lipoylation of the critical lysine residue (Lys 173) and to determine if these amino acids are also important in antibody response to the holodomain. *E. coli* DE3pLysS were transformed with the plasmids containing the mutant or wild type domains and overexpression achieved using IPTG (Figure 4.5). The resultant protein products exhibited  $M_r$  values of approx. 40,000, since these are expressed as C-terminally located GST-fusion proteins. As can be seen from the gel (lane 8), there was no overexpression of mutant 3B.

Having established that overexpression of the majority of the lipoyl domains had occurred, the next stage was a purification of the GST-fusion proteins from the bacterial lysates. Purification was achieved in a single step by affinity chromatography using a glutathione Sepharose 4B column (for overview see Figure 4.6 and Materials and Methods section).

The fusion proteins were eluted over the first two to five fractions (Figure 4.7 demonstrates this in the case of mutant 4A). The fractions were dialysed against distilled water, and then concentrated using Polyethylene Glycol-6000 (PEG-6000) to a final volume of approx. 1ml. The resultant product was run on a 15% SDS-polyacrylamide gel, along with the pre- and post-induction bacterial lysates (Figure 4.8). As a control, the wild type domain (pGLIP-2T) was also treated in a similar manner.

#### **4.8.4 Confirmation of lipoylation of mutant domains and recognition by PD1 monoclonal antibody.**

To determine whether the mutant lipoyl domains were recognised by the *E. coli* lipoylation system, two different techniques were employed:

- (i) Western Blot analysis.
- (ii) Native Gel Electrophoresis.

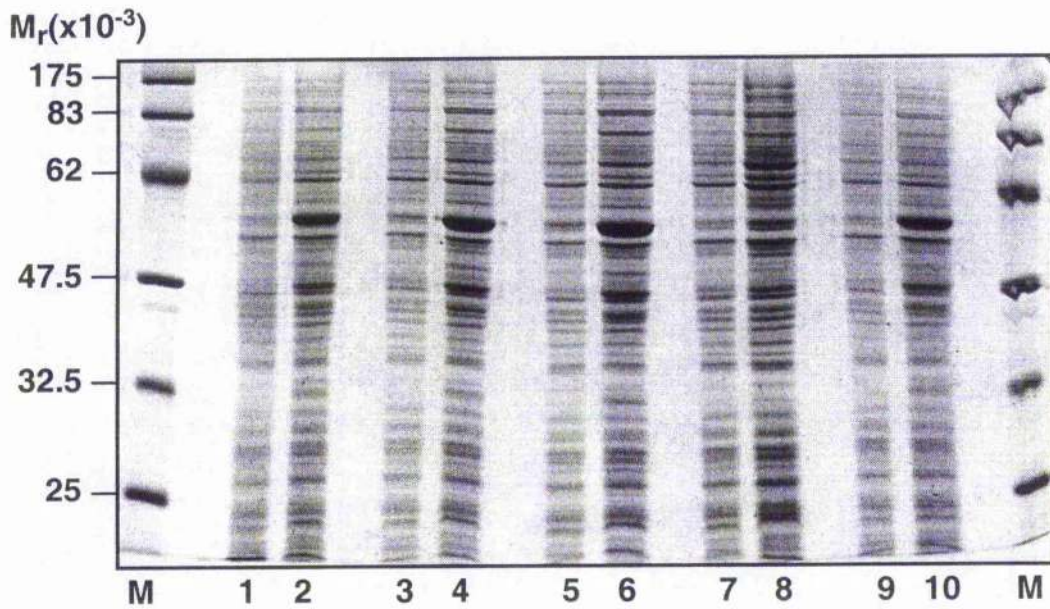


**Figure 4.5 Overexpression of mutant forms of the lipoyl domain from human PDC in *E. coli* DE3pLysS.**

Cultures of *E. coli* DE3plysS (250ml) were induced with IPTG when their  $A_{600}$  reached 0.5. A sample of the pre-induced and 3h post-induction sample were run in adjacent lanes of a 10% SDS-polyacrylamide gel. Proteins were visualised using Coomassie Blue stain. Lane M, molecular mass marker. Lanes 1 and 2, mutant 1A. Lanes 3 and 4, mutant 2A. Lanes 5 and 6, mutant 3A. Lanes 7 and 8, mutant 3B. Lanes 9 and 10, mutant 4A. There was no detectable overexpression of the 3B mutant.

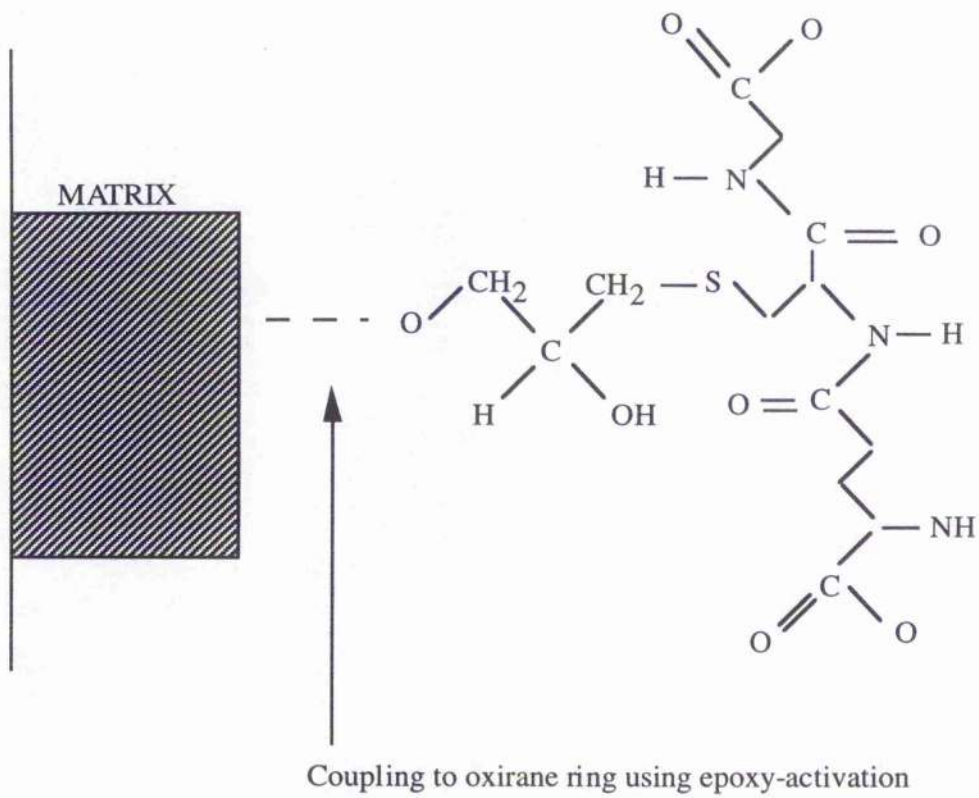


**Figure 4.6 Overview of Glutathione Sepharose 4B column.**

The structure of glutathione, the substrate for GST, permits high affinity binding of the fusion protein and specific, one-step purification by elution with free glutathione.

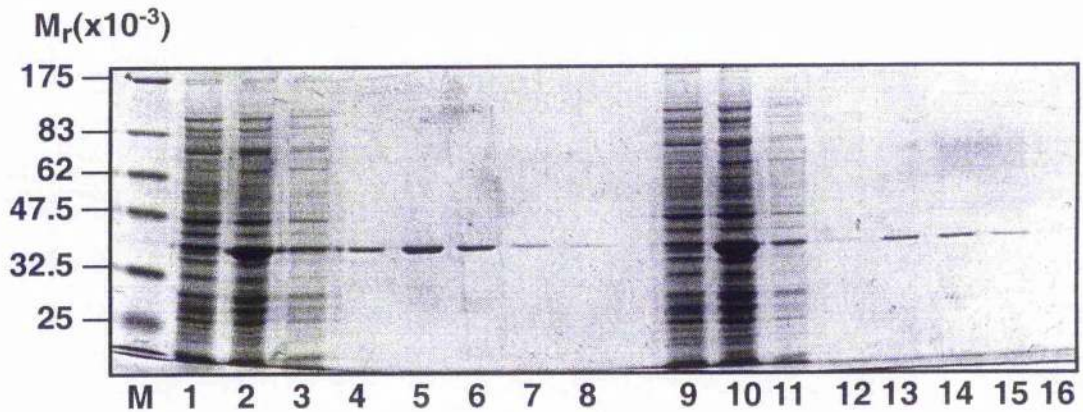


**Figure 4.7. Purification of a mutant lipoyl domain-GST-fusion protein by affinity chromatography on Glutathione Sepharose 4B**

Purification was carried out on the mutant (see Materials and Methods), in this case mutant 1A (Ala174 to Ser174) overexpressed without (lanes 1 to 8) and with (lanes 9 to 16) exogenous lipoic acid in the growth medium. The gel shows the pre- and post-induction samples, (lanes 1, 2; 9 & 10), followed by the flow through from the column, (lanes 3 & 11) then 20 $\mu$ l aliquots of each 1ml fraction eluted from the column, in the presence of 10mM glutathione.

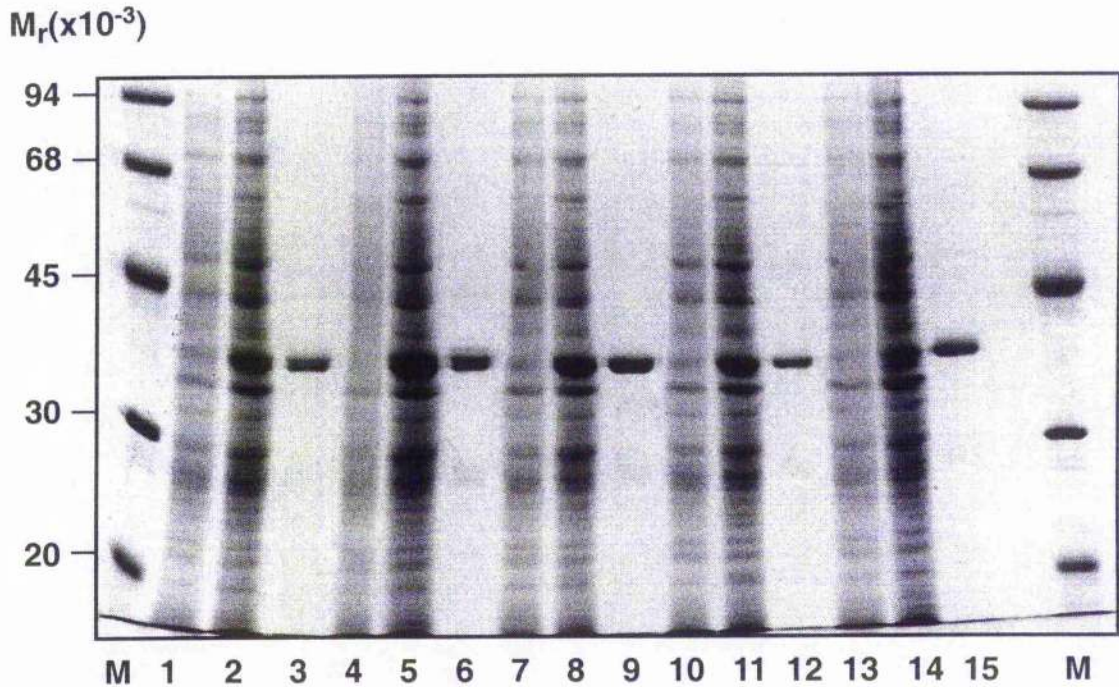


**Figure 4.8** Coomassie Blue-stained gel showing the final purified lipoyl domain mutant proteins.

The fractions containing the affinity purified fusion proteins were pooled and concentrated, then run beside the pre- and 3 hour post-induction samples on a 10% SDS-polyacrylamide gel. Mutant 1A is shown in lanes 1 to 3, mutant 2A in lanes 4 to 6, mutant 3A in lanes 7 to 9, mutant 4A in lanes 10 to 12 and the wild type domain in lanes 13 to 15. M, molecular mass marker.

#### 4.8.4.1 *Western Blot analysis of lipoyl domain mutants.*

Each purified lipoyl domain mutant, in the form of a GST-fusion protein was immunoblotted alongside the wild type domain and native GST (Figure 4.9). The lack of reactivity with GST alone (lane 10) confirmed the antigenicity resulted solely from the presence of the lipoyl domain. The blot shows that, when grown without exogenous lipoic acid, mutants 1A (Ala174 to Ser) and 4A (Asp172 to Asn) react strongly with the lipoylation-specific monoclonal (lanes 1, 2, 7 & 8). There was an extremely faint reaction with the 2A (Glu170 to Gln) mutant. When induced in the presence of the exogenous lipoic acid, lipoylation was enhanced in the cases of 1A and 2A, as evidenced by an enhanced recognition by the monoclonal antibody. There was no recognition of mutant 3A, the lipoyl lysine mutant. Little or no enhancement was observed in the case of mutant 4A suggesting that lipoylation may be complete without the addition of exogenous cofactor.

#### 4.8.4.2 *Native gel electrophoresis of lipoyl domain mutants.*

Native gel electrophoresis was also employed to further establish the lipoylation state and confirm the altered primary sequence of the mutant domains. In this case, electrophoresis was carried out on native polyacrylamide 10% gels (Figure 4.11). Prior to running the samples on a native gel, they were subjected to thrombin cleavage to separate the GST from the lipoyl domain. SDS-PAGE analysis confirmed the completion of cleavage (Figure 4.10). The various mutations altered the overall charge of the domain, thus allowing separation on the basis of altered migration rates. In addition, this separation also allows resolution of the apo- and holo-domains with the lipoylated form migrating more rapidly owing to the removal of a positive charge on the amino group of the lysine side chain on insertion of the prosthetic group.

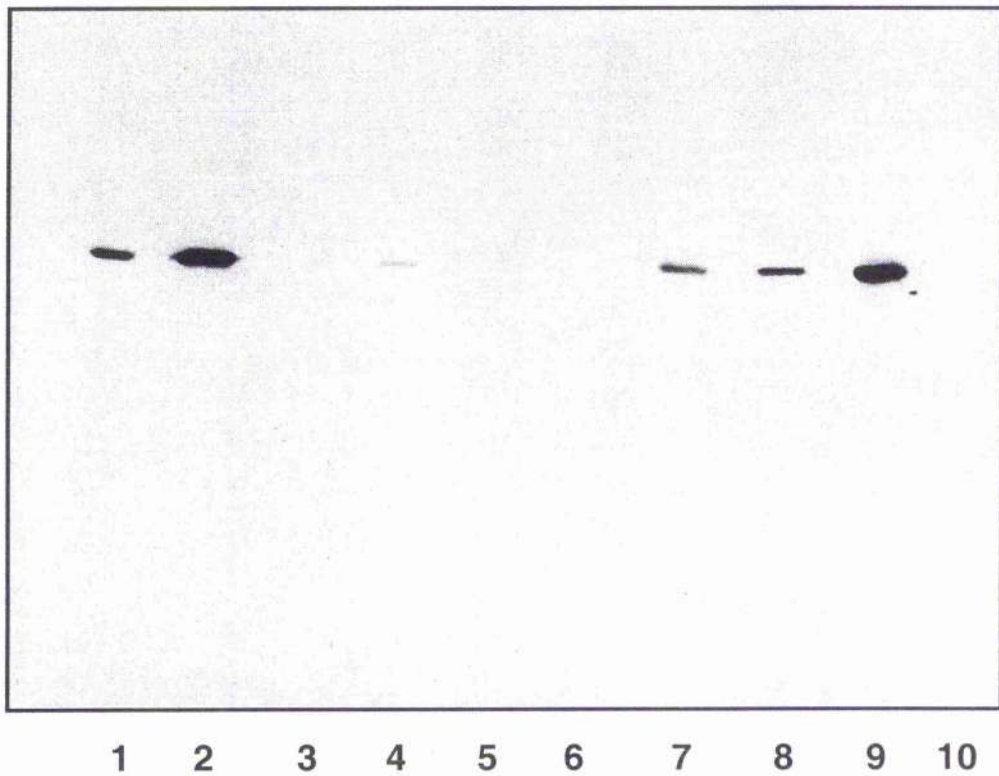


**Fig 4.9 Western Blot of the lipoyl domain mutants induced in the presence or absence of exogenous lipoic acid.**

Lanes 1 and 2 show the result of the immunoblotting of mutant 1A with monoclonal antibody PD1 induced without and with exogenous lipoic acid, respectively. Lanes 3 and 4, mutant 2A. Lanes 5 and 6, mutant 3A. Lanes 7 and 8, mutant 4A. Wild type domain (from pGLIP-2T) was resolved in lane 9 and purified GST in lane 10. The samples were run on a 15% SDS-polyacrylamide gel.

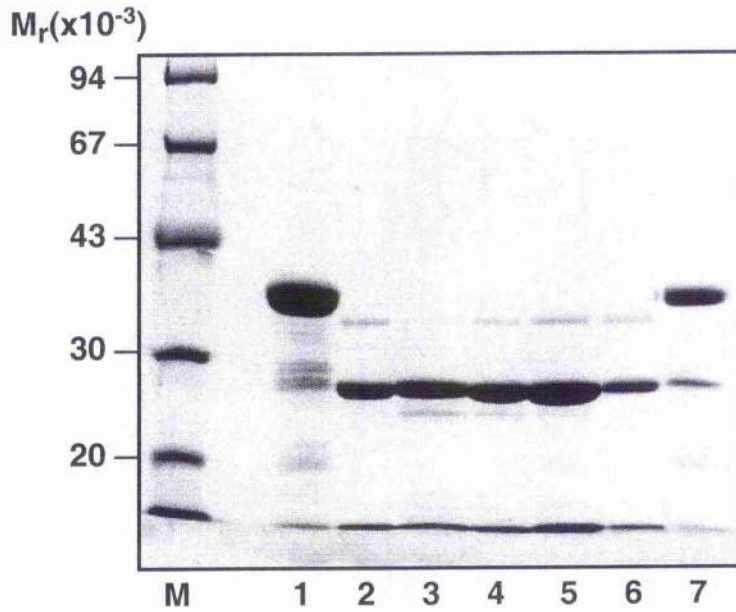


**Figure 4.10. Thrombin cleavage of GST-fusion proteins.**

Each of the purified mutant fusion proteins was subjected to thrombin cleavage for 16h and the resultant products run on a 15% SDS-polyacrylamide gel. Lane 1,  $M_r$  marker. Lanes 2 and 7, mutant 1A and wild type domains prior to cleavage respectively. Lanes 3 to 6 show cleaved mutants 1A, 2A, 3A, & 4A.

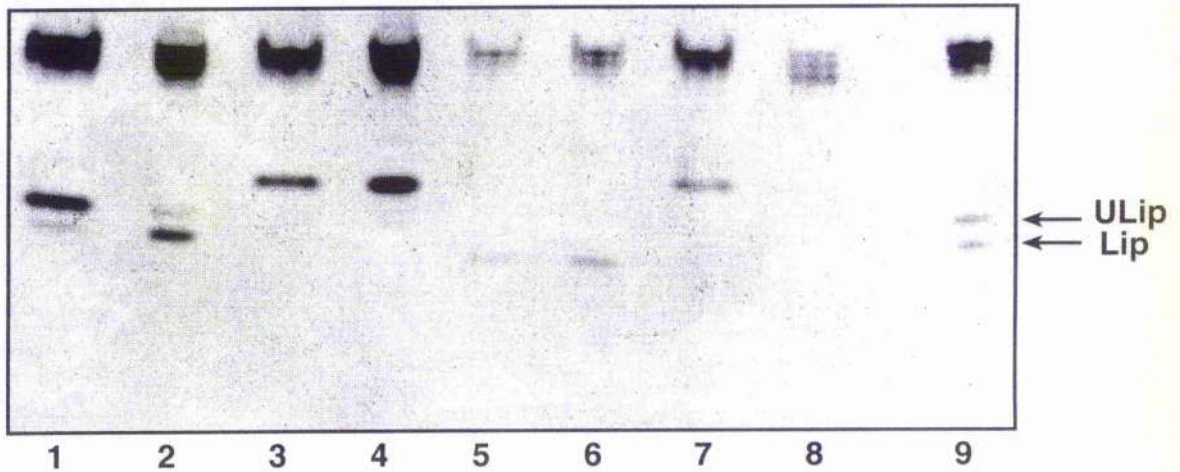


**Figure 4.11. Native gel electrophoresis of the purified lipoyl domain mutants following thrombin cleavage.**

Lanes 1 and 2 of this 10% native gel, mutant 1A unsupplemented and supplemented, respectively, with lipoic acid. Lanes 3 and 4, mutant 2A. Lanes 5 and 6, mutant 3A. Lanes 7 and 8, mutant 4A. The wild type domain, grown without exogenous lipoic acid is shown in lane 9. The arrows labelled ULip and Lip refer to the unlipoylated and lipoylated domains.

## 4.9 Discussion and Conclusions

### 4.9.1 Lipoylation states of intact complexes and subgenes

Lack of cross-reactivity of bovine OGDC and *E. coli* di-domains with monoclonal PD1 was rather surprising in view of the absolute dependence of this antibody on the presence of the covalently-linked lipoyate prosthetic group. These results suggest that the presence of the lipoyate moiety is necessary but not sufficient to induce a positive immune reaction. Additional features such as a specific sequence motif or non-contiguous conformational epitopes may be necessary. Furthermore, there is a lack of protein X reactivity on the blot. This could be a result of the lower levels of protein X in relation to E2-PDC, or the possibility that the monoclonal antibody displays a reduced reactivity as it was raised to the E2-PDC lipoyl domain. A reaction with protein X could perhaps be detected upon over-exposure.

Sequence comparison with bovine OGDC and *E. coli* E2-PDC shows 2 main differences; rat OGDC has a glutamic acid residue 3 residues upstream of the lipoyl lysine and it also has a valine residue 3 residues downstream. Neither of these residues is present in the bovine OGDC or *E. coli* sequences. This suggests that these residues are important for recognition by PD1 in OGDC, regardless of the fact that the enzyme is lipoylated.

Figure 4.4 shows that the di-domains from human PDC, protein X and BCOADC all cross-react strongly with the antibody. The *E. coli* PDC di-domain however failed to exhibit a similar reaction (data not shown). These results indicate that although PD1 was generated against human lipoyl domain, its specificity is more broadly based. They also show that the presence of the lipoic acid cofactor is essential for molecular recognition by monoclonal PD1 in all cases, but that additional factors are also required to achieve a positive response. It was in this context that a comparison of the amino acid

sequences around the site of attachment of the lipoic acid was carried out. Unfortunately there were no obvious differences which could account for the differences observed in the recognition by PD1, with the exceptions that both bovine OGDC and *E. coli* PDC show more sequence variations compared to the human sequence. Both lack the conserved glutamate and valine residues located 5 residues upstream and 4 residues downstream respectively of the lipoyl lysine. Obtaining the human lipoyl domain point mutants meant the possibility of determining whether these residues and others around the lipoic acid attachment site were indeed important for promoting this reactivity.

#### ***4.9.2 Overexpression and purification of human lipoyl domain mutants***

As can be seen on Figure 4.8, the overexpression in *E. coli* DE3 pLysS and subsequent purification of the resultant GST-fusion proteins was successful for all mutants apart from mutant 3B (Gly180-Asn), which failed to overexpress. This could possibly have been due to the mutation resulting in an incorrectly folded product that was rapidly degraded by the *E. coli* proteases. In 1996, Fujiwara *et al.* suggested that a small residue such as glycine or cysteine at this position is essential for correct folding and similar results have been obtained in Newcastle (J. Quinn, personal communication).

#### ***4.9.3 Lipoylation of mutant lipoyl domains.***

The immunoblot (Figure 4.9) clearly shows the differences in the levels of reactivity between the various mutants and the PD1 antibody. What is also obvious is that the presence of exogenous lipoic acid in the growth medium enhances the level of lipoylation as evidenced by the enhanced signals. This was true for the 3 mutants that cross-reacted. As expected, mutant 3A failed to cross-react, since substitution of the lipoyl-lysine moiety removes the critical residue required for the attachment of the lipoic acid prosthetic group.

The apparent lipoylation of mutant 2A contrasts with a report by Quinn *et al.* (1996), who showed that replacing the Glu by Gln caused the abolition of lipoylation as judged by growing the cultures in the presence of [ $^3\text{H}$ ] lipoate and measuring the incorporation of the radiolabelled prosthetic group into TCA-precipitated material. The low levels of cross-reaction observed here, which are enhanced to more detectable levels by exogenous lipoic acid, indicate that this mutant domain is an extremely poor substrate for the lipoylation reaction. Thus the sensitive detection method employed in this study could be the cause of this apparent disagreement.

These results are consistent with those of Wallis & Perham (1994), who showed that changing the equivalent residue (Asp172 to Asn) in *E. coli* E2-PDC had no effect on the ability of the lipoyl lysine to be lipoylated. They also demonstrated that this change caused a reduction in the rate of reductive acetylation by the E1 enzyme.

Moreover, our results in agreement with those obtained for *in vitro* assays on mutant forms of H-apoprotein by Fujiwara *et al.* (1996). The group showed that the glutamic acid residue, three residues upstream of the lipoyl lysine is important for lipoylation by the mammalian lipoyltransferases. Their suggestion was that the residue acts as a recognition signal for the enzyme. In fact, they demonstrated a 100-fold decrease in the rate of lipoylation when glutamic acid was replaced by glutamine.

Our evidence also suggests that the two residues flanking the lipoyl lysine are not critical for lipoylation, since both mutants 1A and 4A are lipoylated when induced in the presence or absence of exogenous lipoic acid. Furthermore, the immunoblot demonstrates the need for the lysine residue at position 173 (in the human domain) for lipoylation, since neither mutant 3A grown with or without exogenous lipoic acid appear to be lipoylated.

Since the rate of migration of individual lipoyl domains on native polyacrylamide gels is primarily dependent on their net charge, mutations that remove a negatively charged amino acid will decrease the mobility. In contrast, neutral replacements should have little or no effect on mobility compared to the wild type domain. In addition, lipoylation itself results in the removal of a positively charged lysine side chain, resulting in increased migration. The nature of the mutations are such that mutants 1A and 4A migrate similarly to the wild-type, 2A migrates more slowly than the wild type and 3A display a higher mobility.

In agreement with Western blot analysis, the 1A mutant is predominantly in the unlipoylated state when grown without lipoic acid, but in the presence of it, there is a shift to the almost fully lipoylated form. This is shown by the presence of two bands on the gel. As already stated, the unlipoylated domain migrates slower on the native gel than the lipoylated form owing to the difference in charge as the lipoic acid forms an amide linkage, increasing the overall net negative charge. The gel also shows that the samples of mutant 2A grown +/-lipoic acid seem to run similarly. The Western blot of these two samples showed both to be lipoylated at extremely low levels. It is likely that these bands actually represent the unlipoylated forms, but there is a tiny percentage of lipoylated domain that is detected by the antisera. In the case of the lysine mutant (3A), both the + and - lipoic acid samples run identically. Neither is lipoylated, as demonstrated by immunoblotting. Mutant 4A, grown without lipoic acid seems to only show one band, which must be assumed to be the lipoylated form. It is possible that the particular mutation makes the domain a better substrate for lipoylation.

#### 4.10 Concluding remarks

Taking the results obtained in this chapter together with those of other groups, it is possible to draw the following conclusions regarding the mammalian and *E. coli* lipoylation systems:

(i) Despite the conserved DKA sequence motif forming a 3-D  $\beta$ -turn, the aspartic acid and alanine residues are not the recognition signal for the enzyme selecting the lysine residue for lipoylation.

(ii) As far as the mammalian system is concerned, the conserved upstream glutamic acid is important, but conversion to Gln leads to greatly reduced but not to total abolition of lipoylation as reported previously.

(iii) The mode of recognition of the substrate by the lipoylating enzyme(s) are similar in both mammalian and prokaryotic systems, with neither the amino acid sequence *per se* nor a structural cue being exclusive for the process of recognition by the lipoylation enzymes.

(iv) The basis of the positive response of individual lipoylated domains by monoclonal antibody PD1 is still unclear; however, it is apparent that conserved Asp and Ala residues forming the DKA motif at the site of lipoylation are not directly involved. Moreover, the conserved Glu also appears not to be essential for cross-reaction. The involvement of conserved Val located 3 residues downstream of the lipoate attachment site in positively-reacting domains was not investigated at this stage.

## CHAPTER 5

**OVEREXPRESSION AND PURIFICATION OF N-TERMINAL FRAGMENTS OF THE E1 COMPONENT OF HUMAN OGDC: USE AS COMPETING INHIBITORY PEPTIDES IN OGDC RECONSTITUTION STUDIES.**

## 5.1 Introduction.

The structure and subunit organisation of the mammalian OGDC complex appears to differ markedly from the other members of the family of 2-oxoacid dehydrogenase complexes, namely PDC and BCOADC. The E1 enzyme of OGDC is a high  $M_r$  homodimer with a subunit of  $M_r$  110,000, in contrast to the  $\alpha_2\beta_2$  tetrameric structures of the analogous components of PDC and BCOADC. Sequence comparisons with protein X and E2-PDC from various sources show significant homology, particularly within the N-terminal region and includes a variation on the characteristic motif PALSP/GTM found in lipoyl domains, which in E1-OGDC is PFLSGT'S. Indeed, using specific proteolysis and N-terminal sequencing, it has been shown that there is a 'lipoyl-like' region at the N-terminus of the E1 component (Figure 5.1).

In this context, the cloning of the genes for human (Nakano *et al.*, 1994) and rat heart (Nakano *et al.*, 1991) E2-OGDC failed to detect the presence of an E1 or E3-binding domain, which is apparent in the E2-OGDC genes cloned from non-mammalian sources such as *E. coli* (Spencer *et al.*, 1984) and indeed in all E2 core assemblies determined to date. Human E2-BCOADC displays a high similarity to E2-OGDC, with the exception of the presence, in the former, of 1 exon encoding the E1/E3-binding domain (Lau *et al.*, 1992). The loss of this exon and the surrounding introns appears to have occurred during the evolution of the complexes. In 1996, Usada *et al.* showed that the *odhA* gene from *Corynebacterium glutanimum* that codes for E1-OGDC, displayed an N-terminal extension with sequence homology to E2s from PDC and OGDC, albeit to their C-termini.

The E1 component is the most proteolytically sensitive enzyme of OGDC (Rice *et al.*, 1992). The addition of protease arg C causes extensive degradation of E1, producing many smaller peptides. Trypsin in contrast, causes very selective degradation. A large stable fragment of subunit 100,000  $M_r$  is produced, termed E1' and a smaller N-

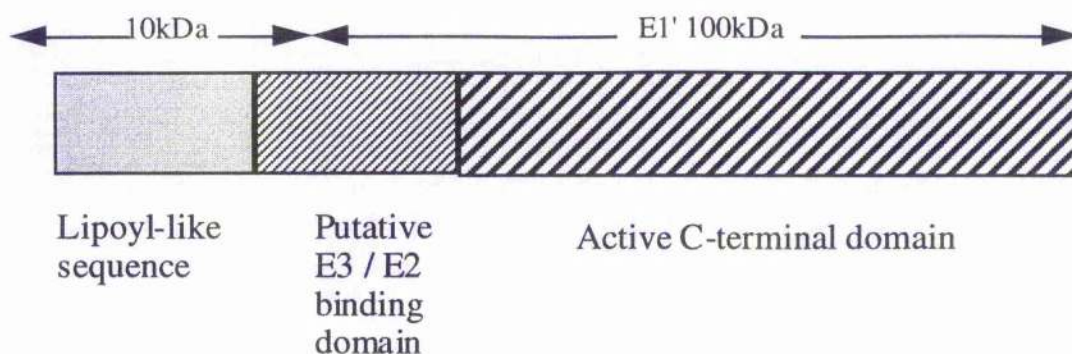


**Figure 5.1 Schematic representation of the E1 component of OGDC.**

At present, the domain organisation of E1-OGDC is poorly understood. What is known is that there is a highly-sensitive tryptic cleavage site which results in the production of a 10kDa fragment plus a 100kDa E1' fragment (as shown). Within the putative E2/E3 binding domain, sequence similarity has been detected to the subunit binding domain of protein X; hence the suggestion that the E1-OGDC binds the E3 as well as the E2 enzyme.

terminal 10,000  $M_r$  peptide is also generated. This pattern of degradation is similar to that obtained by the cleavage of E2-PDC. It generates lipoyl-bearing peptides and C-terminal intersubunit binding domains. The small E1 fragment displays another characteristic of a lipoyl domain in that it is highly immunogenic. The response is greater than that elicited by the large E1' fragment, which retains full catalytic activity. Sequencing of the E1' fragment has confirmed that the small peptide has been cleaved from the N-terminus of E1, a positional similarity to the lipoyl domain.

To date, the precise functional properties and domain boundaries of E1-OGDC been little studied. The main problem is the high affinity which E1 displays for the E2 core. However, a method has been recently developed to release catalytically active E1 from the core using 1M  $MgCl_2$  (McCartney *et al.*, 1998), although the free enzyme is extremely unstable under these conditions. Current evidence indicates that the E1 enzyme of OGDC, in particular the N-terminal region, is important for maintaining overall complex integrity in that it seems to be involved in binding both the E2 and E3 components. Thus a single tryptic cleavage within this region causes total inactivation of the complex by releasing both the E1' and E3 components, which are fully active.

This chapter details the overexpression of various different sized fragments of the N-terminal region of human OGDC. The rationale behind this series of experiments was to map more precisely the boundaries of the putative regions involved in E2 and E3 binding. To do this, it was decided to generate, by PCR, a series of N-terminal fragments of the E1 component and subsequently overexpress them as GST-fusion proteins in *E. coli* for use in competition studies. Investigations would centre on whether these fragments displayed the ability to bind to E2 and/or E3 and could thus compete for binding when E3 and/or E1 and E3 were added back to the E2-OGDC core.

## 5.2 Materials

The PCR amplification was carried out using human fetal liver cDNA (Clontech) as the template. The primers were designed to the known E1 sequence and are detailed in section 5.5. The expression vector pGEX-2T was used for insertion into *E. coli* DH5 $\alpha$ . The recombinant plasmids were subsequently used to transform *E. coli* DE3 pLysS. Glutathione Sepharose 4B (Pharmacia) was employed to purify the GST fusion proteins.

## 5.3 Methods

Initial investigations involved PCR amplification of DNA fragments from human fetal heart cDNA, corresponding to the first 80, 100 and 120 N-terminal amino acids of E1-OGDC. Primers were designed on the basis of the sequence published by Koike *et al*, (1992) (see section 5.4). The products were inserted into a pET11d expression vector and the protein overexpressed in *E. coli* DE3 pLysS. This method was subsequently adapted to that detailed below as it was deemed easier to purify the overexpressed proteins when generated as GST-fusion proteins.

This adapted method again involved the PCR amplification of three different sized fragments of the N-terminal of E1, (60, 110 and 160 amino acids) but differed from the first method in that the primers were designed to allow the insertion of the PCR products into a pGEX-2T vector to form a GST fusion protein, by engineering Bam HI restriction sites onto each end of the PCR products (see section 5.4). A further notable difference was that high fidelity Pfu DNA polymerase was used for the PCR amplification to minimise mis-incorporation.

### 5.4 Aims of this chapter

1. PCR amplification and subsequent cloning of 3 N-terminal fragments of the E1 enzyme of OGDC.
2. Competition studies for E1 and E3-binding between the N-terminal fragments and the OGDC core.
3. Draw conclusions regarding the regions of the E1 enzyme of OGDC involved in binding E2 and E3.

### 5.5 Polymerase Chain Reaction (PCR) of the OGDC E1 N-terminus

Four oligonucleotides were designed to allow the insertion of the PCR product into pGEX-2T for expression as a GST fusion protein. The underlined sequences in the 5' primer (OGDC-UP) and the 3' primers (OGDC-60, OGDC-110 and OGDC-160) denote the Bam HI restriction sites.

OGDC-UP	CAGATTCGGGGAT <u>CCCTCTGCACCTGTTGCTGCTG</u>
OGDC-60	CACAGCAGCGGAT <u>CCAGTTCGGCTCAGGGAAGG</u>
OGDC-110	CAGATCAGCGGAT <u>CCAGTCCCCAGGGGGTCCAG</u>
OGDC-160	GATCTCCCGGGAT <u>CCAGTTCGCTGATTCCTGTCC</u>

In combination with OGDC-UP, OGDC-60 was used to amplify the first 60 amino acids, OGDC-110 the first 110 and OGDC-160 the first 160. High fidelity Pfu DNA polymerase was used for the PCR to minimise misincorporation. The cycling conditions of the PCR differed to those previously employed, when Taq DNA polymerase was used for the amplification. Pfu polymerase catalyses base-incorporation more slowly than Taq, as a result of its increased proofreading exonuclease activity and thus requires a far greater extension time. The programme consisted of an initial denaturation of 95°C for 45 sec, then 35 cycles of the following (95°C for 45 sec, 65°C for 30 sec, 72°C for 10min), followed by a final extension time of 15 min.

## 5.6 Results

### 5.6.1 PCR amplification of N-terminal fragments of E1-OGDC

The human fetal liver cDNA template was subjected to PCR using the OGDC-UP and OGDC-160 primers. This generated the largest PCR fragment (OGDC-160). Restriction digest of the PCR product, with Bam HI, was carried out as detailed in the Materials and Methods section and the product subsequently ligated into pGEX-2T. Recombinant plasmid was amplified in *E. coli* DH5 $\alpha$ . The plasmid was then used as template for the remaining two PCR reactions. All three products were visualised on a 2% TAE-agarose gel, under UV transillumination (Figure 5.2).

### 5.6.2 Construction of recombinant plasmid

Each PCR product was purified using a Qiagen gel extraction kit, then digested with Bam HI. Following further gel purification, the PCR products were ligated overnight into pGEX-2T. Ligations were carried out over a range of vector to insert ratios and a 1:1 ratio deemed optimal. Positive clones were detected by successful release of the appropriate-sized fragment from the recombinant vector. Initially only 2 positive colonies were isolated. Their failure to overexpress when transformed into *E. coli* DE3 pLysS suggested that the cloned fragment had ligated into the vector in the inverse orientation. To overcome this, the insert was re-digested from the vector, re-purified and subsequently re-ligated back into the digested vector. This increased the frequency of positive colonies and permitted isolation of plasmid with the PCR product inserted in the correct orientation.

### 5.6.3 Overexpression of the 3 N-terminal fragments of E1-OGDC

Overexpression of each of the 3 N-terminal fragments was observed following the transformation of *E. coli* DE3 pLysS cells (Materials and Methods section 2.15) using IPTG induction (Materials and Methods section 2.16). Visualisation of the GST-fusion proteins was carried out by resolution on a 12% SDS-polyacrylamide gel (Materials and

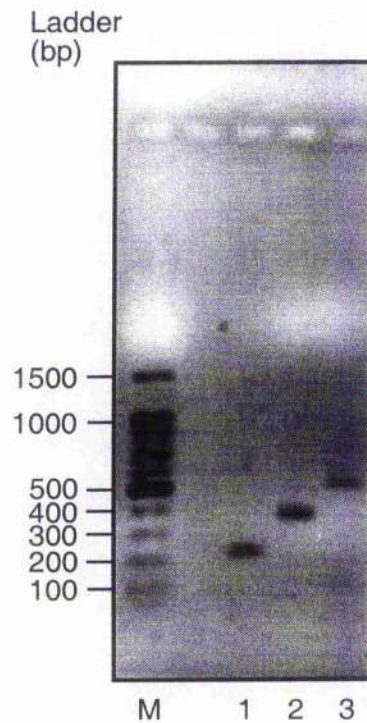


**Figure 5.2. Agarose gel of the PCR amplification of the three N-terminal fragments of E1-OGDC.**

Lane 1, OGDC-60. Lane 2, OGDC-110. Lane 3, OGDC-160. Lane M, 100bp size ladder. The gel was visualised under UV illumination following staining with ethidium bromide.

Methods section 2.2.16) and staining with Coomassie Brilliant Blue. A substantial overexpression was observed within an hour of induction in all cases (Figure 5.3).

#### **5.6.4 Purification of the 3 N-terminal fragments of E1-OGDC**

On achieving successful overexpression of the fragments; the next stage was purification of the GST-fusion proteins from the bacterial lysates. This was achieved in a single step by affinity chromatography using a bench-top glutathione Sepharose 4B column, as detailed in the Materials and Methods section. The fusion proteins were eluted over the first one to five 1ml fractions. Figure 5.4 demonstrates the purification profile of OGDC-60. The fractions were dialysed against distilled water then concentrated using polyethylene glycol-6000 (PEG-6000) to a final volume of approx. 1ml.

### **Part 2**

#### **5.7 Competition studies using the N-terminal fragments as inhibitors of OGDC reconstitution**

##### **5.7.1 Dissociation of native OGDC using 1M NaCl**

After successful purification of the 3 N-terminal fragments of E1-OGDC, the next stage was to discover whether they were capable of inhibiting reconstitution of OGDC. Thus the ability of the N-terminal fragments to inhibit the reconstitution of dissociated OGDC was tested by competing for E3 binding. The E3 enzyme of the 2-oxoacid dehydrogenase complexes can be selectively released by incubating the complex in 1M NaCl at 4°C for 20min (Sanderson *et al.*, 1996).

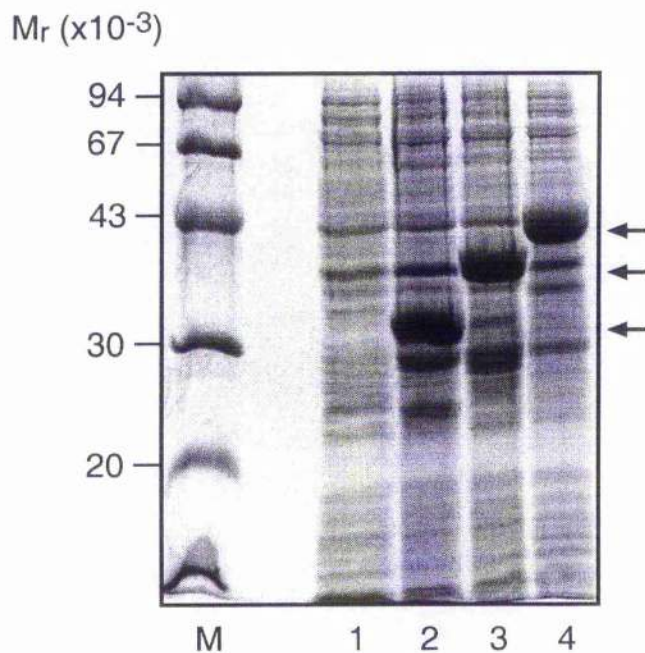


**Figure 5.3. SDS-PAGE analysis of the overexpression of the N-terminal fragments of E1-OGDC in *E. coli* DE3 pLysS.**

Lane 1, pre-induced whole cell extract. Lane 2, overexpressing OGDC-60. Lane 3, overexpressing OGDC-110. Lane 4, overexpressing OGDC-160. M, molecular mass marker.

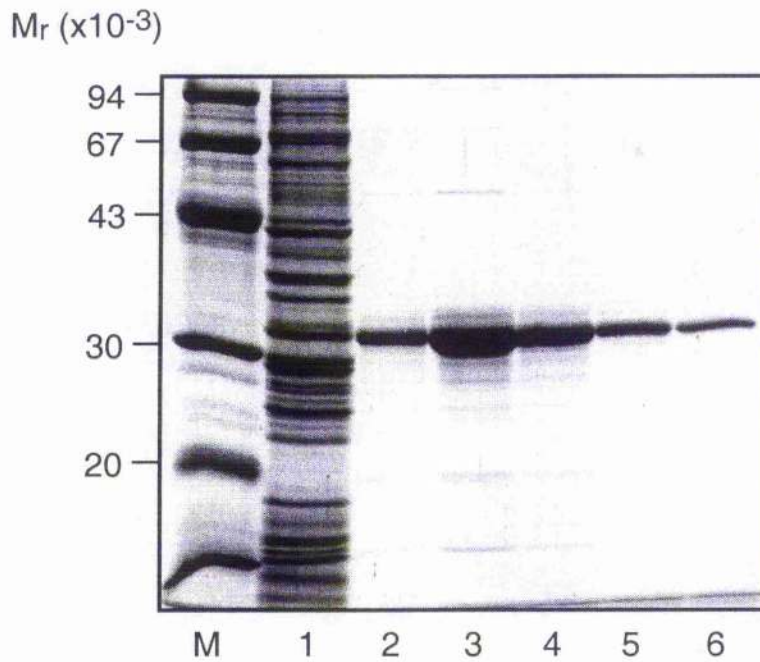


**Figure 5.4. Purification profile of OGDC-60, purified as a GST-fusion protein on a glutathione Sepharose 4B column.**

Lane 1, flow through following loading of the sample onto the column. Lanes 2 to 6 show samples ( $10\mu\text{l}$ ) from successive 1ml fractions collected following addition of the elution buffer to the column.

To assess the extent, if any, of E3 binding by the fragments (detected by the inhibition of OGDC recovery) it was first necessary to determine the efficiencies of reassociation of OGDC after salt treatment. OGDC (10 $\mu$ g) was reconstituted at 20°C for 20 min. in 670 $\mu$ l solution A and 14 $\mu$ l of solution B (Materials and Methods section 2.2.23.1) following the dissociation in 1M NaCl. In order to initiate NADH production, 14 $\mu$ l of 100mM 2-oxoglutarate was added to the assay components. The activity measured, expressed as a percentage of initial OGDC activity, prior to salt treatment was 47.7% (+/- 2.5%) (Figure 5.5).

Subsequently, this experiment was repeated in the presence, in the assay buffer, of a 10-fold stoichiometric excess of each of the E1-OGDC N-terminal fragments. On the addition of the substrate 2-oxoglutarate, the activity of the OGDC complex was measured and again expressed as a percentage of reconstituted complex. Figure 5.5 demonstrates that despite the large excess of E1-GST, there is no significant inhibition of reconstitution of the OGDC complex, with values in the presence of OGDC-60, OGDC-110 and OGDC-160 of 92.2% (+/-2.6%), 88.9% (+/-4.8%) and 95.6% (+/- 4.9%) respectively. Furthermore, to confirm that the GST was not hindering access to the E3 components, the fusion proteins were subjected to cleavage by thrombin, to release the GST component. E1-GST fusion protein (10 $\mu$ g) was incubated overnight at 16°C with 20 units thrombin and the resultant cleaved fragments added to the OGDC reassociation mix. The results obtained were indistinguishable to those for the intact GST-fusion proteins, indicating that the GST does not interfere with any potential intra-complex interactions.

### 5.7.2 Dissociation using 1M MgCl<sub>2</sub>.

In contrast to the E3 component of OGDC, the E1 enzyme is very tightly bound to the E2 core. Previous studies have shown however that high concentrations of divalent cations, especially Mg<sup>2+</sup>, are capable of disrupting the strong interaction, whilst also causing the release of the E3 enzyme (McCartney *et al.*, 1998).

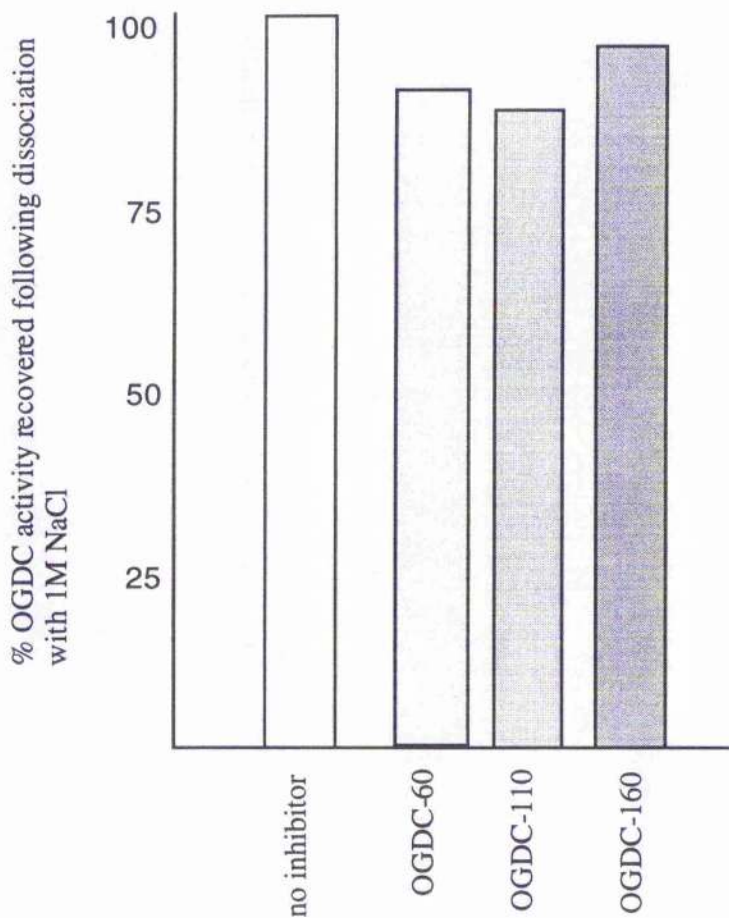


**Figure 5.5 Reconstitution of native OGDC in the absence and presence of the E1-OGDC N-terminal fragments.**

Following the dissociation of the OGDC complex in 1M NaCl, samples (10 $\mu$ g) were removed and incubated for 20 min. In reassociation buffer, prior to being assayed for OGDC activity. The activity recovered was expressed as a percentage of the original activity prior to dissociation. Assay values were the result of duplications which differed by no more than  $\pm 5\%$ . In the presence of each of the N-terminal fragments, there is no significant inhibition of reconstitution.

This technique was employed here to determine whether the E1-OGDC N-terminal fragments had any effect upon the subsequent reconstitution of the complex following its dissociation in the  $MgCl_2$ . An inhibition of assembly would indicate interference of the reassociation of the E1 component to the E2 core.

In order to determine the effect on reconstitution of the N-terminal fragments; OGDC-60, OGDC-110 and OGDC-160, each fragment was added to the reassociation mix in a 10-fold stoichiometric excess. Dissociated OGDC (10 $\mu$ g) was incubated for 20min at 20°C, then assayed to determine the extent of reconstitution (Figures 5.6a, b and c). When each fragment was added to the reassociation buffer, there was a significant decrease in the amount of activity that was regained relative to the values for reconstitution in the absence of inhibitor. With OGDC-60 61.3% (+/-4.2%) returned, with OGDC-110 68.1% (+/-3.6%) returned and with OGDC-160 70.2% (+/-2.1%) returned.

As already mentioned, these N-terminal fragments had been engineered as GST fusion proteins, giving rise to the question of whether the GST was in any way interfering with their mode of action. Thus, they were subjected to thrombin cleavage (10 $\mu$ g of fragment was incubated overnight at 16°C with 20 units thrombin) and the resultant cleaved fragments added to the OGDC reassociation mix. Again the OGDC assays were performed and the results are shown in Figures 5.6a to c, alongside those of the uncleaved and the pre-dissociation samples. What is clear is that the removal of the GST from the fragments causes a small but significant enhancement in the inhibition of complex reassociation, with 50.3%, (+/-3.5%) 58.8% (+/-2.9%) and 61.2% (+/-1.8%) of activity returning in the presence of OGDC-60, OGDC-110 and OGDC-160 respectively.

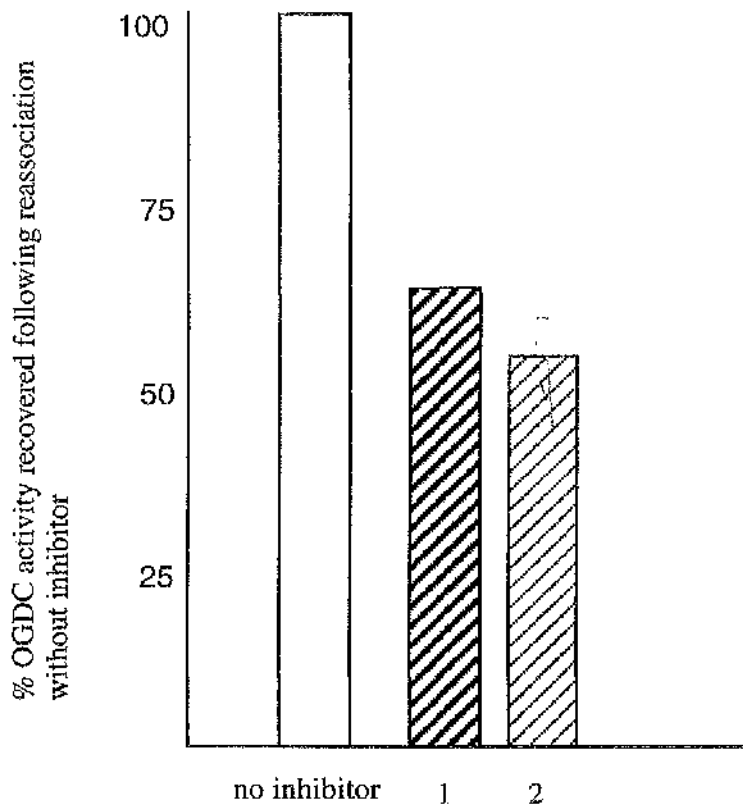


**Figure 5.6a Reconstitution of OGDC, in the presence of OGDC-60, following dissociation of the complex in 1M MgCl<sub>2</sub>.**

Samples (10 $\mu$ g) were removed from the dissociation buffer and incubated for 20mins in reassociation buffer (Materials and Methods section 2.2.23.1). The sample was then assayed for OGDC activity and expressed as a percentage of the activity recovered following salt treatment in the absence of inhibitor. Column 1 shows the activity returned in the presence of a 10-fold stoichiometric excess of OGDC-60. Column 2 shows the activity returned in the presence of thrombin protease-treated OGDC-60.

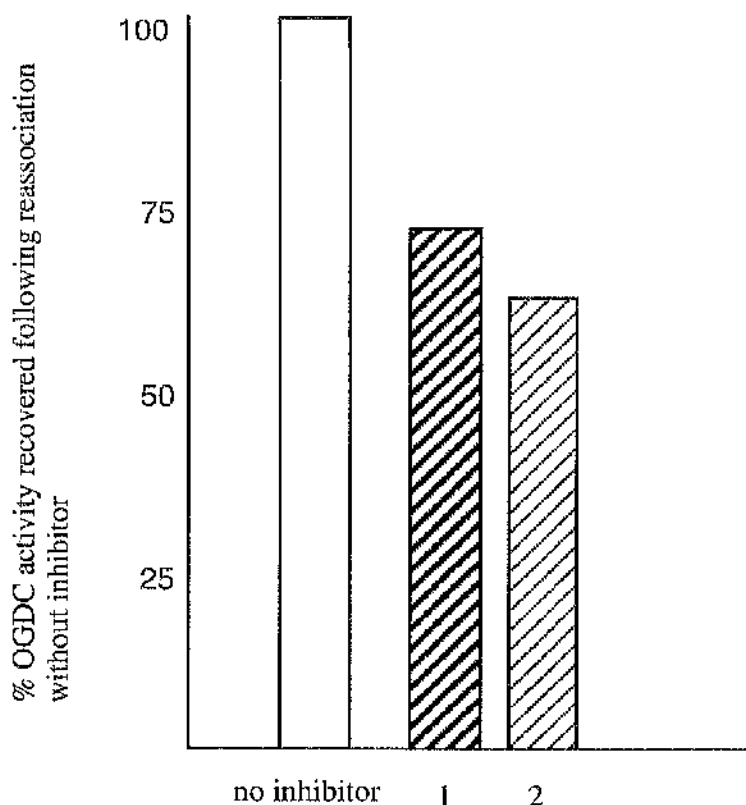


**Figure 5.6b Reconstitution of OGDC, in the presence of OGDC-110, following dissociation of the complex in 1M MgCl<sub>2</sub>.**

Samples (10 $\mu$ g) were removed from the dissociation buffer and incubated for 20mins in reassociation buffer (Materials and Methods section 2.2.23.1). The sample was then assayed for OGDC activity and expressed as a percentage of the activity recovered following salt treatment in the absence of inhibitor. Column 1 shows the activity returned in the presence of a 10-fold stoichiometric excess of OGDC-110. Column 2 shows the activity returned in the presence of thrombin protease-treated OGDC-110.

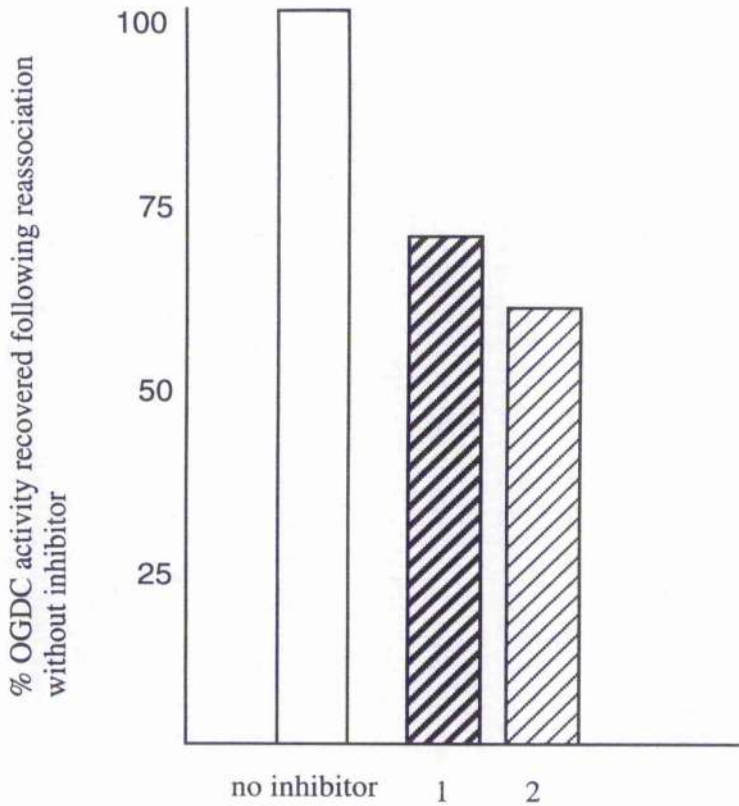


**Figure 5.6c Reconstitution of OGDC, in the of OGDC-160, following dissociation of the complex in 1M MgCl<sub>2</sub>.**

Samples (10 $\mu$ g) were removed from the dissociation buffer and incubated for 20mins in reassociation buffer (Materials and Methods section 2.2.23.1). The sample was then assayed for OGDC activity and expressed as a percentage of the activity recovered following salt treatment in the absence of inhibitor. Column 1 shows the activity returned in the presence of a 10-fold stoichiometric excess of OGDC-160. Column 2 shows the activity returned in the presence of thrombin protease-treated OGDC-160.

## 5.8 Discussion

### 5.8.1 Overexpression and purification of N-terminal fragments

The first section of this chapter detailed the successful overexpression and subsequent purification of three N-terminal fragments of E1-OGDC. The construction of *E. coli* strains capable of overexpressing a gene, or subgene of interest allows production of large quantities of protein in a relatively short time. In the case of the N-terminal fragments, these were generated as GST-fusion proteins by ligating into pGEX-2T. The rationale behind the use of this particular vector was the subsequent single-step purification procedure by affinity chromatography, using glutathione Sepharose 4B. The protein is recovered from the matrix under mild elution conditions which normally preserves its antigenicity and functionality. Cleavage of the GST is possible using a site-specific protease, whose recognition sequence is located immediately upstream from the multiple cloning site on pGEX plasmids. Previous cloning work had employed the pET 11 series of vectors which proved problematic when attempts at purification were carried out. Thus the generation of three N-terminal fragments of E1-OGDC in high yield has allowed investigations into this critical region of the enzyme. Their ability to compete with the native components of the complex following dissociation is studied here in detail.

### 5.8.2 Dissociation of native OGDC

The mammalian 2-oxoglutarate complex seems to have evolved with structural and organisational differences far diverged from the other two 2-oxoacid dehydrogenase complexes. The cloning of the gene for mammalian E2-OGDC failed to show the presence of a peripheral subunit-binding motif, which is apparent in the E2 genes of PDC. There are sequence similarities between E1-OGDC protein X of PDC, suggesting that the E1 enzyme has evolved a degree of bi-functionality by carrying out the E3-binding functions along with its well-documented catalytic role. In this regard, a direct

interaction between E1-OGDC and E3 has been reported recently by McCartney *et al.* (1998).

It was hoped that the competition studies in part two of this chapter would go some way to defining the boundaries of the E3-binding domain on the E1 enzyme and also the region involved in E2 binding. Three different sized N-terminal fragments were generated, encoding the first 60, 110 and 160 amino acids, then used to inhibit the reconstitution of native OGDC, following its dissociation by either NaCl or MgCl<sub>2</sub> treatment. These fragments span the proteolytic cleavage site which results in the release of both an active E1' species and E3, causing inhibition of overall complex activity. Hence this region is thought to be important in the binding of both E1 and E3 to the E2 core.

Partial dissociation of native OGDC can be successfully carried out using 1M NaCl. This causes specific release of the E3 enzyme, whereas the E1/E2 subcomplex remains intact under these conditions. In order to fully disassemble the complex into its three constituent enzymes, high concentrations of MgCl<sub>2</sub> are required (McCartney *et al.*, 1998). Complete dissociation could only be deemed successful if each of the components were functionally active following the high salt treatment. This was confirmed by the reconstitution studies. The levels of reconstitution obtained following 1M NaCl and 1M MgCl<sub>2</sub> treatments were between 45% and 54%, indicating that the individual enzymes did indeed remain functionally active and that significant levels of complex reconstitution could be achieved. These levels are lower than the 60% to 80% reconstitution levels obtained for PDC previously in our laboratory (Sanderson *et al.*, 1996). This is likely to be a reflection of the harsher conditions required for the dissociation. Dissociation of PDC in high salt results in the release of the E1 and E3 components while the E2/X core remains intact, enabling easier reassociation. This further highlights the possible functional comparison between E1-OGDC and protein X of PDC with both enzymes being tightly bound to their respective E2 cores. To date,

structural analysis of the OGDC core has yet to determine whether the E1 enzyme binds with the same orientation as protein X does to the PDC E2 core, *i.e.* that it is associated with each of the individual faces. Further work is also required to determine the optimum length of incubation time in reassociation conditions to obtain maximum OGDC activity. Owing to the instability of dissociated E1, extended incubation will possibly result in reduced recovery of activity. The pH of the dissociation reactions would appear, from previous studies, to be an important contributing factor in the level of reconstitution. McCartney *et al.* (1998) demonstrated that dissociation under acidic conditions results in a slow loss of activity and high levels of recovery. In contrast, they showed that under alkaline conditions, there is a far more rapid loss of activity and lower levels of recovery. This is possibly due to an incomplete dissociation of E1 from the E2 core at more acidic or neutral pH.

The experiments in this chapter were all conducted at pH 7.6, which are too alkaline to allow maximal recovery of OGDC activity following dissociation but are required to promote complete release of the E1 component (McCartney *et al.*, 1998).

### **5.8.3 Reconstitution of native OGDC**

#### **(1) Effect of N-terminal fragments on E3-binding**

Reconstitution analysis showed that the individual components of OGDC were capable of reforming active complex following dissociation. The N-terminal fragments; OGDC-60, OGDC-110 and OGDC-160 had been designed with the view that they may be able to bind the E3 enzyme. This ability would present itself in the form of an inhibition of OGDC reconstitution, as the fragments would compete with the native E2/E1 subcomplex for E3 binding.

The results, however, did not suggest that any of the fragments had the ability to inhibit E3-binding. This is highlighted in Figure 5.5, where it can be clearly seen that the presence of each of the individual fragments in a 10-fold excess has no effect on the

level of complex reconstitution. As a further confirmation of this result, each fragment (10 $\mu$ g) was incubated with purified E3, then the sample analysed by non-denaturing PAGE (data not shown). The gel showed the presence of two bands corresponding to E3 and the N-terminal fragment, but no discrete band representing an E3-N-terminal fragment complex. Adding overexpressed parent GST to the reassociation assay provided information that the GST was not interfering directly with reassociation.

As a control to rule out the possibility of the GST part of the fusion protein interfering with any E3 interaction, it was cleaved away from the N-terminal fragment using thrombin. The reconstitution analysis was then repeated, in the presence of the thrombin-treated fragments. The results were as before, with no inhibition of reconstitution occurring. Interpretation of the data should be carefully considered. As of yet there is no real knowledge of the domain organisation of E1 or whether the N-terminal fragments are capable of correct folding. It is possible that the fragments generated are too small to form stable domains. Furthermore a dimeric structure could be required for binding and finally, the binding site may be composed of other regions outwith the boundaries of the N-terminal fragments. Obviously further work with large excesses of the N-terminal fragments may generate further inhibition of OGDC activity if they are able to compete more strongly with native E1. The experimental series reported here was limited by the amounts of E1-GST fragments generated. To this end, lack of positive effects on OGDC reconstitution must be treated with caution at this stage.

## **(2) Effect of N-terminal fragments on E1 and E3 binding**

The second series of reconstitution studies were performed following dissociation with 1M MgCl<sub>2</sub> which releases both the E1 and E3 components. The reassociation and subsequent OGDC assay was carried out in the presence of a 10-fold excess of each N-terminal fragment. The results demonstrated a significant inhibition of OGDC reconstitution in the presence of each fragment. In fact there was a decrease in complex

activity of approx. 50% when compared to reconstitution in the absence of any of the N-terminal fragments. As with the previous set of reconstitution experiments, they were repeated following the removal of the GST from the fragment with thrombin. The results here showed an enhanced level of inhibition of complex formation. These results show that in this case, the GST is interfering to some extent with the mode of action of the N-terminal fragments. These results implicate the importance of this region of the E1 component in interacting with the E2 core as evidenced by the ability of the fragments to reassociate with E2 and E3 into the native complex. There is no significant difference between each fragment, but they all show the same degree of inhibition. It appears therefore that each fragment, despite having no functional ability to bind E3, can interact with the E1 binding sites on the E2 core, thus inhibiting the levels of reconstitution in this manner.

In summary, these studies have been unable to define regions of E1-OGDC involved in E3-binding. It is possible that the N-terminal fragments that were generated cannot form a stable domain structure to retain this function; however, they have shown the ability promote partial inhibition of E1 binding when present in a 10-fold excess which argues against this hypothesis. Previous studies have shown that the native E1 and E3 interact directly, whereas this is not the case for the stable E1' species produced by tryptic cleavage. Perhaps there are also sequences further downstream whose presence is required to allow the binding of E3. It may still be possible to define the E3-binding region, by generating larger fragments. However, all that can be concluded at present is that the N-terminal region of E1 appears to be involved in promoting its interaction with the E2 core. Current work is concentrating on extending the series of truncated forms of E1 to span the complete open reading frame of this polypeptide. Future analysis should elucidate the domain organisation of the E1-OGDC enzyme as well as leading to more conclusive evidence regarding the diverse properties of this component.

**CHAPTER 6**

**BIACORE STUDIES OF BINDING INTERACTIONS BETWEEN THE  
DI-DOMAINS OF PROTEIN X AND E2-PDC AND E3 ENZYMES  
FROM VARIOUS SOURCES.**

## 6.1 Introduction

Having demonstrated earlier in this thesis, the ability to generate significant quantities of lipoyl domain plus peripheral subunit binding domain, termed the di-domain from various sources, the possibility of studying the kinetics and affinities of binding between specific di-domains and the E3 enzyme becomes available. Very few such investigations have been feasible until recently owing to the constraints of technology. However, with the development of surface plasmon resonance (SPR) in particular, such studies have now been made possible. One such system is BIAcore, which was employed here. BIAcore is an analytical system allowing real-time biomolecular interactions to be monitored where the binding of analytes to surface immobilised ligands can be directly observed.

The detection principle relies on SPR, which is an optical phenomenon arising when light illuminates a film of conducting material under specific conditions. In summary, polarised light which is reflected at an interface between media of 2 refractive indices separated by a thin film of conducting material will resonate at a specific angle and result in a reduction in intensity of the reflected light at that angle. An electromagnetic evanescent wave then propagates away from the interface into the lower refractive index medium. The wave decays exponentially with distance from the interface so can only travel a distance of about 300nm. Thus SPR only detects changes in refractive index very close to the chip surface. Biomolecular interactions occurring at the sensor surface alter the solute concentration and the change in mass causes a depletion in the quantity of reflected light, thus altering the refractive index. SPR can therefore be used to monitor these interactions. One important advantage in using SPR is that there is no requirement for the labelling of the components being studied to permit their detection.

For these binding and kinetic experiments a CM5 sensor chip was used. It has a surface matrix consisting of non-crosslinked carboxy-methylated dextran with approximately

one carboxyl group per glucose residue. Each chip displays four separate channels on its surface, called flow cells. These can be independently modified, to study the interactions of one analyte with different ligands at any one time. The carboxyl groups are used for covalent immobilisation of the ligand (in this case the E3 enzyme of the 2-oxoacid dehydrogenase complexes) via amine, thiol and aldehyde or carboxyl groups. The matrix is hydrophilic and gives little non-specific binding, allowing very selective analysis when the analyte is in crude samples such as cell extracts. Due to the covalent nature of the bound ligand, the chip surface can be regenerated following the passage of analyte over its surface for repetitive measurements of binding. The output signal of a BIAcore is measured in resonance units (RU), with 1000 RU equal to 1ng of mass per  $\text{mm}^2$ . Inclusive software packages are available allowing calculations of association rate constants ( $k_{\text{ON}}$ ), dissociation rate constants ( $k_{\text{OFF}}$ ) and affinity ( $K_{\text{A}}$ ) or dissociation constants ( $K_{\text{D}}$ ).

A recent series of experiments was carried out by Lessard *et al.* (1996), with a degree of relevance to the work of this chapter. The group employed the biosensor system to study interactions between *B. stearothermophilus* E2-PDC with both the E1 and E3 enzymes of the complex. It has been demonstrated that one subunit binding domain of *B. stearothermophilus* is capable of binding either one E1 tetramer or one E3 dimer, but not both simultaneously (Lessard and Perham, 1995). The use of the biosensor allowed the determination of accurate measurements of the kinetics of the interactions. For the experimental series, the di-domain from *B. stearothermophilus* was attached to the surface of a CM5 chip, through the lipoyl group on the lipoyl domain. The oxidised form of the lipoyl group was used to generate a disulphide bridge with the thiol groups introduced to the chip surface. Samples of E1 and E3 were then passed over the immobilised di-domain and kinetic constants obtained. Values for  $k_{\text{ON}}$  were calculated to be identical for the E1-di-domain and E3-di-domain complexes ( $3.26 \times 10^6 \text{ M}^{-1} \text{ sec}^{-1}$ ). The rates of dissociation in contrast were vastly different:  $1.06 \times 10^{-3} \text{ sec}^{-1}$  and  $1.87 \times 10^3 \text{ sec}^{-1}$  respectively. Thus the experiments confirmed that the affinity of the

di-domain for E1 is greater than for E3 due entirely to the kinetics of dissociation. Further experiments were carried out by the group to define precisely the interactions between E1 and the binding domain. They were able to confirm that binding occurs solely through the E1 $\beta$  subunit, with no detectable binding between the E1 $\alpha$  subunit and the binding domain on E2.

As has been mentioned earlier, it appears that with regard to PDC, a separate gene product, namely protein X, has evolved with the ability to bind the E3 enzyme. Indeed, the removal of protein X from the PDC core results in a large decrease in whole complex activity. However, approx. 20% of this loss of activity can be regained by the addition of 100 fold excess amounts of E3.

It was with this in mind that the following BIAcore studies were performed. Having successfully overexpressed the di-domains of both E2-PDC and protein X, their ability to bind the E3 enzyme was investigated to determine whether indeed binding to protein X is stronger and to calculate the amount of residual binding to E2-PDC. Three sources of the E3 enzyme; human, porcine and yeast, were tested to determine whether protein X has indeed evolved with an increased ability to bind E3, over E2-PDC. Reconstitution studies in our laboratory (McCartney *et al.*, 1998) have shown that for maximal PDC activity to be recovered it is necessary to add back the parent E3, therefore it was investigated whether this result could be confirmed more precisely using the BIAcore instrument. Further studies in Glasgow had also demonstrated that the addition of yeast E3 causes a pronounced inhibition of recovery of mammalian PDC activity. In the following studies, yeast E3 was used as a substrate in an attempt to deduce whether its mode of inhibition involves high affinity binding to protein X, or if its mode of inhibition is by another means.

## 6.2 Aims of chapter.

1. Coupling of the E3 enzyme from porcine, human and yeast sources to a CM5 sensor chip.
2. Optimisation of the conditions required to study the interaction of the above-mentioned E3 enzymes with the overexpressed di-domains of protein X and E2-PDC, generated in an earlier chapter.
3. Obtaining kinetic and affinity data relating to the binding interactions.

## 6.3 Results

### 6.3.1 Immobilisation of various E3 enzymes onto the surface of a CM5 sensor chip.

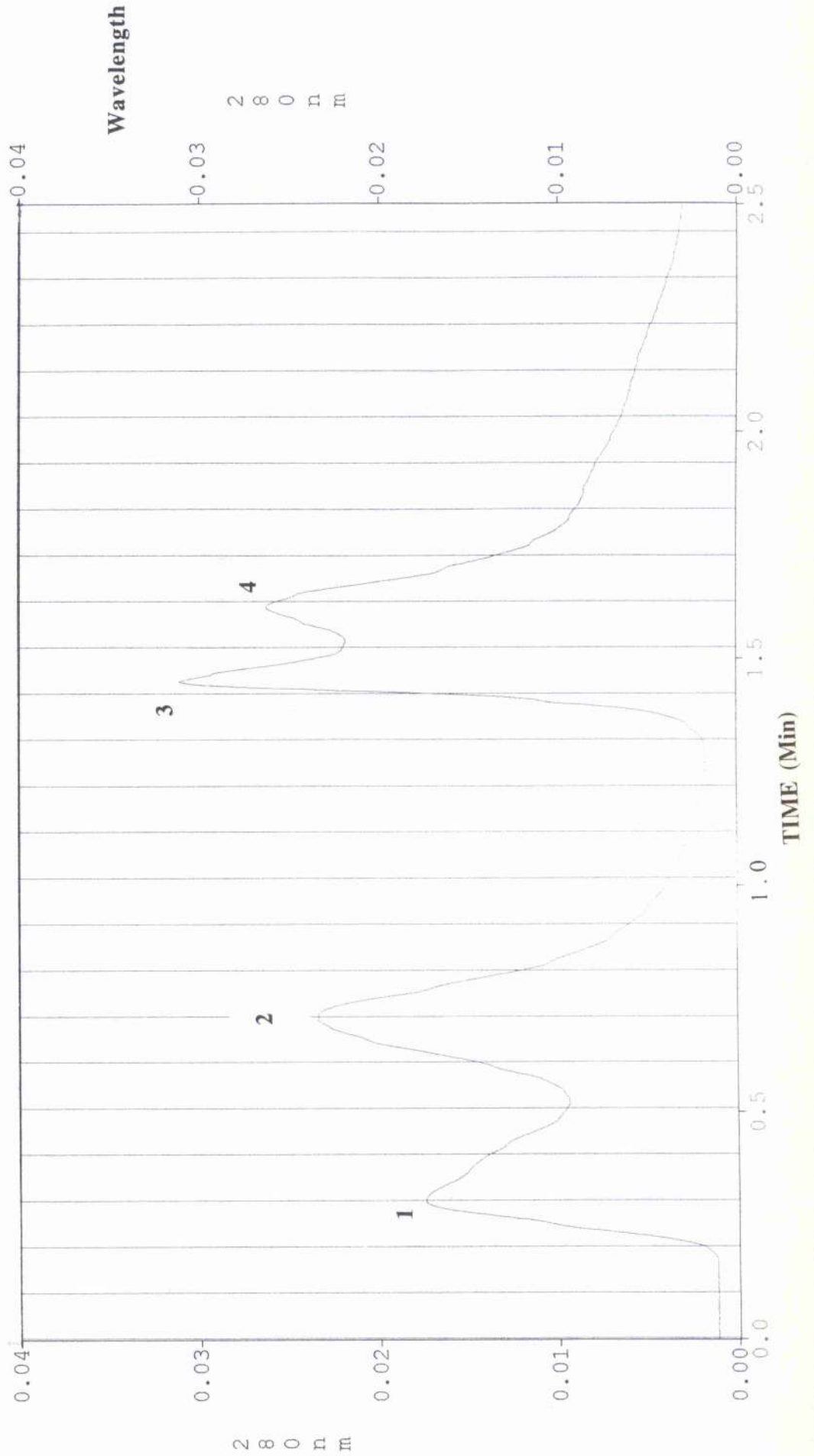
Commercial porcine and yeast E3s (Sigma) were used for immobilisation along with E3 isolated from partially purified human OGDC (Materials and Methods, section 2.2.22). The final stage in the purification of the human E3 involved the use of a Poros 20PSi column on the BioCAD Sprint Perfusion Chromatography System (PerSeptive Biosystems, Inc). The flow rate was set to 10ml/min, and the column equilibrated in a 25mM Bis/Tris propane buffer (pH 7.5), prior to loading the sample (1ml). A NaCl gradient was programmed to run from 400mM to 800mM over 15 column volumes. Fractions (1ml) were collected during this time. A final 10 column wash of 2M NaCl was carried out to remove any remaining material bound to the column. The final E3 sample was run in parallel with the same sample prior to purification. Figure 6.1, obtained following a 1ml injection of salt and heat-treated complex, shows 4 main peaks at 280nm. A sample (10 $\mu$ l) of each 1ml fraction corresponding to these peaks was resolved by SDS-PAGE analysis, to determine where the E3 had eluted. Having determined that the second peak was the one of relevance, fractions 4 to 7 were pooled together and concentrated using PEG-6000. Figure 6.2 shows a sample (10 $\mu$ l) of this purified E3 resolved by SDS-PAGE analysis, run in parallel with an equal volume of sample, prior to the column purification step.

### Footnote for Figure 6.1

**Figure 6.1 Elution profile obtained for the purification of the E3 enzyme from human OGDC complex using the BioCAD Sprint Perfusion Chromatography System.**

Following heat treatment at 65°C in the presence of high salt (see Materials and Methods), a 1ml sample of crude complex preparation was injected onto a Poros 20PSi column. Four major peaks of absorbance were observed at 280nm. A sample (10µl) of each corresponding 1ml fraction was analysed by SDS-PAGE to identify peak 2 as being the purified E3 enzyme.

Figure 6.1



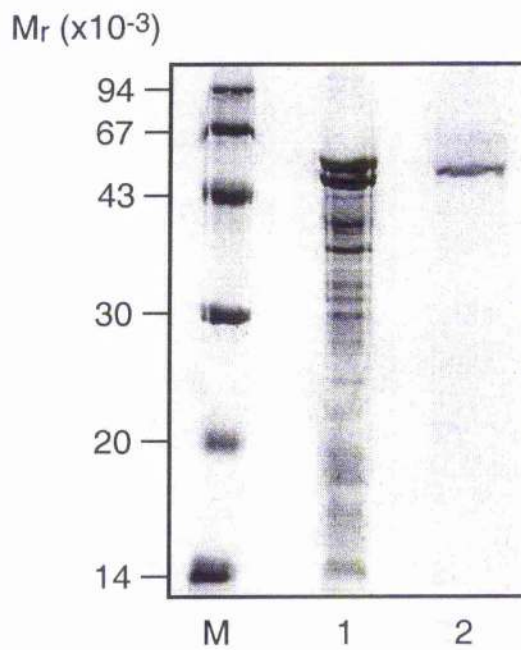


**Figure 6.2** Coomassie Blue-stained SDS-PAGE demonstrating the final step in the purification of the E3 enzyme from human OGDC.

Lane 1 shows the OGDC sample (10 $\mu$ l) following a 65 $^{\circ}$ C heat treatment. Lane 2 shows sample (10 $\mu$ l) following ion-exchange on a BioCAD Sprint Perfusion Chromatography system. M, molecular mass marker.

Each E3 was at a final concentration of 50 $\mu$ g/ml in 10mM sodium acetate buffer (pH 4.5) when injected over the surface of a CM-5 sensor chip. The immobilisation used NHS [N-hydroxysuccinimide] and EDC [N-ethyl-N'- (3-dimethylaminopropyl) carbodiimide hydrochloride] in accordance with the manufacturers' protocol for amine coupling. In each case, the flow rate was set to 5 $\mu$ l/min and sample was manually injected so that binding of ligand reached levels of between 1000 and 2000 RU. This level was deemed optimal for kinetic analysis studies. The true rates of association and dissociation can be limited by mass transport of the analyte (in these studies, the di-domains) to and from the binding surface. Relatively low levels of immobilised ligand help to keep intrinsic binding rates low so that mass transport effects are reduced to a minimum. Mass transport is influenced by the diffusion coefficient, which itself is dependent on molecular mass. An indication of mass transport limitations is if the value for the association constant increases as the concentration of analyte increases. Regeneration of the chip surface between analyte passages was achieved using 1M NaCl.

Figure 6.3 shows a theoretical sensorgram for an immobilisation sequence. The numbered points refer to the following stages in the process.

- (i) Baseline response for the pre-modified sensor chip surface, with a continuous flow of buffer across its surface.
- (1) Activation of the surface with NHS/EDC causes an initial increase in signal caused by the change in refractive index.
- (2) The base-line following activation is increased by approx. 250 RU due to the activation of NHS-esters.
- (3) Injection of ligand causes coupling to the chip surface. The ligand solution is still in contact with the sensor chip, so the response includes both the immobilised and non-covalently bound ligand. The sharp fall back to base line occurs when the solution has fully passed over the surface, taking with it any non-bound ligand.

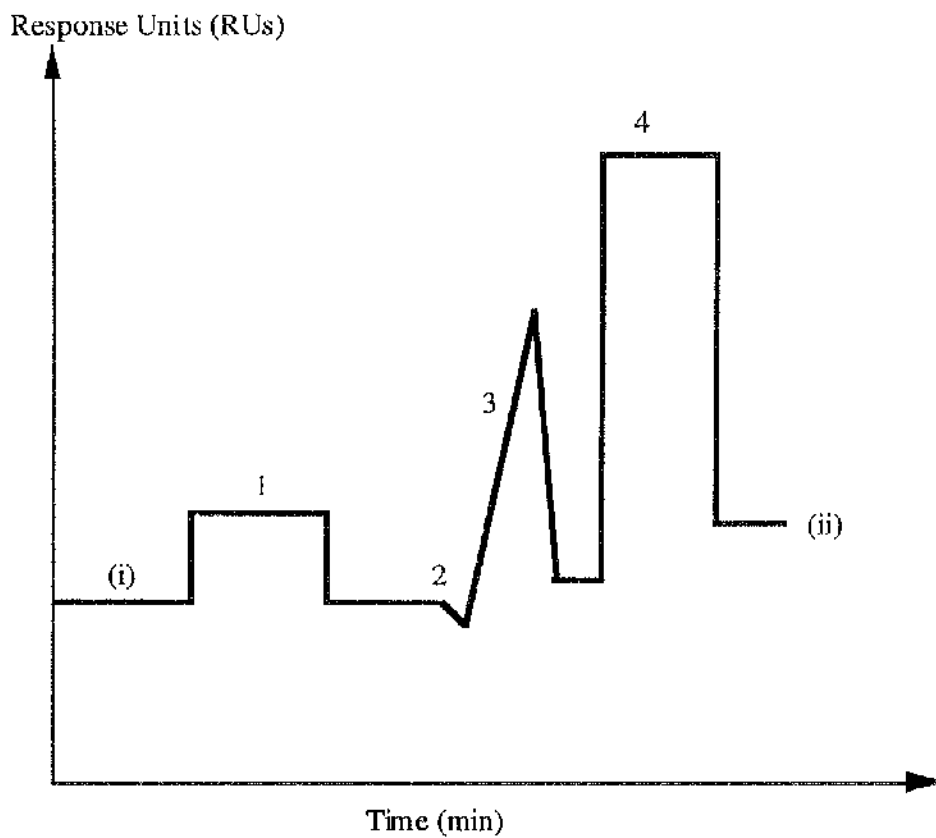


**Figure 6.3** Theoretical sensorgram showing the trace expected when coupling ligand to the flow-cells of the chip.

1. Surface activation with NHS/EDC.
2. Injection of ligand.
3. Coupling to the chip surface.
4. Blocking non-specific binding with ethanolamine.

The difference between (i) and (ii) represents the amount of ligand bound to the chip surface, in terms of response units, with 1,000RU being equivalent to 1ng protein per square mm.

- (4) Deactivation of unreacted NHS-esters by the addition of ethanolamine hydrochloride. Any ligand bound electrostatically is also removed.
- (ii) The amount of immobilised ligand after deactivation.

The immobilisation profiles of the E3 enzymes are shown by Figures 6.4a, b and c (sensorgrams A, B and C), corresponding to porcine, human and yeast sources. From the sensorgrams, the injection of each E3 enzyme gave the following results:

Porcine E3	1865 RU of binding
Human E3	1667 RU of binding
Yeast E3	1048 RU of binding

### **6.3.2 Interactions between the protein X and E2-PDC di-domains with the immobilised E3 samples.**

In order to study binding interactions between the previously generated di-domains and the E3 samples, 50ml cultures were IPTG-induced to overexpress the relevant di-domain and the pellets resuspended in HBS buffer (10mM HEPES (pH 7.4), 15mM NaCl, 3.4mM EDTA, 0.005% surfactant P20) to a final concentration of 1mg/ml. It was estimated from the SDS-PAGE analysis that the di-domain represented approx. 10% of the total protein in the cell extract, hence was at a concentration of approx. 0.1mg/ml, which corresponds to a 50 $\mu$ M solution. Each (60 $\mu$ l) extract was passed over the chip surface at a rate of 30 $\mu$ l/min, followed by 10 $\mu$ l 1M NaCl to regenerate the chip surface between analyte samples. Separate runs were carried out over a range of concentrations, from 50 $\mu$ M to 250nM. Reproducibility was confirmed using fresh cell extracts. Control injections were carried out by having a flow cell on the chip that had

**Figure 6.4a Sensorgram A, showing immobilisation of porcine E3 to a CM5 chip.**

Immobilisation was carried out using standard amine chemistry. E3 was passed over the chip surface at a final concentration of 50 $\mu$ g/ml and at a flow rate of 5 $\mu$ l/min until binding reached the level of 1865 RU. Any unbound E3 was washed away from the chip surface using 1M ethanolamine hydrochloride. The first X on the trace represents the point of injection of the E3. The second X represents the end of the manual injection. The third X represents the end of the second manual injection. The difference in RU between the first and third points shows the level of immobilisation.

# Sensorgram A

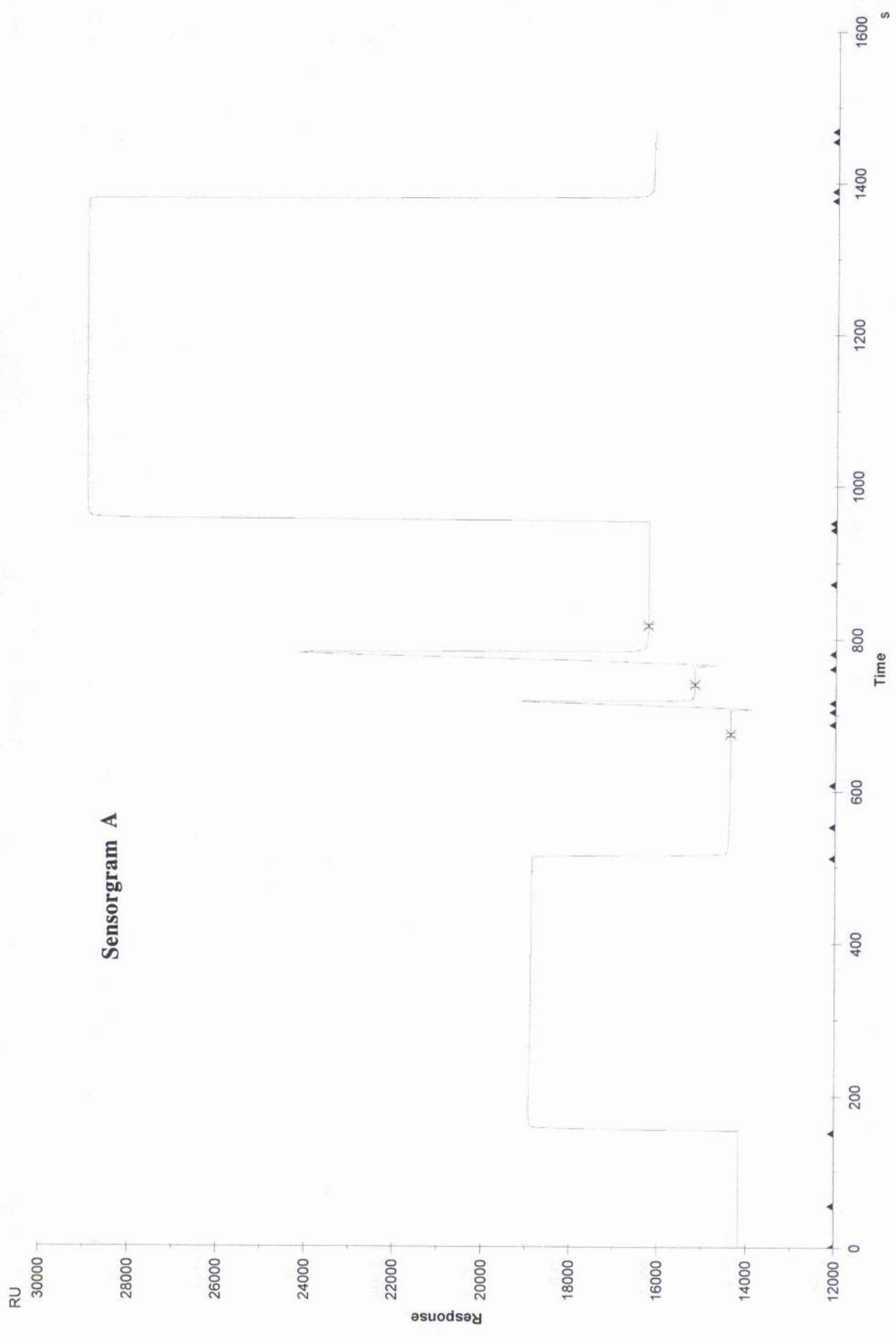


**Figure 6.4b Sensorgram B, showing immobilisation of human E3 to a CM5 chip.**

Immobilisation of porcine E3 was carried out using standard amine chemistry. E3 was passed over the chip surface at a final concentration of 50µg/ml and at a flow rate of 5µl/min until binding reached the level of 1667 RU. Any unbound E3 was washed away from the chip surface using 1M ethanolamine hydrochloride. The three spikes in the initial activation phase are an artefact caused by a reaction between NHS and EDC. This causes air bubbles to be produced, which are subsequently introduced during the injection phase. The three sites designated X are explained in the footnote for sensorgram A.

# Sensorgram B

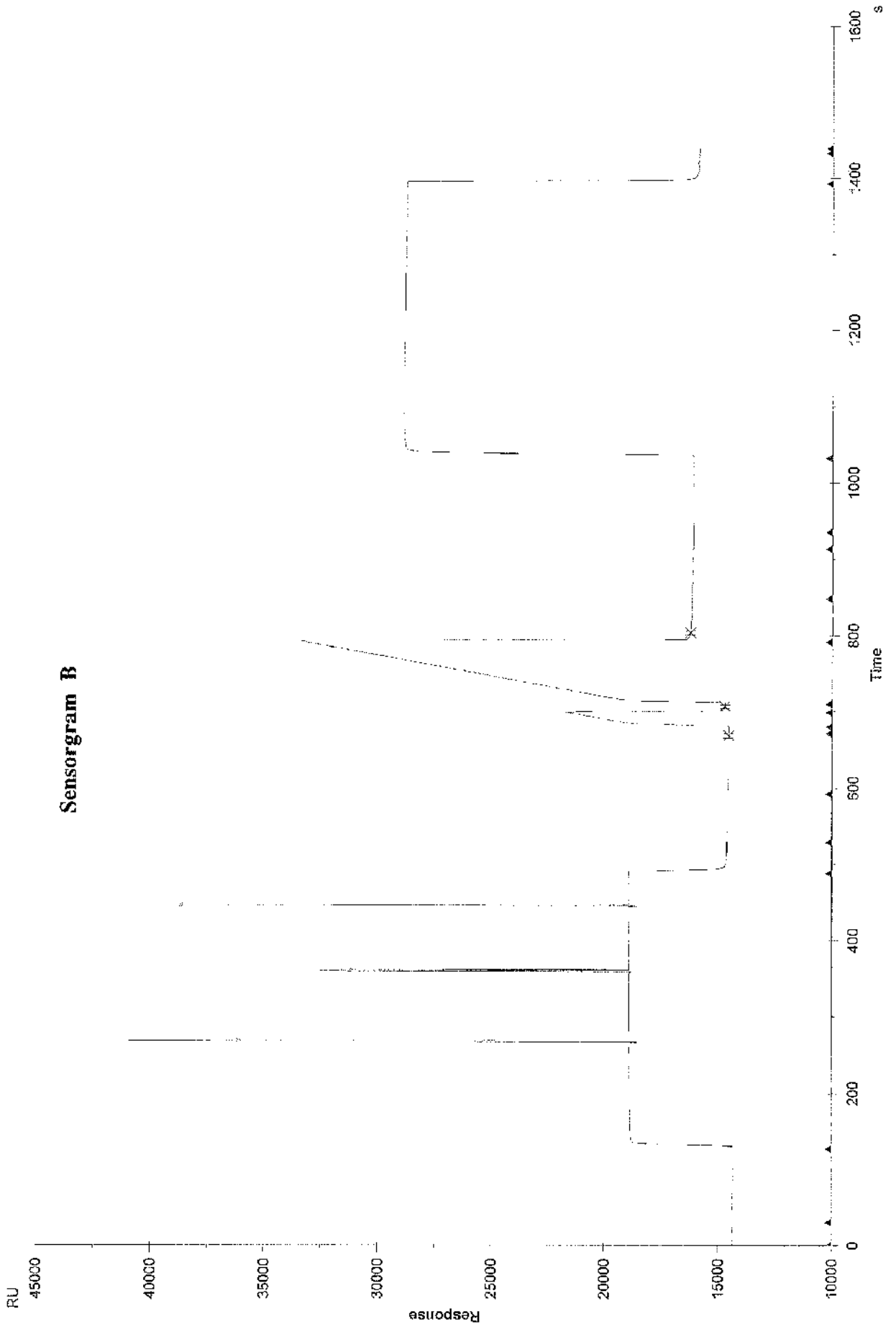
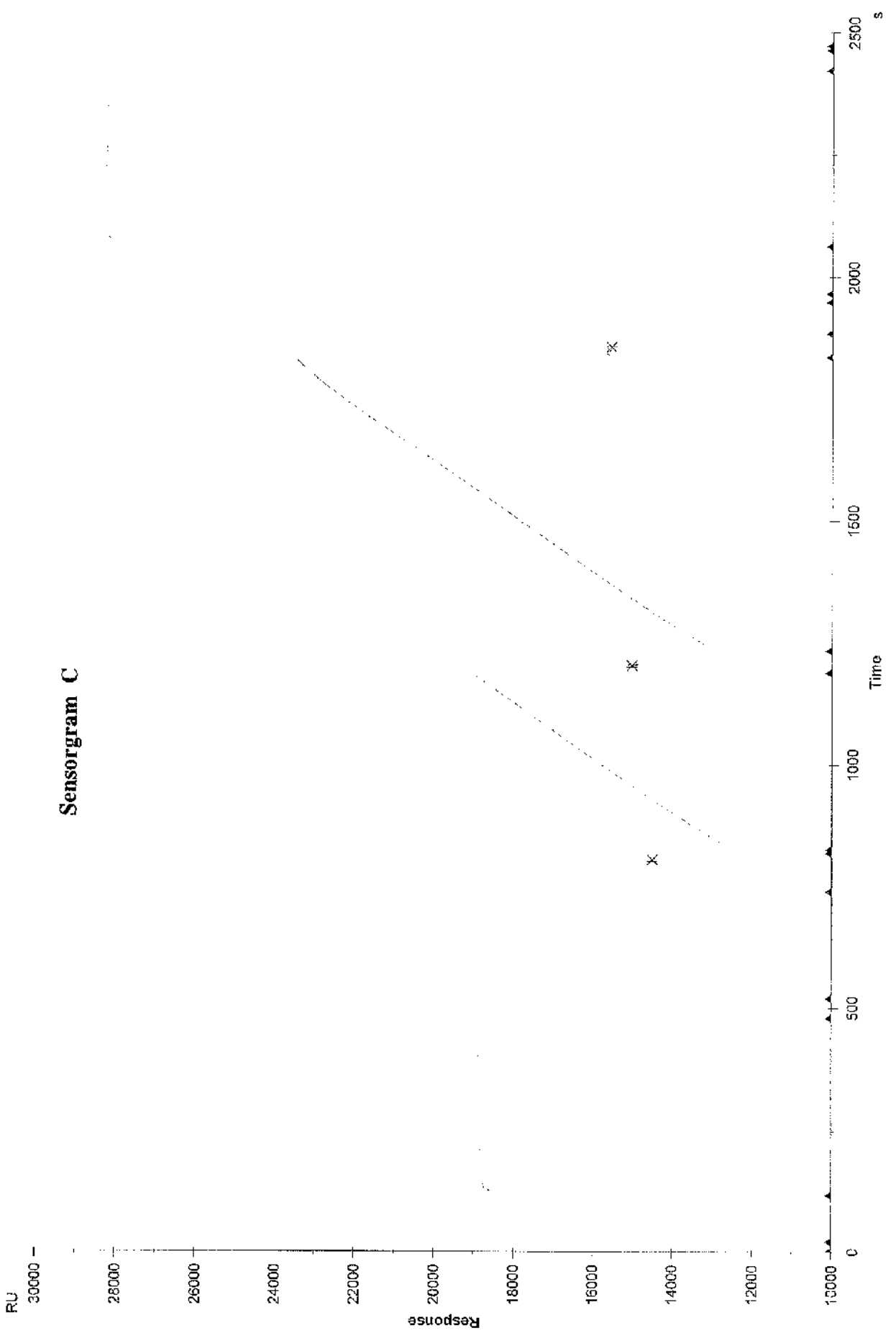


**Figure 6.4c Sensorgram C, showing immobilisation of yeast E3 to a CM5 chip.**

Immobilisation of yeast E3 was carried out using standard amine chemistry. E3 was passed over the chip surface at a final concentration of 50 $\mu$ g/ml and at a flow rate of 5 $\mu$ l/min until binding reached the level of 1048 RU. Any unbound E3 was washed away from the chip surface using 1M ethanolamine hydrochloride. As with the previous 2 sensorgrams, 2 manual injections were carried out to obtain the level of immobilisation of E3 required for these studies. The 3 sites designated X are explained in the footnote for sensorgram A.

# Sensorgram C



been treated by the same immobilisation protocol as for the E3 enzymes, with the exception of having no E3 in the sample. This allowed any background interactions with the chip surface to be detected and thus correcting the base-line binding levels. As a further control, an extract of *E. coli* DE3 pLysS was passed over the chip surface. It was noted that no significant binding occurred. Table 6.1 shows the rate and affinity constants obtained between the various E3 enzymes and protein X (A) and E2-PDC (B) di-domains.

**Table 6.1A Rate and affinity constants for the protein X di-domain interacting with the immobilised E3 enzymes.**

E3 source	$K_{on}$ $M^{-1}s^{-1}$	$K_{off}$ $s^{-1}$	$K_a$ $M^{-1}$	$K_d$ $M^{-1}$
Human E3	$6.98 \times 10^5$	$3.71 \times 10^{-3}$	$1.88 \times 10^8$	$5.31 \times 10^{-9}$
Porcine E3	$1.14 \times 10^5$	$5.21 \times 10^{-3}$	$2.18 \times 10^7$	$4.58 \times 10^{-8}$
Yeast E3	$1.02 \times 10^4$	$1.16 \times 10^{-2}$	$8.79 \times 10^5$	$1.14 \times 10^{-6}$

**Table 6.1B. Rate and affinity constants for the E2-PDC di-domain interacting with the immobilised E3 enzymes.**

E3 source	$K_{on}$ $M^{-1}s^{-1}$	$K_{off}$ $s^{-1}$	$K_a$ $M^{-1}$	$K_d$ $M^{-1}$
Human E3	$8.32 \times 10^3$	$3.27 \times 10^{-3}$	$2.52 \times 10^6$	$3.93 \times 10^{-7}$
Porcine E3	$1.47 \times 10^4$	$4.01 \times 10^{-3}$	$3.67 \times 10^6$	$2.72 \times 10^{-7}$
Yeast E3	2.15	$1.12 \times 10^{-5}$	$1.91 \times 10^5$	$5.23 \times 10^{-6}$

### **6.3.3 Interactions between full-length protein X and full-length E2-PDC and the immobilised E3 samples.**

As a comparison to the kinetic data obtained for the protein X and E2-PDC di-domain interactions with E3, the full-length mature protein X and E2-PDC genes were overexpressed in *E. coli* DE3 pLysS and the whole cell extracts passed over the surface of the CM5 chip, as before with the extracts of the overexpressed di-domains. Primers were designed to the published E2-PDC and protein X sequences, to allow PCR amplification. The PCR products were ligated into pET14b, which resulted in the generation of a His-Tag protein. The recombinant plasmids were amplified in *E. coli* XL-10 Gold. Following transformation into DE3 pLysS, the genes of interest were induced with IPTG and the whole cell extracts analysed by SDS-PAGE to confirm successful overexpression. The protein X gene generated a protein of  $M_r$  approx. 50,000 and the E2-PDC gene generated a protein of  $M_r$  approx. 70,000. (These initial stages were kindly carried out by Miss Audrey Brown in the laboratory). Tables 6.2A and 6.2B below show the rate and affinity constants obtained between the protein X and E2-PDC and the various E3 enzymes.

**Table 6.2A** Rate and affinity constants for full-length protein X interacting with the immobilised E3 enzymes.

E3 source	$K_{on}$ $M^{-1}s^{-1}$	$K_{off}$ $s^{-1}$	$K_a$ $M^{-1}$	$K_d$ $M^{-1}$
Human E3	$5.11 \times 10^5$	$4.81 \times 10^{-3}$	$1.06 \times 10^8$	$9.42 \times 10^{-9}$
Porcine E3	$4.58 \times 10^5$	$9.03 \times 10^{-3}$	$5.06 \times 10^7$	$1.97 \times 10^{-8}$
Yeast E3	$1.04 \times 10^4$	$1.07 \times 10^{-2}$	$9.66 \times 10^5$	$1.04 \times 10^{-6}$

**Table 6.2B** Rate and affinity constants for full-length E2-PDC interacting with the immobilised E3 enzymes.

E3 source	$K_{on}$ $M^{-1}s^{-1}$	$K_{off}$ $s^{-1}$	$K_a$ $M^{-1}$	$K_d$ $M^{-1}$
Human E3	$1.6 \times 10^5$	$1.91 \times 10^{-2}$	$8.38 \times 10^6$	$1.19 \times 10^{-7}$
Porcine E3	$1.42 \times 10^4$	$3.84 \times 10^{-3}$	$2.57 \times 10^6$	$2.70 \times 10^{-7}$
Yeast E3	<b>2.99</b>	$1.0 \times 10^{-5}$	$2.99 \times 10^5$	$3.36 \times 10^{-6}$

## 6.4 Discussion.

The advent of surface plasmon resonance (SPR) detection has now opened the way for in-depth investigations of the precise kinetics of interactions between proteins, which has particular relevance to the 2-oxoacid dehydrogenase complexes. The mobility of the individual domains hampers crystallisation studies and thus also the study of how the various components interact. SPR measurements are at the forefront of advancing this area of study.

The peripheral subunit-binding domain of *B. stearrowthermophilus* E2-PDC is known to interact strongly with both the E1 enzyme and the E3 component of the complex. Furthermore actual affinity constants have been determined, showing that vast differences in dissociation rates are primarily responsible for the differences in the observed binding affinities. Thus interactions between E1 and E3 and the binding domain occur in a non-simultaneous manner. In mammals, protein X has evolved as a separate gene product which is capable of binding the E3 enzyme, with high affinity. Surface plasmon resonance has been employed here as a way of studying the binding interactions between the peripheral subunit binding domains of E2-PDC and the equivalent putative binding domain of protein X with E3.

Prior to analysis of E2-E3 and protein X-E3 interactions on the BIAcore 2000 apparatus, a preliminary investigation had to be undertaken to confirm the stability of the E3 enzyme in the acidic conditions required during the immobilisation process. E3 assays were carried out at 4.5, following overnight incubation, to see what effect, if any the low pH would have on the enzyme. The activity of the enzyme was seen to reduce by 25%, when compared to E3 incubated at the normal assay pH of 7.6 (data not shown). The incubation time was far greater than that required for the immobilisation process, so it was decided that this decrease was not large enough to affect the experimental series. E3 is known to be a very robust enzyme, extremely resistant to proteolysis and capable of resisting degradation on heating to 65°C for

prolonged periods of time. Optimal immobilisation to the sensor chip surface requires low pH to keep the ligand protonated to interact with the negatively charged chip surface. Indeed, the pH was maintained at 1 pH unit below the pI of the enzyme. Furthermore, the actual buffer itself required to have no free amine groups, as this too would hinder the immobilisation process.

Before reliable rate constants and subsequently the dissociation constant ( $K_d$ ) can be determined for the interactions between the di-domains and the E3 enzymes, it is necessary to carry out a systematic series of experiments. The on rate constant ( $k_{on}$ ) can only be measured under non-equilibrium conditions *i.e.* where the rate of di-domain-E3 complex formation does not equal the rate of dissociation of the 2 components. A series of dilutions of the analyte solution (the di-domain) are therefore passed over the chip surface. These ranged from 250nM to 50 $\mu$ M. At the higher concentrations it was observed that equilibrium was reached too rapidly for the measurement of  $k_{on}$ .

Analysis of the dissociation constants ( $K_d$ ) for the various E3 interactions with E2 and protein X shows values in the  $\mu$ M to nM range. The lowest value of  $5.31 \times 10^{-9} \text{ M}^{-1}$  was obtained for the interaction between the protein X di-domain and human E3. Furthermore a similar value was obtained for the interaction between the full-length protein X and human E3 ( $9.42 \times 10^{-9} \text{ M}^{-1}$ ). These results would seem to substantiate the hypothesis that protein X has originated from E2 by gene duplication and has subsequently evolved a specific role in binding E3. Similar  $K_d$  values are observed for the interaction between a heterologous mammalian E3 (porcine) and the protein X di-domain ( $4.58 \times 10^{-8} \text{ M}^{-1}$ ) and also full length protein X ( $1.97 \times 10^{-8} \text{ M}^{-1}$ ). As reported previously, reconstitution is optimal when the E3 and subunit binding domains are from the same, *i.e.* parental source. The affinities of the interactions involving human E3 with the E2-PDC di-domain and full length E2 are lower than those involving protein X, although E2 displays a residual ability to bind E3 as expected from

previous biochemical studies. As is the case with protein X, the highest affinities are seen when the E3 is from the parental source. There is an obvious discrepancy between the values for the on and off constants obtained for full length E2 and the E2 di-domain which may be a result of full length E2 forming 60meric structures. In contrast, no such difference is observed between full length protein X and the di-domain, the former exhibiting a monomeric structure.

Analysis of the full length E2-PDC and the di-domain interactions with the human and porcine E3 enzymes shows that there is a decrease in the affinity of binding compared to the full-length protein X and the protein X di-domain. This again substantiates recent work demonstrating the necessity for the parental enzyme for restoring maximal affinities on reconstitution.

With regard to the interactions involving yeast E3, the dissociation constants are much greater than for the other two E3 enzymes from mammalian sources;  $1.14 \times 10^{-6} \text{ M}^{-1}$  for protein X di-domain,  $1.04 \times 10^{-6} \text{ M}^{-1}$  for full-length protein X,  $3.36 \times 10^{-6} \text{ M}^{-1}$  for full length E2-PDC and  $5.23 \times 10^{-6} \text{ M}^{-1}$  for the E2-PDC di-domain. This again shows the necessity for parental source interactions for high affinity interaction. As mentioned earlier, yeast E3 has been shown, in experiments carried out in our laboratory, to inhibit the reconstitution of mammalian PDC, when added in excess to the reconstituting enzyme components. The results obtained here from the BIAcore instrument show that the yeast E3 does not discriminate between E2 and protein X as the affinity constants are relatively similar. Taking this evidence together, would suggest that it is the binding to and interaction with the protein X or E2-E3-binding domain that causes the inhibition of the PDC complex reconstitution. Once bound to the main E3 binding site, the yeast E3 prevents interaction with the parental E3 enzyme.

The use of the full-length protein X and E2-PDC genes in the latter part of this chapter has provided further confirmation that the di-domains are fully functional subgenes of the mature E2-PDC and protein X genes. The BIAcore software does have some limitations because it assumes a 1:1 binding of analyte to ligand. Therefore the data obtained for full-length E2 should be interpreted with caution as it is likely that the recombinantly-expressed E2 which is fully active will be present as a 60meric assembly.

The experiments reported here involve, in effect, a simple immobilised ligand plus analyte format. Future investigations could employ a capture system employing the previously described monoclonal antibody PD1. As it recognises the lipoyl domain of the di-domain, a practical scenario would be to immobilise the antibody onto the chip surface. This process involves the Fc region, leaving the antigen recognition sites free for binding. Next, the cell extracts containing the overexpressed di-domains or full-length proteins would be passed over and allowed to interact with the antibody. Finally the various E3 enzymes would be passed over the Ab-E2 or Ab-protein X complexes allowing on and off rates and dissociation constants to be determined. This may potentially be a better system than that employed in this chapter because in addition to supplying data about two sets of binding constants (the antibody-di-domain interaction could be measured too), would reduce the chance of any non-specific reaction. The presence of the lipoyl domain attached to the subunit binding domain provides an ideal route for the attachment of the binding domain to the chip, whilst not interfering with subunit binding domain interactions.

Future studies could be conducted to confirm the accuracy of the binding data. Crude extracts may not represent the ideal source of di-domain or full-length protein and attempts are currently being made in the laboratory to generate them as GST-fusion proteins, which would make their purification easier. Research is also being carried out to generate the subunit binding domains of human E2 and protein X individually as

GST-fusion proteins. In addition, a purification strategy has been devised so that pure E2-PDC and protein X can be generated, following their construction as His-Tagged proteins.

These initial binding experiments have certainly proved that the BIAcore 2000 instrumentation is a powerful tool, capable of generating much needed quantification of the interactions of the individual components of the 2-oxoacid dehydrogenase complexes. The evidence obtained to date supports biochemical evidence that protein X has evolved a specific role in high affinity E3-binding; however, as suggested from biochemical studies on protein X-deficient complexes, the E2 subunit binding domain retains an appreciable affinity for the E3 components and is able to sustain partial PDC function in the presence of an excess of this enzyme. Future work will hopefully give an insight into the OGDC complex in particular, as little is currently known about subunit interactions involved in maintaining complex integrity. Along with crystallography studies, studies of the dynamics of protein-protein interactions by evolving technologies such as SPR will lead to a rapid increase in our understanding of structure-function relationships in multisubunit systems.

## GENERAL DISCUSSION

The family of mitochondrial 2-oxoacid dehydrogenase complexes represent the largest multienzyme systems studied to date and serve as paradigms for molecular enzymologists in their analysis of the enhancement of catalytical efficiency and regulatory control conferred by organisation into multisubunit structures. In addition, these complexes have several other unique properties: (a) as their subunits are nuclear encoded, these massive arrays must be assembled *in situ* within the mitochondrial matrix inner membrane compartment following import of their individual component polypeptides as larger precursors from the cytoplasm; (b) the activity states of PDC and BCOADC, uniquely amongst mitochondrial enzymes, are regulated by a phosphorylation/dephosphorylation cycle involving tightly-associated kinases and loosely-bound phosphatases, indicative of their key roles in carbohydrate and amino acid metabolism respectively; (c) defects in the catalytic function, import and biogenesis of the complexes are implicated in a wide range of biochemical and genetic disorders including various types of metabolic lactic acidosis (Robinson *et al.*, 1990), Alzheimers disease (Shen *et al.*, 1994) and autoimmune conditions such as primary biliary cirrhosis (Sherlock & Doolcy, 1993). The multifaceted nature of research into these complexes has meant that they have been subjected to extensive investigation from a number of directions in recent years. Despite this increased attention however, much remains to be learned about their structure-function relationships and involvement in a variety of pathological processes.

Until recently, models for their organisation have been based on our knowledge of bacterial PDCs, which have been subjected to intensive scrutiny. In the bacterial complexes, the oligomeric E2 assembly provides the structural and mechanistic framework for the complexes with the E1 and E3 components, non-covalently bound to a common or partially overlapping subunit binding domain, located in the N-terminal region immediately adjacent to the lipoyl domains. As has been observed in this thesis,

the E2 polypeptide possesses a multidomain organisation. This modular design permits the generation and subsequent overexpression of subgenes and individual domains as functional entities. An extra component of human PDC, termed protein X has a similar domain structure and has evolved from E2-PDC as a separate gene product, displaying a binding affinity for E3. Protein X has not been found in any bacterial sources.

In chapter three, we have overexpressed a subgene of the E2-PDC component from various sources and human protein X, which we have termed the di-domain. With the exception of Quinn *et al*, (1997), who successfully overexpressed the human lipoyl domain, this is the first reported overexpression of human and bovine subgenes in *E. coli*. Subsequently we have confirmed that these subgenes are correctly folded by two independent methods: (a) the mammalian domains are able to cross-react with a monoclonal antibody (PD1) raised specifically to the lipoylated form of the human lipoyl domain. Any incorrect folding would result in an inability to be recognised by the *E. coli* lipoyl ligase enzyme, responsible for the attachment of the prosthetic group; (b) surface plasmon resonance studies have also confirmed that the subunit binding domains of these subgenes are correctly folded by measuring the kinetics of binding interactions between the di-domains and various E3 enzymes.

A number of factors must be involved in the recognition by the lipoylating enzymes, in order that only the specific Lys residue within the lipoyl domain is lipoylated. The positioning of this residue is such that it extends outwards from the folded domain at the tip of a  $\beta$ -turn structure. In conjunction with the spacial positioning of the lipoyl-lysine, it is postulated that amino acid residues in the vicinity are also important in the recognition processes. In chapter four we have obtained the human lipoyl domain plus a series of point mutations of the domain in order to investigate the role of several residues in affecting the efficiency of lipoylation. We have shown that the residues immediately flanking the lipoyl-lysine are not necessary for lipoylation. Furthermore, we have shown, in agreement with Fujiwara *et al*, (1996) that the conserved upstream

Glu is important, as conversion to Gln leads to greatly reduced although not to total abolition of lipoylation. The possibility of a downstream conserved residue being of importance has still to be investigated.

As already mentioned, the individual components of the multienzyme complexes show a modular design, with each enzyme displaying several domains within its structure. The organisation of the 2-oxoglutarate complex (OGDC) is quite distinct to that of PDC, with regard to the ability of each of the components to interact with one another. As with PDC, the E2 polypeptides form an organisational framework, which provide binding sites for the other components; E1 and E3. Unlike PDC, E3 does not appear to bind directly to the E2 core. Instead, it does so via the E1 enzyme, in an association within its N-terminal region. Previous studies have been limited due the tight binding of E1 to the E2 core and also the instability of E1 on its release, thus the domain boundaries remain as yet ill-defined, so in chapter five we devised an experimental series to map more precisely the boundary of the E3-binding site on E1 in mammalian OGDC (a bovine heart source). Several N-terminal subgenes of E1 were generated as GST-fusion proteins and overexpressed then their ability to bind E3 was investigated. A direct interaction between E1-OGDC and E3 has been reported recently by McCartney *et al.*, (1998). However, the N-terminal fragments failed to exhibit any ability to interact with E3 as detected by their failure to act as competing inhibitory peptides. We were unable to confirm, at this stage whether these E1-GST fragments had folded correctly. It is possible that incorrect folding would prevent interaction with E3, however, they did partially inhibit reassociation following the release of both E1 and E3 from the E2 core.

The vast array of molecular biological techniques now available have opened many new avenues for research. One such field is that of surface plasmon resonance, using a BIAcore 2000 machine. In chapter six we have shown its usage in obtaining precise binding constants for interactions between human protein X and PDC-E2 with E3. This

technique is likely to recreate an environment similar to that *in vivo*, where binding is a continuous process, which reaches a state of equilibrium. It was possible to substantiate the hypothesis that protein X evolved a specific role in binding E3. The data demonstrated that the affinity of interaction between protein X and human E3 is greater than that for the interaction between human E2-PDC and human E3. It was shown that E2-PDC has retained an ability to bind E3, despite protein X being the main E3-binding protein. This is in agreement with clinical studies where patients lacking an immunologically detectable protein X, still retain a residual level of PDC activity. By using heterologous sources of E3, previous work has been further substantiated which showed the need for the parental E3 to gain optimal reconstitution. The binding affinities for the interaction between the porcine E3 and both protein X and E2-PDC were significantly lower than those involving human E3. This technique should, in future studies be able to provide a large amount of data regarding the numerous interactions that occur within the multienzyme complexes.

What should be recognised from this thesis and other studies recently being undertaken, is the speed at which our knowledge about these large 2-oxoacid dehydrogenase complexes is expanding. With the ability to generate vast quantities of material using a variety of expression systems and purification techniques now available, structure-function relationships and the molecular basis for many disease states associated with these 2-oxoacid dehydrogenase multienzyme complexes can now be investigated.

## **BIBLIOGRAPHY**

Ali, M.S., Shenoy, B.C., Eswaran, D., Anderson, L.A., Roche, T.E. and Patel, M.S. (1995) Identification of the tryptophan residue in the thiamin pyrophosphate binding site of the mammalian pyruvate dehydrogenase. *J. Biol. Chem.* **270**, 4570-4574.

Ali, S.T. and Guest, J.R. (1990) Isolation and characterisation of lipoylated and unlipoylated domains of the E2p subunit of the pyruvate dehydrogenase complex of *E. coli*. *Biochem. J.* **271**, 139-145.

Allen, A.G., Perham, R.N., Allison, N., Miles, J.S. and Guest, J.R. (1989) Reductive acetylation of tandemly repeated lipoyl domains in the pyruvate dehydrogenase multienzyme complex of *E. coli* in random order. *J. Mol. Biol.* **208**, 623-633.

Allen, M.D. PhD Thesis, 1995.

Barrera, C.R., Namihara, G., Hamilton, L., Munk, P., Eley, M.H., Linn, T.C. and Reed, L.J. (1972)  $\alpha$ -keto acid dehydrogenase complexes. *Arch. Biochem. Biophys.* **148**, 343-358.

Bates, D.L., Danson, M.J., Hale, G., Hooper, E.A. and Perham, R.N. (1977) Self-assembly and catalytic activity of the pyruvate dehydrogenase multienzyme complex of *Escherichia coli*. *Nature* **268**, 313-316.

Beal, M.F. (1992) Does impairment of energy-metabolism result in excitotoxic neuronal death in neurodegenerative illnesses? *Ann. of Neurol.* **31**, 119-130.

Behal, R.H., Browning, K.S., Hall, T.B. and Reed, L.J. (1989) Cloning and nucleotide sequence of the gene for protein X from *Saccharomyces cerevisiae*. *Proc. Natl. Acad. Sci. USA* **86**, 8732-8736.

Berg, A., De Kok, A. and Vervoort, J. (1994) Sequential  $^1\text{H}$  and  $^{15}\text{N}$  nuclear magnetic resonance assignments and secondary structure of the N-terminal lipoyl domain of the dihydrolipoyl transacetylase component of the pyruvate dehydrogenase complex from *A. vinelandii*. *Eur. J. Biochem.* **221**, 87-100.

Bleile, D.M., Hackert, M.L., Pettit, F.H. and Reed, L.J. (1981) Subunit structure of dihydrolipoyl transacetylase component of pyruvate dehydrogenase complex from bovine heart. *J. Biol. Chem.* **194**, 95-102.

Bleile, D.M., Munk, P., Oliver, R.M. and Reed, L.J. (1979) Subunit structure of dihydrolipoyl transacetylase component of pyruvate dehydrogenase complex from *Escherichia coli*. *Proc. Natl. Acad. Sci. USA* **76**, 4385-4389.

Borges, A., Hawkins, C.F., Packman, L.C. and Perham, R.N. (1990) Cloning and sequence analysis of the genes encoding the dihydrolipoamide acetyltransferase and dihydrolipoamide dehydrogenase components of the pyruvate dehydrogenase multienzyme complex of *B. stearothermophilus*. *Eur. J. Biochem.* **194**, 95-102.

Bowker-Kinley, M.M. and Popov, K.M. (1997) Site-directed mutagenesis of pyruvate dehydrogenase kinase isoform 2 reveals a new class of protein kinases. *FASEB J.* **11**, 9, SS, 2634.

Brookfield, D.E., Green, J., Ali, S.T., Machado, R.S. and Guest, J.R. (1991) Evidence for two protein-lipoylation activities in *E. coli*. *FEBS Letts.* **295**, 13-16.

Carothers, D.J., Pons, G. & Patel, M.S. (1989) Dihydrolipoamide dehydrogenase - Functional similarities and divergent evolution of the pyridine nucleotide-disulfide oxidoreductases. *Arch. Biochem. and Biophys.* **268**, 2, 409-425.

Danson, M.J., McQuattie, A. & Stevenson, K.J. (1986) Dihydrolipoamide dehydrogenase from *Halophilic Archaeobacteria* - Purification and properties of the enzyme from *Halobacterium-halobium*. *Biochemistry*, **25**, 13, 3880-3884.

Dardel, F., Packham, L.C. and Perham, R.N. (1990) Expression in *Escherichia coli* of a sub-gene encoding the lipoyl domain of the pyruvate dehydrogenase complex of *Bacillus stearothermophilus*. *FEBS Letts*. **264**, 206-210.

Dardel, F., Laue, E.D. and Perham, R.N. (1991) Sequence specific  $^1\text{H}$ -NMR assignments and secondary structure of the lipoyl domain from *B. stearothermophilus* pyruvate dehydrogenase multienzyme complex. *Eur. J. Biochem.* **201**, 203-209.

Dardel, F., Davis, A.L., Laue, E.D. and Perham, R.N. (1993) Three-dimensional structure of the lipoyl domain from *Bacillus stearothermophilus* pyruvate dehydrogenase multienzyme complex. *J. Mol. Biol.* **229**, 1037-1048

De Kok, A. and Westphal, A.H. (1985) Hybrid pyruvate dehydrogenase complexes reconstituted from components of the complexes from *E. coli* and *A. vinelandii*. *Eur. J. Biochem.* **152**, 35-41.

De Marcucci, O.G.L., Hunter, A. and Lindsay, J.G. (1986) Precursor forms of the constituent polypeptides of pyruvate dehydrogenase and 2-oxoglutarate dehydrogenase complexes from ox heart. *Biochemical Society Transactions*, *617th meeting*, **14**, 870.

De Marcucci, O. and Lindsay, J.G. (1985) Component X. An immunologically distinct peptide associated with mammalian pyruvate dehydrogenase multienzyme complex. *Eur. J. Biochem.* **149**, 641-648.

De Marcucci, O.L., Hunter, A. and Lindsay, J.G. (1985) Low immunogenicity of the common lipoamide dehydrogenase subunit (E3) of mammalian pyruvate dehydrogenase and 2-oxoglutarate dehydrogenase multienzyme complexes. *Biochem J.* **226**, 509-517.

De Meirleir, L., Lissens, W., Benelli, C., Marsac, C., De Klerk, J., Scholte, J., Van Diggelen, O., Kleijer, W., Seneca, S. and Liebaers, I. (1998) Pyruvate dehydrogenase complex deficiency and absence of subunit X. *J. Inher. Metab. Dis.* **21**, 9-16.

Endo, T., Mitsui, S., Nakai, M., and Roise, D. (1996) Binding of Mitochondrial Presequences to Yeast Cytosolic Heat Shock Protein 70 depends on the Amphiphilicity of the Presequence. *J. Bio. Chem.* **271**, (8), 4161-4167.

Frey, P.A., Fluornoy, D.S., Gruys, K. and Yang, Y-S. (1989) Intermediates in reductive transacetylase catalysed by pyruvate dehydrogenase complex. *Ann. N.Y. Acad. Sci. USA.* **573**, 21-35.

Fujiwara, K., Okamura-Ikeda, K. and Motokawa, Y. (1990) cDNA sequence, *in vitro* synthesis, and intramitochondrial lipoylation of H-protein of the glycine cleavage system. *J. Biol. Chem.* **265**, 17463-17467.

Fujiwara, K., Okamuraikeda, K. and Motokawa, Y. (1991) Lipoylation of H-protein of the glycine cleavage system - The effect of site-directed mutagenesis of amino acid residues around the lipoyllysine residue on the lipoate attachment. *FEBS Letts.* **293**, 115-118.

Fujiwara, K., Okamura-Ikeda, K. and Motokawa, Y. (1992) Expression of mature bovine H-protein of the glycine cleavage system in *E. coli* and *in vitro* lipoylation of the apoform. *J. Biol. Chem.* **267**, 20011-20016.

Fujiwara, K., Okamura-Ikeda, K. and Motokawa, Y. (1994) Purification and characterisation of lipoyl-AMP-N-epsilon-lysine lipoyltransferase from bovine liver mitochondria. *J. Biol. Chem.* **269**, 24, 16605-16609.

Fujiwara, K., Okamura-Ikeda, K. and Motokawa, Y. (1996) Lipoylation of Acetyltransferase Components of  $\alpha$ -Ketoacid Dehydrogenase Complexes. *J. Biol. Chem.* **271**, 12932-12936.

Fuller, C.C., Reed, L.J., Oliver, R.M. and Hackert, M.L. (1979) Crystallization of a dihydrolipoyl transacetylase-dihydrolipoyl dehydrogenase subcomplex and its implications regarding the subunit structure of the pyruvate dehydrogenase complex from *Escherichia coli*. *Biochem. Biophys. Res. Commun.* **90**, 431-438.

Fussey, S.P.M., Guest, J.R., James, O.F.W., Bassendine, M.F. and Yeaman, S.J. (1988) Identification and analysis of the major M2 autoantigens in primary biliary cirrhosis. *Proc. Natl. Acad. Sci. USA* **85**, 8654-8658.

Fussey, S.P.M., Ali, S., Guest, J.R., James, O.F.W., Bassendine, M.F. and Yeaman, S.J. (1990) Reactivity of primary biliary cirrhosis with *Escherichia coli* dihydrolipoamide acetyltransferase (E2p): characterisation of the main immunogenic region. *Proc. Natl. Acad. Sci. USA* **87**, 3987-3991.

Garland, P.B. and Randle, P.J. (1964) Control of pyruvate dehydrogenase in the perfused rat heart by the intracellular concentration of acetyl-coenzyme A. *Biochem J.* **91**, 6c-7c.

Geoffroy, V., Benelli, C., Poggi, F., Saudubray, J.M., Lissens, W., De Meirleir, L., Marsac, C. and Lindsay, J.G. (1996) Defect in the X-lipoyl-containing component of

the pyruvate dehydrogenase complex in a patient with neonatal lactic acidemia. *Pediatrics*, **97**, 267-272.

Glover, L.A. and Lindsay, J.G. (1992) Targeting proteins to mitochondria: a current overview. *Biochem. J.* **284**, 609-620.

Gottschalk, W. K., Lammers, R. and Ullrich, A. (1992) The carboxy terminal 110 amino acids portion of the insulin receptor is important for insulin signalling to pyruvate dehydrogenase. *Biochem. and Biophys. Res. Com.* **189**, 906-911.

Graham, L.D., Guest, J.R., Lewis, H.M., Miles, J.S., Packman, L.C., Perham, R.N. and Radford, S.E. (1986) The pyruvate-dehydrogenase multi-enzyme complex of *Escherichia coli* - genetic reconstitution and functional analysis of the lipoyl domains. *Phil. Trans. R. Soc. Lond. A.* **317**, 391-404.

Graham, L.D., Packman, L.C. and Perham, R.N. (1989) Kinetics and specificity of reductive acylation of lipoyl domains from 2-oxo acid dehydrogenase multienzyme complexes. *Biochemistry*, **28**, 1574-1581.

Green, J.D.F., Laue, E.D., Perham, R.N., Ali, S.T. and Guest, J.R. (1995) Three-dimensional structure of a lipoyl domain from the dihydrolipoyl acetyltransferase component of the pyruvate dehydrogenase multienzyme complex of *Escherichia coli*. *J. Mol. Biol.* **248**, 328-343.

Griffin, T.A. and Chuang, D.T. (1990) Genetic reconstruction and characterisation of the recombinant transketolase (E2b) component of bovine branched-chain  $\alpha$ -keto acid dehydrogenase complex. *J. Biol. Chem.* **265**, 13174-13180.

Gruys, K.J., Datta, A. and Frey, P.A. (1989) 2-acetylthiamin pyrophosphate (acetyl-TPP) pH-rate profile for hydrolysis of acetyl-TPP and isolation of acetyl-TPP as a transient species in pyruvate dehydrogenase catalysed reactions. *Biochemistry* **28**, 9071-9080.

Guest, J.R., Angier, S.J. and Russell, G.C. (1989) Structure, expression and protein engineering of the pyruvate dehydrogenase complex in *Escherichia coli*. *Ann. N. Y. Acad. Sci.* **573**, 76-99.

Guest, J.R. (1987) Functional implications of structural homologies between chloramphenicol acetyltransferase and dihydrolipoamide acetyltransferase. *FEMS Microbiol. Lett.* **44**, 417-422.

Guest, J.R., Lewis, H.M., Graham, L.D., Packman, L.C. and Perham, R.N. (1985) Genetic reconstruction and functional analysis of the repeating lipoyl domains in the pyruvate dehydrogenase multienzyme complex of *E. coli*. *J. Mol. Biol.* **185**, 743-754.

Hackert, M.L., Xu, W-X., Oliver, R.M., Wall, J.S., Hainfield, J.F., Mullinax, T.R. and Reed, L.J. (1989) Branched-chain  $\alpha$ -ketoacid dehydrogenase complex from bovine kidney: radial distribution of mass determined from dark-field electron micrographs. *Biochemistry* **28**, 6816-6821.

Hale, G., Wallis, N.G. and Perham, R.N. (1992) Interaction of avidin with the lipoyl domains in the pyruvate dehydrogenase multienzyme complex: three dimensional location and similarity to biotinyl domains in carboxylases. *Proc. R. Soc. Lond. B.* **248**, 247-253.

Hale, G. and Perham, R.N. (1979) Primary structure of the swinging arms of the pyruvate dehydrogenase complex of *E. coli*. *FEBS Letts.* **105**, 263-266.

- Hanemaaijer, R., Janssen, A., De Kok, A. and Veeger, C. (1989) The dihydrolipoyl transacetylase component of the pyruvate dehydrogenase complex from *A. vinelandii*. *Eur. J. Biochem.* **174**, 593-599.
- Harris, R.A., Hawes, J.W., Popov, K.M., Zhao, Y., Shimomura, Y., Sato, J., Jaskiewicz, J. & Hurley, T.D. (1997) Studies on the regulation of the mitochondrial alpha-ketoacid dehydrogenase complexes and their kinases. *Advances in Enzyme Regulation*, **37**, 271-293.
- Hawkins, C.F., Borges, A. and Perham, R.N. (1989) A common structural motif in thiamin pyrophosphate-binding enzymes. *FEBS Letts.* **255**, 77-82.
- Hayden, M.A., Huang, I., Bussiere, D.E. and Ashley, G.W. (1992) The biosynthesis of lipoic acid. *J. Biol. Chem.* **267**, 9512-9515.
- Heijne, G.V., Steppuhn, J. and Herrmann, R.G. (1989) Domain structure of mitochondrial and chloroplast targeting peptides. *Eur. J. Biochem.* **180**, 535-545.
- Henderson, C.E. and Perham, R.N. (1980) Purification of the pyruvate dehydrogenase multienzyme complex of *B. stearothermophilus* and resolution of its four component polypeptides. *Biochem. J.* **189**, 161-172.
- Hemila, H., Palva, A., Paulin, L., Arvidson, S. and Palva, I. (1990) Secretory S complex of *B. subtilis*: sequence analysis and identification to pyruvate dehydrogenase. *J. Bacteriol.* **172**, 5052-5063.
- Hipps, D.S. and Perham, R.N. (1992) Expression in *Escherichia coli* of a sub-gene encoding the lipoyl domain and peripheral subunit binding domains of the

dihydrolipoamide acetyltransferase component of the pyruvate dehydrogenase complex of *Bacillus stearothermophilus*. *Biochem. J.* **283**, 665-671.

Hipps, D.S., Packham, L.C., Allen, M.D., Fuller, C., Sakaguchi, K., Appella, E. and Perham, R.N. (1994) The peripheral subunit binding domain of the dihydrolipoamide acetyltransferase component of the pyruvate dehydrogenase complex of *Bacillus stearothermophilus*: preparation and characterization of its binding to the dihydrolipoamide dehydrogenase component. *Biochem. J.* **297**, 137-143.

Indo Y. and Matsuda, I. (1996) Molecular defects of the branched-chain  $\alpha$ -keto acid dehydrogenase complex: maple syrup urine disease due to mutations of the E1 $\alpha$  and E1 $\beta$  subunit gene. *Alpha-Keto Acid Dehydrogenase Complexes*. Patel, M.S., Roche, T.E. and Harris, R.A. (eds.) Birkhauser Verlag, Basel.

Jilka, J.M., Rahmatullah, M., Kazemi, M. and Roche, T.E. (1986) Properties of a newly characterised protein of the bovine kidney pyruvate dehydrogenase complex. *J. Biol. Chem.* **261**, 1858-1867.

Joplin R.E., Wallace, L.L., Lindsay, J.G., Palmer, J.M., Yeaman, S.J. and Neuberger, J.M. (1997) The human biliary epithelial cell plasma membrane antigen in primary biliary cirrhosis: pyruvate dehydrogenase X? *Gastroenterology* **113**, (5), 1727-1733.

Kalia, Y.N., Brocklehurst, S.M., Hipps, D.S., Appella, E., Sakaguchi, K. and Perham, R.N. (1993) The high-resolution structure of the peripheral subunit-binding domain of dihydrolipoamide acetyltransferase from the pyruvate dehydrogenase multienzyme complex of *Bacillus stearothermophilus*. *J. Mol. Biol.* **230**, 323-341.

Kanzaki, T., Hayakawa, T., Hamada, M., Fukuyoski, Y. and Koike, M. (1969) Mammalian  $\alpha$ -keto acid dehydrogenase complexes. IV. Substrate specificities and kinetic properties of the pig heart pyruvate and 2-oxoglutarate dehydrogenase complexes. *J. Biol. Chem.* **244**, 1183-1187.

Kaplan, M.M. (1987) Primary biliary cirrhosis. *N. Engl. J. Med.* **316**, 521-528.

Keha, E.E., Ronft, H. and Kresze, G-B. (1982) On the origin of mitochondria: a re-examination of the molecular structure and kinetic properties of pyruvate dehydrogenase complex from brewer's yeast. *FEBS Letts.* **145**, 289-292.

Khailova, L.S., Khorochkina, L.G. and Severin, S.E. (1989) Organisation and functioning of muscle pyruvate dehydrogenase active centers. *N. Y. Acad. Sci. USA* **573**, 36-54.

Kim, H. and Patel, M.S. (1992) Characterisation of two site-specifically mutated human dihydrolipoamide dehydrogenase (His-452 to Gln and Glu-457 to Gln). *J. Biol. Chem.* **267**, 5128-5132.

Kleanthous, C. and Shaw, W.V. (1985) Catalytic mechanism of chloramphenicol acetyltransferase - Evidence from kinetic and chemical modification studies. *Biochem. Soc. Transactions*, **13**, 1, 247-248.

Kochi, H. and Kikuchi, G. (1976) Mechanism of Reversible Glycine Cleavage Reaction in *Arthrobacter globiformis*. Function of Lipoic Acid in the Cleavage and Synthesis of Glycine. *Arch. Biochem. Biophys.* **173**, 71-81.

Koike, K., Urata, Y. and Goto, S. (1992). Cloning and nucleotide sequence of the cDNA encoding human 2-oxoglutarate dehydrogenase (lipoamide). *Proc. Natl. Acad. Sci. USA* **89**, 1963-1967.

Komuniecki, R., Rhee, R., Bhat, D., Duran, E., Sidaway, E. and Song, H. (1992) The pyruvate dehydrogenase complex from the parasitic nematode *Ascaris suum*: novel subunit composition and domain structure of the dihydrolipoyl transacetylase component. *Arch. Biochem. Biophys.* **296**, 115-121.

Kraulis, P.J. (1991) A program to produce both detailed and schematic plots of protein structures. *J. Applied Crystallography.* **24**, 5, 946-50.

Larner, J., Huang, C., Suzuki, S., Tang, G., Zhang, C., Schwartz, C.F.W., Romero, G., Luttrell, L. and Kennington, A.S. (1989) Insulin mediators and the control of pyruvate-dehydrogenase complex. *Ann. NY Acad. Sci.* **573**, 297-305.

Lewendon, A., Murray, I.A., Kleanthous, C., Cullis, P.M. and Shaw, W.V. (1988) Substitutions in the active site of chloramphenicol acetyltransferase: role of a conserved aspartate. *Biochemistry* **27**, 7385-7390.

Leslie, A.W.G. (1990) Refined crystal structure of type III chloramphenicol acetyltransferase at 1.75Å resolution. *J. Mol. Biol.* **213**, 167-186.

Lessard, I.A.D., Fuller, C. and Perham, R.N. (1996) Competitive Interaction of Component Enzymes of the Peripheral Subunit-Binding Domain of the Pyruvate Dehydrogenase Multienzyme Complex of *Bacillus stearothermophilus*: Kinetic Analysis Using Surface Plasmon Resonance Detection. *Biochemistry* **35**, 16863-16870.

Lessard, I.A.D. and Perham, R.N. (1995) Interaction of component enzymes with the peripheral subunit binding domain of the pyruvate dehydrogenase multienzyme complex of *Bacillus stearothermophilus*: Stoichiometry and specificity in self-assembly. *Biochem. J.* **306**, 727-733.

Lessard, I.A.D. and Perham, R.N. (1994) Expression in *E. coli* of genes encoding the E1 $\alpha$  and E1 $\beta$  subunits of the pyruvate dehydrogenase complex of *B. stearothermophilus* and assembly of a functional E1 component ( $\alpha_2\beta_2$ ) *in vitro*. *J. Biol. Chem.* **269**, 10378-10383.

Lindqvist, Y., Schneider, G., Ermler, U. and Sundstrom, M. (1992) Three-dimensional structure of transketolase, a thiamin diphosphate dependent enzyme at 2.5Å resolution. *EMBO J.* **7**, 2373-2379.

Ling, M., McEachern, G., Seyda, A., MacKay, N., Scherer, S.W., Bratinova, S., Beatty, B., Giovannucci-Uzielli, M.L. and Robinson, B.H. (1998) Detection of a homozygous four base pair deletion in the protein X gene in a case of pyruvate dehydrogenase complex deficiency. *Human Mol. Genet.* **7**, 501-505.

Liu, T-C., Kim, H., Arizmendi, C., Kitano, A. and Patel, M.S. (1993) Identification of two missense mutations in a dihydrolipoamide dehydrogenase-deficient patient. *Proc. Natl. Acad. Sci. USA* **90**, 5186-5190.

Logan, T.M., Theriault, Y. and Fesik, S.W. (1994) Structural characterization of the FK506 binding protein unfolded in urea and guanidine hydrochloride. *J. Mol. Biol.* **236**, 637-648.

Lowe, P.N., Hodgson, J.A., and Perham, R.N. (1983) Dual role of a single multienzyme complex in the oxidative decarboxylation of pyruvate and branched-chain 2-oxoacids in *B. subtilis*. *Biochem. J.* **215**, 133-140.

Lowry, O.H., Rosebrough, N.J., Farr, A.L. and Randall, R.J. (1951) Protein Measurement with the Florin Phenol Reagent. *Biol. Chem.* **193**, 265-275.

Machado, R.S., Guest, J.R. and Williamson, M.P. (1993) Mobility in pyruvate-dehydrogenase complexes with multiple lipoyl domains. *FEBS Letts.* **323**, 243-246.

Maedayorita, K., Russell, G.C., Guest, J.R., Massey, V. & Williams, C.H. (1994) Modulation of the oxidation-reduction potential of the flavin in lipoamide dehydrogenase from *Escherichia-coli* by alteration of a nearby charged residue, K53R. *Biochemistry* **33**, 20, 6213-6220.

Maeng, C-Y., Yazdi, M.A., Niu, X-D., Lee, H.Y. and Reed, L.J. (1994) Expression, purification and characterization of the dihydrolipoamide dehydrogenase binding protein of the pyruvate dehydrogenase complex from *Saccharomyces cerevisiae*. *Biochemistry* **33**, 13801-13807.

Mande, S.S., Sarfaty, S., Allen, M.D., Perham, R.N. and Hol, W.G.J. (1996) Protein-protein interactions in the pyruvate dehydrogenase multienzyme complex: dihydrolipoamide dehydrogenase complexed with the binding domain of dihydrolipoamide acetyltransferase. *Structure* **4**, 277-286.

Markwell, M.A., Haas, S., Bieber, L.L. and Tolbert, N.E. (1978) A Modification of the Lowry Procedure to Simplify Protein Determination in Membrane and Lipoprotein Samples. *Anal. Biochem.* **87**, 206-210.

Marsac, C., Stansbie, D., Bonne, G., Cousin, J., Jehenson, P., Benelli, C., Leroux, J.P. and Lindsay, G. (1993) Defect in the lipoyl-bearing protein X subunit of the pyruvate dehydrogenase complex in two patients with encephalomyelopathy. *J. Pediatr.* **123**, 915-920.

Mattevi, A., Obmolova, G., Kalk, K.H., Westphal, A.H., de Kok, A. and Hol, W.G.J. (1993) Refined crystal structure of the catalytic domain of dihydrolipoyl transacetylase (E2p) from *A. vinelandii* at 2.6Å resolution. *J. Mol. Biol.* **230**, 1183-1199.

Mattevi, A., Obmolova, G., Schulze, E., Kalk, K., Westphal, A.H., de Kok, A. and Hol, W.G.J. (1992) Atomic structure of the cubic core of the pyruvate dehydrogenase multienzyme complex. *Science* **255**, 1544-1550.

Mattevi, A., Schierbeck, A.J. and Hol, W.G.J. (1991) The refined crystal structure of lipamide dehydrogenase from *Azotobacter vinelandii* at 2.2Å resolution. *J. Mol. Biol.* **220**, 975-994.

McCartney, R.G., Rice, J.E., Sanderson, S.J., Bunik, V., Lindsay, H. and Lindsay, J.G. (1998) Subunit interactions in the mammalian alpha-ketoglutarate dehydrogenase complex - Evidence for direct association of the alpha-ketoglutarate dehydrogenase and dihydrolipoamide dehydrogenase components. *J. Biol. Chem.* **273**, 37, 24158-24164.

McCartney, R.G., Sanderson, S.J. and Lindsay, J.G. (1997) Refolding and Reconstitution studies on the Transacetylase-Protein X (E2/X) Subcomplex of the Mammalian Pyruvate Dehydrogenase Complex: Evidence for Specific Binding of the Dihydrolipoamide Dehydrogenase Component to Sites on Reassembled E2. *Biochemistry* **36**, 22, 6819-6826.

Meng, M. and Chuang, D.T. (1994) Site-directed mutagenesis and functional analysis of the active-site residues of the E2 component of branched-chain  $\alpha$ -keto acid dehydrogenase complex. *Biochemistry* **33**, 12879-12885.

Miles, J.S., Guest, J.R., Radford, S.E. and Perham, R.N. (1988) Investigation of the mechanism of active site coupling in the pyruvate dehydrogenase multienzyme complex of *E. coli* by protein engineering. *J. Mol. Biol.* **202**, 97-106.

Miles, J.S., Guest, J.R., Radford, S.E. and Perham, R.N. (1987) A mutant pyruvate dehydrogenase complex of *E. coli* deleted in the (Alanine+ Proline)-rich region of the acetyltransferase component. *Biochim. Biophys. Acta.* **913**, 117-121.

Mori, T., Oshima, Y. and Kochi, H. (1994) Binding properties of the components of branched-chain 2-oxoacid dehydrogenase complex on ELISA. *J. Biochem.* **116**, 1111-1116.

Morris, T.W., Reed, K.E. and Cronan, J.E. (1994) Identification of the gene encoding lipoyl-protein ligase A of *E. coli*. Molecular cloning and characterization of the *lplA* gene and gene-product. *J. Biol. Chem.* **269**, 16091-16100.

Morris, T.W., Reed, K.E. and Cronan, J.E. (1995) Lipoyl acid metabolism in *Escherichia coli* - The *lplA* and *lplB* genes define redundant pathways for ligation of lipoyl groups to apoprotein. *J. Bacteriol.* **177**, 1, 1-10.

Murakami, K. and Mori, M. (1990) Purified presequence binding factor (PBF) forms an import-competent complex with a purified mitochondrial precursor protein. *EMBO J.* **9**, (10), 3201-3208.

Nakano, K., Takase, C., Sakamoto, T., Nakagawa, S., Inazawa, J., Ohta, S. and Matuda, S. (1994) Isolation, characterization and structural organization of the gene and pseudo gene for the dihydrolipoamide succinyltransferase component of the human 2-oxoglutarate dehydrogenase complex. *Eur. J. Biochem.* **224**, 179-189.

Nakano, K. Matuda, S., Yamanaka, T., Tsubouchi, H., Nakagawa, S., Titani, K., Ohta, S. and Miyata, T. (1991) Purification and Molecular cloning of succinyltransferase of the Rat  $\alpha$ -ketoglutarate Dehydrogenase Complex. *J. Biol. Chem.* **266**, 19013-19017.

Neagle, J., De Marcucci, O., Dunbar, B. and Lindsay, J.G. (1989) Component X of mammalian pyruvate dehydrogenase complex: structural and functional relationship to the lipoate acetyltransferase (E2) component. *FEBS Letts.* **253**, 11-15.

Neagle, J. and Lindsay, J.G. (1991) Selective proteolysis of the protein X subunit of the bovine heart pyruvate dehydrogenase complex. (Effects on dihydrolipoamide dehydrogenase (E3) affinity and enzymatic properties of the complex). *Biochem. J.* **278**, 423-427.

Niu, X.-D., Stoops, J.K. and Reed, L.J. (1990) Overexpression and mutagenesis of the catalytic domain of dihydrolipoamide acetyltransferase from *S. cerevisiae*. *Biochemistry* **29**, 8614-8619.

Oliver, R.M. and Reed, L.J. (1982) in "Electron Microscopy of Proteins" (ed. R.Harris) Academic Press, London. **2**, 1-48.

Otulakowski, G. and Robinson, B.H. (1987) Isolation of cDNA clones of porcine and human lipoamide dehydrogenase - homology to other disulphide oxidoreductase. *J. Biol. Chem.* **262**, 17313-17318.

Packman, L.C. and Perham, R.N. (1986) Chain folding in the dihydrolipoyl acetyltransferase components of the 2-oxo-acid dehydrogenase complexes of *E. coli*. *FEBS Letts.* **206**, 193-198.

Packman, L.C. and Perham, R.N. (1987) Limited proteolysis and sequence analysis of the 2-oxo acid dehydrogenase complexes of *E. coli*. *Biochem. J.* **242**, 531-538.

Packman, L.C., Borges, A. and Perham, R.N. (1988) Amino acid sequence analysis of the lipoyl and peripheral subunit-binding domains in the lipoate acetyltransferase component of the pyruvate dehydrogenase complex from *Bacillus stearothermophilus*. *Biochem. J.* **252**, 79-86.

Palmer, T.N., Caldecourt, M.A. and Sugden, M.C. (1983) Adrenergic inhibition of branched-chain 2-oxoacid dehydrogenase in rat diaphragm muscle *in vitro*. *Biochem. J.* **216**, 63-70.

Patel, M.S., Johnson, M., Yang, H-S and Magnuson, T. (1997) Targeted disruption of murine dihydrolipoamide dehydrogenase gene. *FASEB J.* **11**, SS458

Patel, M.S. and Roche, T.E. (1990) Molecular biology and biochemistry of pyruvate dehydrogenase complexes. *FASEB J.* **4**, 3224-3233.

Perham, R.N. (1991) Domains, motifs and linkers in 2-oxo acid dehydrogenase multienzyme complexes : A paradigm in the design of a multifunctional protein. *Biochemistry* **30**, 8501-8511.

Popov, K.M., Hawes, J.W. & Harris, R.A. (1997) Mitochondrial alpha-ketoacid dehydrogenase kinases - A new family of protein kinases. *Advances in second messenger and phosphoprotein research*, **31**, 105-111.

Popov, K.M., Zhao, Y., Shimomura, Y., Jaskiewicz, J.A., Kerdishvili, N.Y., Irwin, J., Goodwin, G.W. and Harris, R.A. (1995) Dietary control and tissue expression of branched-chain  $\alpha$ -ketoacid dehydrogenase kinase. *Arch. Biochem. Biophys.* **316**, 148-154.

Popov, K.M., Kerdishvili, N.Y., Zhao, Y., Gudi, R. and Harris, R.A. (1994) Molecular cloning of the p45 subunit of pyruvate dehydrogenase kinase. *J. Biol. Chem.* **269**, 29720-29724.

Popov, K.M., Kerdishvili, N.Y., Zhao, Y., Shimomura, Y., Crabb, D.W. and Harris, R.A. (1993) Primary Structure of Pyruvate Dehydrogenase Kinase Establishes a New Family of Eukaryotic Protein Kinases. *J. Biol. Chem.* **268**, 26602-26606.

Popov, K.M., Zhao, Y., Shimomura, Y., Kuntz, M.J. and Harris, R.A. (1992) Branched-chain  $\alpha$ -ketoacid dehydrogenase kinase: molecular cloning, expression, and sequence similarity with histidine protein kinases. *J. Biol. Chem.* **267**, 13127-13130.

Quinn, J., Diamond, A.G., Masters, A.K., Brookfield, D.E., Wallis, N.G. and Yeaman, S. (1993) Expression and lipoylation in *Escherichia coli* of the inner lipoyl domain of the E2 component of the human pyruvate dehydrogenase complex. *Biochem J.* **289**, 81-85.

Quinn, J. (1997) Lipoylation of acetyltransferase components of 2-oxoacid dehydrogenase complexes. *Methods in Enzymology*, **279**, 193-202.

Rahmatullah, M., Gopalakrishnan, S., Andrwes, P.C., Chang, C.L., Radke, G.A. and Roche, T.E. (1989) Subunit associations in the mammalian pyruvate dehydrogenase complex. *J. Biol. Chem.* **264**, 2221-2227.

Reed, K.E. and Cronan, J.E. (1993) Lipoic acid metabolism in *E. coli*: sequencing and functional characterisation of the *lipA* and *lipB* genes. *J. Bacteriol.* **175**, 1325-1326.

Reed, L.J. and Yeaman, S.J. (1987) in *The Enzymes* (Boyer, P.D., and Krebs, E.G.) Vol **18**, 77-96, Academic Press, Orlando, FL, USA. Pyruvate Dehydrogenase.

Reed, L.J. (1974) Multienzyme complexes. *Acc. Chem. Res.* **7**, 40-56.

Reed, L.J., Leach, F.R. and Koike, M. (1958) Studies on the lipoic acid activating systems. *J. Biol. Chem.* **232**, 123-142.

Rice, J. E., Dunbar, B. and Lindsay, J.G. (1992) Sequences directing dihydrolipoamide dehydrogenase (E3) binding are located on the 2-oxoglutarate dehydrogenase (E1) component of the mammalian 2-oxoglutarate dehydrogenase multienzyme complex. *EMBO J.* **11**, 9, 3229-3235.

Robien, M.A., Clore, G.M., Omichinski, J.G., Perham, R.N., Appella, E., Sakaguchi, K. and Gronenborn, A.M. (1992) Three-dimensional solution structure of the E3-binding domain of the dihydrolipoamide succinyltransferase core from the 2-oxoglutarate dehydrogenase multienzyme complex of *Escherichia coli*. *Biochemistry* **31**, 3463-3471.

Robinson, B.H., MacKay, N., Petrova-Benedict, R., Ozalp, I., Coskun, T. and Stacpoole, P.W. (1990) Defects in the E2 lipoyl transacetylase and the X-lipoyl

containing component of the pyruvate dehydrogenase complex in patients with lactic acidemia. *J. Clin. Invest.* **85**, 1821-1824.

Roche, T.E. and Patel, M.S. (1989) Alpha-keto acid dehydrogenase complexes- Organisation, regulation and biomedical ramifications - A tribute to Lester J. Reed. *Ann. N.Y. Acad. Sci.* **573**, 1-462.

Roche, T.E., Rahmatullah, M., Powers-Greenwood, S.L., Radke, G.A., Gopalakrishnan, S. and Chang, C.L. (1989) The lipoyl-containing components of the mammalian pyruvate dehydrogenase complex: Structural comparison and subdomain roles. *Ann. N.Y. Acad. Sci.* **573**, 66-75.

Rowles, J., Scherer, S.W., Xi, T., Majer, M., Nickle, D.C., Rommens, J.M., Popov, K.M., Harris, R.A., Riebow, N.L., Xia, J., Tsui, L.C., Bogardus, C. and Prochazka, M. (1996) Cloning and characterization of *PDK4* on 7q21.3 encoding a fourth pyruvate dehydrogenase kinase isoenzyme in human. *J. Biol. Chem.* **271**, 22376-22382.

Russell, G.C. and Guest, J.R., (1991) Sequence similarities within the family of dihydrolipoamide acetyltransferases and discovery of a previously unidentified fungal enzyme. *Biochim. Biophys. Acta.* **1076**, 225-232.

Russell, G.C. and Guest, J.R., (1990) Overexpression of restructured pyruvate dehydrogenase complexes and site-directed mutagenesis of a potential active-site histidine residue. *Biochem. J.* **269**, 443-450.

Sanderson, S.J., Khan, S.S., McCartney, R.G., Miller, C. and Lindsay, J.G. (1996) Reconstitution of mammalian pyruvate dehydrogenase and 2-oxoglutarate dehydrogenase complexes: analysis of protein involvement and interaction of homologous and heterologous dihydrolipoamide dehydrogenases. *Biochem. J.* **319**, 109-116.

Schatz, G. and Dobberstein, B. (1996) Common Principles of Protein Translocation Across Membranes. *Science* **271**, 1519-1526.

Schulze, E., Westphal, A.H., Veeger, C. and De Kok, A. (1992) Reconstitution of pyruvate dehydrogenase complexes based upon dimeric core structures from *A. vinelandii* and *E. coli*. *Eur. J. Biochem.* **206**, 427-435.

Schulze, E., Benen, J.A.E., Westphal, A.H. and De Kok, A. (1991) Interaction of lipoamide dehydrogenase with the dihydrolipoyl transacetylase component of the pyruvate dehydrogenase complex from *A. vinelandii*. *Eur. J. Biochem.* **200**, 29-34.

Shepherd, B.B. and Hammes, G.G. (1976) Fluorescence energy-transfer measurements between CoA and FAD-binding sites of the *E. coli* pyruvate dehydrogenase multienzyme complex. *Biochemistry* **15**, 311-317.

Sherlock, S. and Dooley, J. (1993) Diseases of the liver and biliary system. Blackwell Scientific Publications, Ninth Edition, Oxford, 236-250.

Sheu, K.F., Cooper, A., Koike, K., Koike, M., Lindsay, J.G. & Blass, J.P. (1994) Abnormality of the alpha-ketoglutarate dehydrogenase complex in fibroblasts from familial alzheimers disease. *Ann. of Neurol.* **35**, 3, 312-318.

- Spencer, M.E., Darlison, M.G., Stephens, P.E., Duckenfield, I.K. and Guest, J.R. (1984) Nucleotide sequence of the *sucB* gene encoding the dihydrolipoamide succinyltransferase of *Escherichia coli* K12 and homology with the corresponding acetyltransferase. *Eur. J. Biochem.* **141**, 361-374.
- Stanley, C. and Perham, R.N. (1980) Purification of 2-oxo acid dehydrogenase multienzyme complexes from ox heart by a new method. *Biochem. J.* **191**, 147-154.
- Stephens, P.E., Darlison, M.G., Lewis, H.M. and Guest, J.R. (1983) The pyruvate dehydrogenase complex of *Escherichia coli* K12. The nucleotide sequence encoding the dihydrolipoamide acetyltransferase component. *Eur. J. Biochem.* **133**, 481-489.
- Stephens, P.E., Lewis, H.M., Darlison, M.G. and Guest, J.R. (1983h) Nucleotide sequence of the lipoamide dehydrogenase gene of *Escherichia coli* K12. *Eur. J. Biochem.* **135**, 519-527.
- Stepp, L.R. & Reed, L.J. (1985) Active-site modification of mammalian pyruvate-dehydrogenase by pyridoxal 5'-phosphate. *Biochemistry* **24**, 25, 7187-7191.
- Stoops, J.K., Baker, T.S., Schroeter, J.P., Kolodzie, S.J., Niu, X-D. and Reed, L.J. (1992) Three-dimensional structure of the truncated core of the *S. cerevisiae* pyruvate dehydrogenase complex determined from negative stain and cryoelectron microscopy. *J. Biol. Chem.* **267**, 24769-24775.
- Stuart, R. A., Gruhler, A., Vanderklei, I., Guiard, B., Koll, H. and Neupert, W. (1994) The requirement of matrix ATP for the import of precursor proteins into the mitochondrial matrix and intermembrane space. *Eur. J. Biochem.* **20**, 1, 9-18.

Surh, C.D., Roche, T.E., Danner, D.J., Ansari, A, Coppel, R.L. Dickson, R. and Gershwin, M.E. (1989) Antimitochondrial autoantibodies in primary biliary cirrhosis recognize cross-reactive epitope(s) on protein X and dihydrolipoamide acetyltransferase of pyruvate dehydrogenase complex. *Hepatology* **10**, 2, 127-133.

Vettakkorumakankav, N.N. and Patel, M.S. (1996) Dihydrolipoamide dehydrogenase: Structural and mechanistic aspects. *Indian J. Biochem & Biophys.* **33**, 3, 168-176.

Wagenknecht, T., Grassucci, R., Radke, G.A. and Roche, T.E. (1991) Cryoelectron microscopy of mammalian pyruvate dehydrogenase complex. *J. Biol. Chem.* **266**, 24650-24656.

Wallis, N.G., Allen, M.D., Broadhurst, R.W., Lessard, I.A.D. and Perham, R.N. (1996) Recognition of a Surface Loop of the Lipoyl Domain Underlies Substrate Channelling in the Pyruvate Dehydrogenase Multienzyme Complex. *J. Mol. Biol.* **263**, 463-474.

Wallis, N.G. and Perham, R.N. (1994) Structural dependence of post-translational modification and reductive acetylation of the lipoyl domain of the pyruvate dehydrogenase multienzyme complex. *J. Mol. Biol.* **236**, 209-216.

Wieland, O.H., Urumow, T. and Drexler, P. (1989) Insulin, phospholipase and the activation of the pyruvate dehydrogenase complex: an enigma. *Ann. NY Acad. Sci.* **573**, 274-284.

Williams, C.H. Jr. (1992) Lipoamide dehydrogenase, glutathione reductase, thioredoxin reductase and mercuric reductase-family of flavoenzyme dehydrogenase. In *Chem. and Biochem. of flavoenzymes* (Ed. Muller, F.), **3**, 121-211. CRC Press, Boca, Raton, FL.

Wynn, R.M., Davie, J.R., Cox, R.P. and Chuang, D.T. (1992) Chaperonins GroEL and GroES promote assembly of heterotetramers ( $\alpha$ -2- $\beta$ -2) of mammalian mitochondrial branched-chain- $\alpha$ -keto acid decarboxylase in *E. coli*. *J. Biol. Chem.* **267**, 12400-12403.

Yang, H., Hainfield, J.F., Wall, J.S. and Frey, P.A. (1985) Quaternary structure of pyruvate dehydrogenase complex from *E. coli*. *J. Biol. Chem.* **260**, 80, 6049-6051.

Yang, Y-S. and Frey, P.A. (1986) Dihydrolipoyl transacetylase of *E. coli*. Formation of 8-S-acetyldihydrolipoamide. *Biochemistry* **25**, 8173-8178.

Yeaman, S.J. (1989) The 2-oxo acid dehydrogenase complexes: recent advances. *Biochem. J.* **257**, 625-632.

Yeaman, S.J., Danner, D.J., Mutimer, D.J., Fussey, S.P.M., James, O.F.W. and Bassendine, M.F. (1988) Primary Biliary Cirrhosis - Identification of 2 major M2 mitochondrial auto-antigens. *Lancet* **1**, 8594, 1067-1070.

Yeaman, S.J., Hutcheson, E.T., Roche, T.E., Pettit, F.H., Brown, J.R., Reed, L.J., Watson, D.C. and Dixon, G.H. (1978) Sites of phosphorylation on pyruvate dehydrogenase from bovine kidney and heart. *Biochemistry* **17**, 2364-2370.

